Sirindhorn International Institute of Technology
Thammasat University

Thesis CE-MS-2010-02

EFFECT OF CONCRETE PROPERTIES AND EXPOSING CONDITION ON HALF-CELL POTENTIAL MEASUREMENT

Kitipoom Chansuriyasak

EFFECT OF CONCRETE PROPERTIES AND EXPOSING CONDITION ON HALF-CELL POTENTIAL MEASUREMENT

A Thesis Presented

by

Kitipoom Chansuriyasak

Master of Science in Engineering
School of Civil Engineering and Technology
Sirindhorn International Institute of Technology
Thammasat University
August 2010

EFFECT OF CONCRETE PROPERTIES AND EXPOSING CONDITION ON HALF-CELL POTENTIAL MEASUREMENT

A Thesis Presented

By

Kitipoom Chansuriyasak

Submitted to

Sirindhorn International Institute of Technology

Thammasat University

In partial fulfillment of the requirement for the degree of

MASTER OF SCIENCE IN ENGINEERING

Approved as to style and content by

Advisor and
Chairperson of Thesis Committee _____

Assoc. Prof. Waree Kongprawechnon, Ph.D.

Co-Advisor _____

Prof. Somnuk Tangtermsirikul, D. Eng.

Committee Member and
Chairperson of Examination Committee _____

Assoc. Prof. Chalie Charoenlarpnopparut, Ph.D.

Committee Member _____

Chalermchai Wanichlamlert, Ph.D.

Committee Member _____

Pakawat Sancharoen, D. Eng.

External Examiner: Assoc. Prof. Sumimol Sajjvanich, Ph.D.

August 2010

Acknowledgements

I warmly thank my advisor, Assoc. Prof. Dr. Waree Kongprawechnon, for her guidance, advice, and continuous support. Her extensive discussions and interesting explorations have been very helpful for my thesis. I would like to express my deep and sincere gratitude to my co-advisor, Prof. Dr. Somnuk Tangtermsirikul, head of the Construction and Maintenance Technology Research Center (CONTEC). His wide knowledge and his logical way of thinking have been of great value for me. His understanding, encouraging and personal guidance have provided a good basis for the present thesis.

I wish to express my sincere appreciations to Assoc. Prof. Dr. Chalie Charoenlarpnopparut , Dr. Chalermchai Wattanalamlerd and Dr. Pakawat Sancharoen, who served as my thesis committee members, and give me important guidance during my first step into studies of corrosion of steel bar in concrete and gave good advice and guidance since the start until the completion.

I would like to express special thanks to all staff at the Civil Engineering Laboratory in School of Civil Engineering and Technology, Sirindhorn International Institute of Technology, Thammasat University (SIIT), for their help in providing facilities and materials for my experiment. Also, I would like to convey special thanks to all students in CONTEC for their cooperation and experiments. I’m deeply indebted to the CONTEC and SIIT for providing me a scholarship to study at Sirindhorn International Institute of Technology.

Finally, my graduation would not be completed without best wish from my parents, Mr.Kitisak and Mrs.Somchit Chansuriyasak, who help me for everything and always give me greatest love, willpower and financial support until the completion of this thesis. And at last, special thanks are given to my friends for their help and encouragement.

Abstract

The initiation time of chloride induced reinforcement corrosion in concrete needs to be anticipated so that appropriate maintenance program can be applied before corrosion occurs. The interpretation of half-cell potential measurement on reinforced concrete structures can be a major challenge in the field of civil engineering. The main reason for this is that half-cell potential mapping provides information to predict the probability of corrosion in concrete. But it does not give clear insight on the rate and the nature of corrosion. Typically for general uniform corrosion, half-cell potential data can provide valuable information about the probability of corrosion. In case of localized corrosion, the interpretation of half-cell measurement can be misleading. This thesis is aimed to study the effect of concrete properties and deterioration on effectiveness of the half-cell potential measurement for monitoring corrosion of steel bars in concrete.

In this experiment, concrete specimens were prepared with different fly ash replacement ratios (FA=0%, 20%, 30%, 50%) and different limestone powder replacement ratios (LP=0%, 5%, 10%, 15%). In addition, some mix proportions were prepared by combination of two binders (20% fly ash and 10% limestone powder). Specimens both of plain concrete and reinforced concrete ware submerged in sodium chloride (NaCl) solution, exposed to carbon dioxide (CO_2), and combined cyclic exposure to NaCl solution and CO_2. The corrosion activities of steel bar in concrete were investigated by half-cell potential measurement for interpretation of initial corrosion. Although, half-cell potential measurement can be used to investigate probability of corrosion of reinforcement, corrosion current density was also measured to be compared with half-cell potential data for corrosion activity interpretation. Carbonation depth measurement and chloride content measurements of concrete specimens were also conducted for verification. The findings in this study are useful for improving the understanding and efficiency of the half-cell potential measurement to investigate probability of corrosion of reinforcement in the reinforced concrete structures.

Results exhibited that half-cell potential reading can be effectively used to investigate probability of steel corrosion in case of chloride environment. This summary is supported by the results of chloride content and corrosion current density. However, half-cell potential reading may not well interpret corrosion due to carbonation, when it is compared by carbonation depth results and corrosion current density value. In addition, corrosion starting times of concrete specimens exposed to combined environment between chloride attack and carbonation were faster than those of chloride only and carbonation only, respectively. This study clearly shows that half-cell potential is much more effective for detecting the corrosion of steel bars in concrete exposed to chloride than carbonation. Moreover, half-cell potential method is better than corrosion current density method for investigating corrosion starting time in laboratory.

Table of Contents

Table of Contents

List of Figures

List of Figures

List of Tables

List of Tables

Chapter 1

Introduction

1.1 General

Deterioration of infrastructures due to corrosion of steel in reinforced concrete structures (RC) has become a serious issue world wide. The corrosion problem has grown to extent that maintenance and repair work cost a huge amount of money annually. Additionally, corrosion can cause serious damage to reinforced concrete structures especially in case of severe environmental conditions. Generally, concrete structures are expected to last for more than 50 years. The concrete cover is designed to protect rebars by preventing the ingress of dangerous substances and setting a high alkalinity around the rebars. Nevertheless, carbon dioxide can decrease this alkalinity substantially and chloride can destroy the passivation film around the steel bars depending on severity of the surrounding environment. In this condition and with the presence of oxygen and water, steel corrosion will occur and shorten the service life of the RC structures.

In normal environment, a RC structure can resist the attacks and shows good long-term durability. However, corrosion problems arrive when the structures are located in severe environments, especially marine. In this environment, the RC structures can deteriorate by chloride attack. The penetrations of chloride ions though concrete causes the depassivation of reinforcing bars and may shorten the life of the structures. The service lifetime of the RC structures can be simply divided into an initiation stage and propagation stage (Bertolini, 2000). The period of initiation stage, controlled by chloride ion penetration to reach the embedded steel, depends on the microstructure of concrete, the external concentration of the chlorides, the transport distance (thickness of concrete cover), condition of sub environment such as wet-dry, etc. as well as the existence of cracks. Subsequently, the propagation stage is followed by the starting of electro-chemical process, which is controlled by the availability of oxygen, the relative humility in the concrete and the temperature around the corrosion area. A schematic sketch of steel corrosion sequence in concrete is shown in Fig 1.1.

This requires counter measure to repair damaged structures and more importantly to protect them from corrosion. These works can only be carried out efficiently after diagnosis of corrosion. The corrosion of steel embedded in concrete can be detected simply by visual inspection. Because of the expanded volume of corrosion products around the reinforcement, internal stress is present and resulting in crack at the concrete surface. Concrete delamination and rust staining can be observed in case of heavy corrosion. Visual inspection provides the first indication of corrosion state, however, it dose not give sufficient information. For investigating corrosion and evaluating corrosion risk even before corrosion took place, a number of methods have been developed.

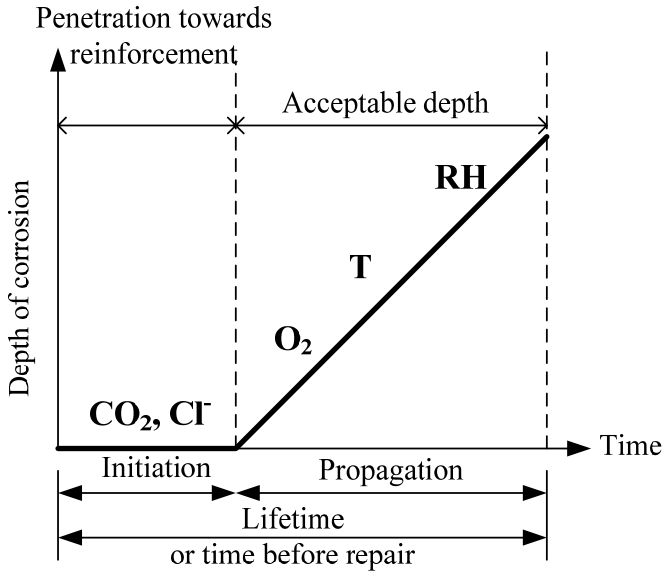

Figure 1.1 Schematic sketch of steel corrosion sequence in concrete (Bertolini, 2000).

In case of destructive testing method, concrete and steel samples are selected from representative locations on structures for assessment. Some basic parameters of steel corrosion such as mass loss and corroded area; and parameters on concrete such as chloride content, carbonation depth, and so on are measured. Furthermore, permeability or diffusions for oxygen and chloride ions, indicating the ease by which aggressive substances can enter concrete structures, can be tested. This method provides insights into the corrosion state and its progress but it is time consuming and so costly. In certain circumstances, this method is impractical due to damages imposed on the structures and so a non-destructive testing method is an alternative providing electrochemical information about the corrosion process.

The corrosion process includes the formation of anodic and cathodic sites on reinforcing steel because of different chemical reactions. Subsequently, a potential difference is observed between the anode and the cathode. The amount of current flow in the corrosion process is determined by this potential difference. Basically, a non-destructive testing method, based on measurement of electrical potential and magnitude of corrosion current, indicates the probability of corrosion, the trends of changes in corrosion process and corrosion rate. The method includes several techniques such as half-cell potential measurement, polarization resistance, electrical resistance, galvanostatic pulse, electrochemical noise, etc.

One of the famous nondestructive techniques is half-cell potential measurement and is available in practice. Half-cell potential measurement is simple and inexpensive to assess the corrosion risk of reinforcing steel. This method can be used to estimate the corrosion risk of steels even if there is no sign of corrosion on the concrete surface and it provides a significant advantage for inspecting existing concrete structures. By this method, the electrical potential difference between the reinforcing steel and a standard portable reference electrode in contact with the concrete surface is measured. The HCP values are then plotted on schematic diagram of the investigated structure as an equipotential contour map.

There are many reports showed recommendations to use the half-cell potential measurement. For instance, The ASTM standard C876 provides general guidelines for the interpretation of the HCP data. According to these guidelines, the probability of corrosion of the reinforcing steels is less than 10% if the potential is greater than -200 mV, whereas potential values lower than - 350 mV indicate a high probability (> 90%) that corrosion is active. The HCP values between these limits indicate areas where the corrosion activity is uncertain.

Although half-cell potential measurement is famous for assessing the corrosion risk, many reports have shown that efficiency of measurement depends on many factors. For example, the potentials measured are very sensitive to moisture content, thickness of concrete cover, surface coating and resistivity of concrete. In addition, different organizations have different recommendations on half-cell potential measurements. ASTM C 876 suggests numerical criteria for assessing the corrosion risk of steels based on a survey of concrete bridge decks. Meanwhile, RILEM TC 153-EMC recommends that numerical criteria from ASTM C 876, lead to misinterpretation because the measured values of the potential fluctuate due to various factors.

1.2 Objectives and scope of study

The interpretation of half-cell potential measurements (HCP) in reinforced concrete structures can be a major challenge for civil engineers. The main reason for this is that HCP mapping provides information to detect the probability of corrosion in concrete. However, the influence of concrete properties such as mix proportions, concrete cover thickness and deterioration of concrete such as chloride attack and carbonation can affect half-cell potential values.

The main objective of the present work is to provide a tool for engineers to effectively interpret the results of HCP measurements. Moreover, this thesis presents the influence of concrete properties and deterioration on HCP reading for monitoring corrosion state of reinforcing steel.

On the basis of this phenomenon, the present study was aimed to:

1. Investigate the efficiency of HCP method to indicate the corrosion state of reinforcing steel due to chloride attack. The HCP values are investigated with macro-cell corrosion current to recheck the corrosion.
2. Study the influence of carbonation of concrete on HCP measurement.
3. Verify proper methods for testing depassivation of steel bars in concrete which is attacked by chloride and carbonation in laboratory.
4. Study effect of water to binder ratio, fly ash and limestone powder replacement, concrete cover thickness on half-cell potential.
5. Study effect of combined cyclic chloride environment and carbonation on half-cell potential values.

Chapter 2

Literature Review

2.1 General

Presented in this chapter are literature reviews for this study. Topics of the reviews are focused on mechanisms of steel corrosion in concrete, types of corrosion, principle of carbonation, corrosion of in concrete steel due to chloride attack, methodology of half-cell potential measurement and principle of corrosion current density. Literature reviews are presented in the following sections.

2.2 Principles of steel corrosion in concrete

In order to understand how to reduce or prevent steel corrosion in reinforced concrete, a basic understanding of the corrosion related reactions and processes that take places in the reinforced concrete is necessary. An electrochemical process occurs once steel reinforcement corrodes in the concrete. The products of corrosion are created through the electrochemical reactions of iron, water, and oxygen. These electrochemical reactions are generally composed of four processes.

The first reaction is the anodic process in which the oxidation of iron occurs at the anode area of the steel. At the anode areas of the steel, electrons are released and metallic ions are formed on the steel surface which is represented as

$$Fe \rightarrow Fe^{2+} + 2e^{-} \qquad (2.1)$$

Actual metal loss will occur at the anode area. During the anodic reaction, electrons are deposited on the surface of the steel, increasing the electrical potential (Bentur et al, 1997).The ferrous ions that are produced dissolve in the water solution surrounding the steel and produce acidic conditions as given

$$Fe^{2+} + 2H_2O \rightarrow Fe(OH)_2 + 2H^{+} \qquad (2.2)$$

The electrons that are released during the anodic reaction are consumed by the cathodic reaction, the second electrochemical reaction needed in order to complete corrosion process. The reduction of oxygen occurs and can be represented as

$$O_2 + 2H_2O + 4e^{-} \rightarrow 4OH^{-} \qquad (2.3)$$

The third process occurs with "the transport of electrons within the metal from the anodic regions, where they become available, to the cathodic regions where they are consumed" (Bertolini, 2003). The electrons that are deposited on the surface of the steel will migrate toward a lower electrical potential, the cathode area. The flow of electrons

from the anode, through the steel, to the cathode creates an electrical current within the steel reinforcing bar and forms a closed loop with the hydroxyl ion migrating from cathode area to the anode area, sometimes referred as galvanic corrosion. This represents the fourth process (Chess, 1998).

All four processes must occur at the same rate and must be equal in order to complete corrosion. The corrosion rate will be controlled by the slowest of the four processes mentioned above. The anode and cathode reactions must also be balanced in order to continue the corrosion process to continue. The number of electrons that are received by the cathode area must equal to the number or electrons that are contributed by the anode area (Bentur et al., 1997).

However, the reactions that take place at the anode and cathode do not complete the process to create rust. There are several more reactions that must be explained in order to fully understand the formation of rust. The additional reactions needed are as shown in Eqs (2.4) to (2.6)

$$Fe^{2+} + 2OH^{-} \rightarrow Fe(OH)_2 \quad (2.4)$$

$$4Fe(OH)_2 + O_2 + 2H_2O \rightarrow 4Fe(OH)_3 \quad (2.5)$$

$$2Fe(OH)_3 \rightarrow Fe_2O_3H_2O + 2H_2O \quad (2.6)$$

From equation (2.4), ferrous hydroxide is formed. The ferrous hydroxide then forms ferric hydroxide which in turn forms hydrated ferric oxide which is more commonly referred to as rust as shown in equations (2.5) and (2.6). The ferric oxide that is produced in equation (2.6) has a volume that is twice that of steel (Broomfield, 1997). The corrosion process of steel bar in concrete is presented in Fig 2.1. Once the ferric oxide hydrates, it swells, and becomes more porous. This increase in volume may eventually create a pressure great enough to exceed the tensile capacity of the concrete which can lead to cracking, spalling, and delamination of the cover concrete (ACI Committee 222, 1996).

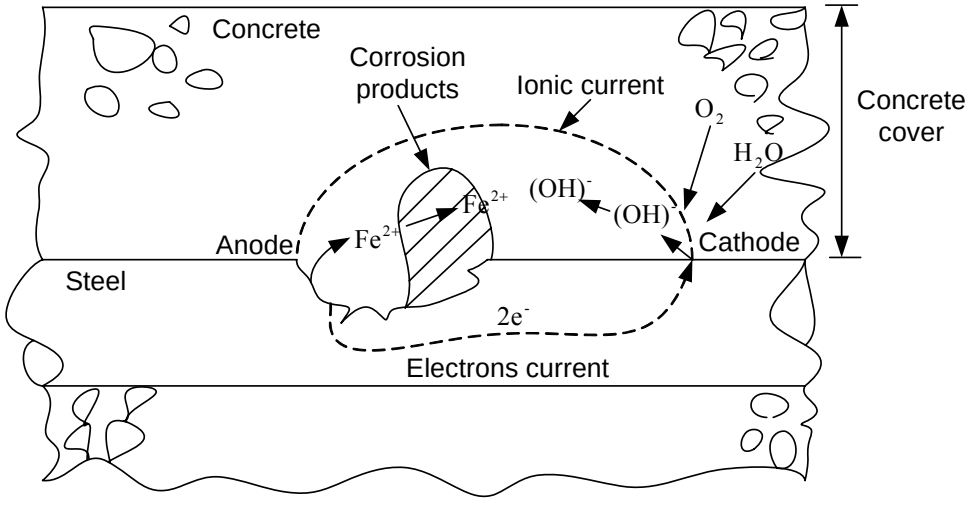

Figure 2.1 Schematic of the corrosion process

The most common occurrences of corrosion in reinforced concrete structures, as stated earlier, are caused by the intrusion of chlorides and carbonation. Both processes are detrimental once present at the depth of the reinforcing steel. Appropriate measures must be taken to minimize both effects in order to prevent the premature failure of the structures.

2.2.1 Mechanisms of micro and macro-cell corrosion

Two mechanisms of corrosion that are often discussed are those of micro-cells and macro-cells. Different spatial locations of both the anode and the cathode leads to different forms of corrosion of the reinforcing steel in concrete (Elsener, 2002).

Micro-cell corrosion

Micro-cell corrosion is observed when the anodic and cathodic reactions take place adjacently to one another. Micro-cell corrosion is commonly referred to as localized corrosion and occurs at isolated locations along the bar as pitting corrosion. Because the reactions are in such close proximity, uniform iron dissolution occurs over a relatively large area of the surface. The pairs of adjacent anodes and cathodes give the appearance that the removal of steel is uniform (Elsener, 2002 and Raupach, 1996). The uniform corrosion is generally a result of carbonation of the concrete (Elsener, 2002 and Raupach, 1996). Knowledge of the effects of micro-cell corrosion is important as they can augment the effects of macro-cell corrosion.

Macro-cell corrosion

Macro-cells often develop as a result of the presence of large anodic reinforcement areas that are in electrical contact with the cathodic areas (Andrade, C. et al 1991 and Keddam, M. et al 1994). The concrete acts as the electrolyte in order to complete the galvanic cell. The macro-cells tend to form in anodic areas where the critical chloride content has been attained, often leading to pitting (Elsener, B. 2002 and Raupach, M. 1996). One important aspect that has gained much attention is that the microcell corrosion should not be disregarded when macro-cells are present (Felier, S. et al 2005 and Clemena, G. 2003). In order to accurately reflect the corrosion occurring within the structure, the corrosive actions of the micro-cells should be added to that of the macro-cells (Andrade, C. et al 1991). This is especially significant when the cathodic area is much larger than the anodic area such as in bridge decks especially where truss bars are utilized.

The macro-cell current is difficult to predict due to the many influencing factors that must be analyzed. Schiessl (1986) reported that the combined effects between micro-cell and macro-cell need to be considered. So, the corrosions current, I_{corr} represents the combined activity of the micro plus macro-cell activity and can be represented in Eq (2.7).

$$I_{corr} = \frac{B}{R_p} \qquad (2.7)$$

Where, I_{corr} is a corrosion rate in ampere/cm^2, B is a constant in volts and R_p is polarization resistance in ohms$\cdot$cm^2. While I_{corr} provides information on both the micro and macro-cell corrosion mechanisms

The effects of differences in clear spacing on macro-cell corrosion

Bertolini (2004) reported that low resistivity concrete permits cathodic current to travel distances in the range of one meter to the local anode. However, Schiessel (1998) reported that distance between anode and cathode in the range of 80 to 640 millimeters had practically no effect on macro-cell corrosion in the case of Portland cement concrete.

There are many reports that show macro-cell corrosion rate depended on the ratio of the cathode area to the anode area greatly affects the rate of corrosion. According to Andrade (1991), micro-cell corrosion occurs when ratio of the anode area and the cathode area equate. Then, corrosion in reinforced concrete is uniformly distributed. It is well known that this phenomenon is uniform corrosion. But it is different when ratio of cathode areas increases. Very large cathode area may accelerate the rate of corrosion, because large amount of electrons from small anode area can be simply moved to the large cathode area. Consequence, the increased rate of corrosion may be as great as 0.5 to 1.0 mm/year (Elsener, 2002).

However, experimentation has shown that only when the cathodic area is in the range of 41 times greater than the anodic area, the macro-cell corrosion is three to six times greater than that of the micro-cells (Andrade, 1991). The results support the hypothesis that macro-cell corrosion is most likely formed in very large structures that have very large passive areas in comparison to that of the anode areas and that micro-cell corrosion is most often the dominant corrosion mechanism measured.

2.2.2 Corrosion rate

The corrosion rate, induced by chloride ions, can be formulated by theory of macro-cell corrosion which is determined by the degree of polarization of anode or cathode. The difference between the potentials of an electrode with and without current is call electrochemical polarization. This polarization represents an over potential defined as shown in Eqs (2.8) to (2.9)

$$\eta_a = E_{corr} - E_a \tag{2.8}$$

$$\eta_c = E_c - E_{corr} \tag{2.9}$$

where η_a, η_c are the over potentials and E_a, E_c are the equilibrium potentials for anode and cathode, respectively. E_{corr} is corrosion potential.

Even (1960) introduced a simplified graphic method for representing the relationship between current (I) and potential (E). Figure 2.2 illustrates the simplest example of an Evens diagram. The intersection of two curves represents the conditions at which the anodic and cathodic current are equal and no net external current flows and, thus, defines the corrosion potential (E_{corr}), and corrosion current (I_{corr}).

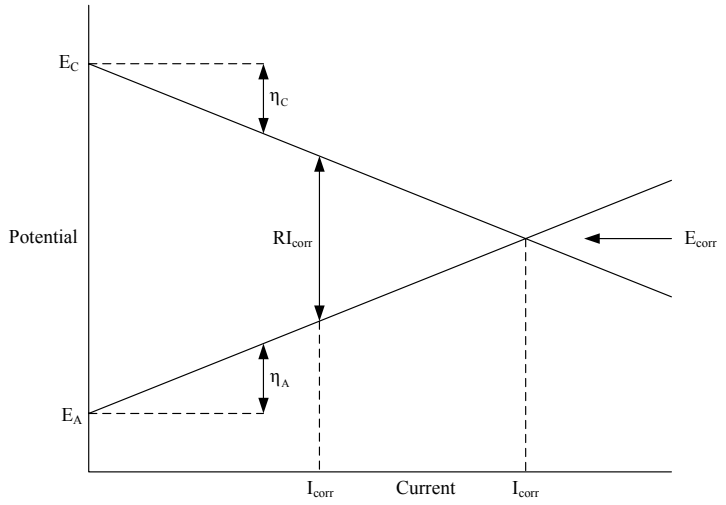

Figure 2.2 Schematic of Evens diagram (Evens, 1960)

2.3 Carbonation

Carbon dioxide is one of the most common gases that can penetrate in to concrete and destroy the protective passive layer of steel reinforcement. Carbonation occurs when the carbon dioxide within the atmosphere reacts with $Ca(OH)_2$ inside the pores of the concrete to form calcium carbonate (Revie, 2000). The acid then reacts with the calcium and other hydroxides to form solid carbonates (Revie, 2000). Carbonation can be a result of poor concrete cover, poor concrete quality, and poor consolidation. The following reaction is associated with carbonation as

$$Ca(OH)_2 + CO_2 \rightarrow CaCO_3 + H_2O \quad (2.10)$$

or

$$3CaO{\cdot}2SiO_2{\cdot}3H_2O + 3CO_2 \rightarrow 3CaCO_3{\cdot}2SiO_2{\cdot}3H_2O \quad (2.11)$$

Carbonation will initially neutralize the surface of the concrete and then gradually move inwards. The pH levels in the pore solution within the concrete will decrease from a pH level of approximately 12 to a pH level of approximately 8, approaching neutrality (Bertolini, 2004). The decrease in the pH levels decreases the stability of the passive layer. The instability of the passive layer leads to a breakdown of this passive layer which will initiate corrosion.

The rate that corrosion will occur as a result of carbonation depends on environmental factors and factors related to the concrete. Environmental factors include humidity, temperature, and the concentration levels of carbon dioxide while factors related to the concrete involve the alkalinity levels and the permeability of the concrete (Bertolini, 2004). The following equation (2.12) describes the rate of carbonation which decreases with time:

$$d = k\sqrt{t} \quad (2.12)$$

where, d = depth of carbonation (mm)
t = time (years)
k = carbonation coefficient (mm/$\sqrt{\text{year}}$)3

Jibodee (2005) studied effect of fly ash, which was used to partially replace cement, on carbonation coefficient. It was found that carbonation coefficient of concrete increased with the increase of fly ash, content water to binder ratio, and CO_2 concentration in the environment. Moreover, carbonation coefficient incorporating high-CaO fly ash was lower than that of the concrete with low-CaO fly ash.

2.4 Chloride attack

Chlorides penetrate into concrete by absorption of chloride containing water or by diffusion of the ion in the water (Neville, 1995). In a structure permanently submersed in the seawater, chlorides penetrate into concrete considerably. However, corrosion can occur if concrete is exposed to seawater and dried out alternatively. Dry concrete absorbs salt water until the concrete is saturate. When the external environment change to dry, salt water will move from the ends of capillary pore toward the concrete surface where pure water evaporates and salts are left behind. The concentration of salts in the pore water increases near the concrete surface. Thus salts will diffuse from the high concentration zones to the lower ones. After one cycle of wetting and drying the water moves outwards and salt does inwards.

The ingress of chlorides is strongly influenced by length of wetting and drying periods. Wetting occurs very fast and drying does much slower so that the interior of concrete hardly dried out. Extensive drying allows larger amount of chlorides ingress into concrete in the subsequent wetting period due to capillary suction.

There is a level called threshold concentration of chloride that corrosion will be initiated. The total chloride content can be measured by weight of concrete whereas threshold level is commonly presented as percent by weight of cementitious material. The first value can be converted to the second one by multiplying it with the ratio of concrete density to the cement content. Many factors affect the threshold chloride content including external environment, concrete composition (Rosenberg cited in Nicholas 1999). Thus, no single value of threshold chloride content exists. Some previous research sugguested that chloride threshold level can be considered to determine of corrosion risk. A risk classification was proposed as in Table 2.1.

Table 2.1 Corrosion risk

Chloride by weight of cement, %	Risk of corrosion
< 0.4	Negligible
0.4 to 1.0	Possible
1.0 to 2.0	Probable
> 2.0	Certain

Source: Bamforth (1998)

These recommendations are consistent with available data worldwide. For concrete with water to cement ratio less than 0.5 under cyclic wet/dry condition, the chloride threshold level of 0.4 by weight of cement is most applicable. In term of amount of chloride ions by volume of concrete, the threshold value is about 1.2 to 2.4 kg/m^3 according to JSCE (2004).

2.4.1 Oxygen diffusion

In the corrosion process, oxygen is also an important factor. In the cathodic reaction process, oxygen is obviously necessary and the rate of oxygen diffusion through the concrete to the reinforcing steel depends on the quality of concrete. On the other hand, if concrete is completely saturated with water, concrete deterioration may not occur, even if corrosion initiation has taken place at an early stage (Tuutti.K., 1982). Oxygen must diffuse partly through a liquid phase and partly through a gas phase in the pores of concrete expressed by the effective diffusion coefficient of oxygen. Coefficient of oxygen diffusion is traditionally calculated from Fick's first law (Takewaka.K. et.al., 1999).

2.4.2 Moisture content

The effect of moisture content in concrete is expressed in two ways, the diffusion processes of substance and the corrosion rate of steel. In the diffusion processes, the diffusion rates of oxygen and chloride depend on the moisture content in concrete. Higher the moisture content in concrete, causes the higher diffusion rate of chloride, In contrast, the oxygen diffusion is lower (because air-filled pore is less).

Nevertheless, moisture content of the concrete plays a direct role in determining the rate of corrosion of steel embedded in concrete. The water influences the process in at least two ways. One is the degree of water saturation which appears to have a dominating influence on the electrical effect and the diffusivity of oxygen. After exceeding a threshold value from water saturation, corrosion process becomes diffusion governed and the corrosion rate decreases (Balabanic.G. et.al., 1996).

2.5 Methods of assessing extent of corrosion damage in reinforced concrete

Many test methods are available to measure corrosion of reinforced concrete. However, it is uncommon to rely on only one method. Instead, a combination of testing methods are performed and analyzed to predict the presence of corrosion and the rate at which it is occurring. Two of the most commonly used methods, half-cell potential and macro-cell corrosion measurement, are discussed below.

2.5.1 Half – cell potential measurement

Confidence in using half-cell potentials as an indication of corrosion potential has developed from the success of structure corrosion surveys. As a result, potential reading are now commonly conducted on bridges, stadiums, buildings, dams, tunnel liners, and many other structures. Half-cell potential measurements provide a classification of the corrosion activity of the steel and indicate locations where the steel is potentially corroding. Table 2.2 presents the relationship given in ASTM C 876 between the half-cell potential values, reported in mV, and the probability of steel corrosion.

Van Deveer (1975) found that there was a 95% probability of corrosion in regions where the potential was more negative than -350 mV with respect to copper/copper sulphate reference electrode and 5% probability where the potential was less negative than -200 mV. The criteria are indicative rather than absolute and do not imply for example, that 95% of all the steel within areas where potentials is more negative than -350 mV will be corroding.

Table 2.2 Probability of corrosion according to half-cell potential readings

Half-cell potential reading	Corrosion activity
less negative than -200 mV	90% probability of no corrosion
Between -200 mV and -350 mV	an increasing probability
More negative than -350 mV	90% probability of corrosion

Source: ASTM C876-91

A. Poursaee and C.M. Hansson (2007) reported the corrosion behavior of as received steel and sand blasted steel in mortar submersed in a simulated pore solution (NaOH and KOH), the half-cell measurement and linear polarization resistance were used for determining the time required for passivation. The results showed that the as received steel showed higher corrosion rate than the sand-blasted steel but there is no consistency in half-cell potential values. Moreover, all half-cell potential value are between -350 and -200 mV CSE, which is within the range of "uncertainty of active corrosion" according to the ASTM C876 guidelines for interpretation of half-cell potential data. This indicated that the ASTM recommendations are not applicable to measure the earliest stages of passivation of the steel. They concluded that the ASTM criteria cannot be applied to fresh mortar or concrete.

As shown in Figure 2.3, the half-cell potential measurement apparatus consists of a voltmeter with one lead wire connected to a reference electrode, normally a copper copper-sulfate ($Cu/CuSO_4$) electrode, placed on the surface of the concrete and a second lead wire connecting the voltmeter to the reinforcing steel. Current passes from the reference electrode to the concrete surface through a sponge soaked with an electrolytic solution. The objective of the instrumentation is to measure the voltage, or potential difference, between the rebar and the reference electrode. In the half-cell potential setup, the reference electrode behaves as the cathode, as copper is higher in the galvanic series than steel.

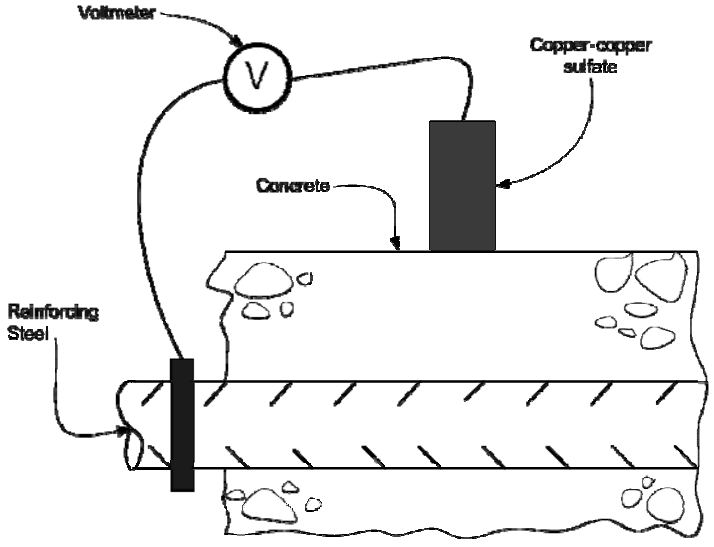

Figure 2.3 Half-cell potential measurement apparatus

Parameters influencing half – cell potential measurement

Above mentioned, the corrosion of steel in concrete is a major type of deterioration in concrete structures. If corrosion activity of the concrete structures is not inspected or monitored, the concrete structures may have severe damages and require intensive maintenance programs earlier than they should. Thus, non-destructive techniques especially half-cell potential method can be used to detect the corrosion activity of steel in concrete (Gu et al., 1998). However, many factors affect the magnitude of the half-cell potential so that it may not indicate true corrosion conditions (Broen et al.1983; Elsener and Bohni 1990; Elsener et al. 1990). Hereafter, parameters influencing half-cell potential measurement are presented.

Concrete repair

B.Elsener (2001), show limitations of half-cell potential measurement as an assessment technique after electrochemical chloride removed. The potential values become more positive by about 80-100 mV indicating the repassivation of steel. Moreover, a five-year record after completion of repair work showed that no corrosion had initiated and the potential fields become more homogeneous. Rilem TC154-EMC (2003), concluded that half-cell potential measurement can be used to evaluate the corrosion state of the steel bar after electrochemically realkalization. Results showed that the potential values after the treatment were shifted up by about 200 mV to more negative values. Therefore, the shift in potential depends on the type of repair technique and its mechanistic action. Half-cell potential mapping can be used to evaluate the effectiveness and durability of repair works with the normal interpretation only when the concrete resistivity is not changed too much after treatment.

Corrosion inhibitors

Rilem TC154-EMC (2003), conclude that testing the efficiency of inhibitors penetrated from the concrete surface by half-cell potential measurement is difficult. Because change in the pore water composition, concrete resistivety as well as different possible mechanisms of the inhibitor action can lead to shifts of the half-cell potential measured from the concrete surface and cannot be interpreted straight forward.

Moisture content

The half-cell measurement is very sensitive to the humidity existing in the concrete. More negative potentials are resulted from concrete with higher degree of saturation. There are many reports showing that moisture content can affect the half-cell reading. For example, Rilem TC154-EMC (2003) concluded that changing the moisture especially wetting of the concrete surface led to a shift of the whole potential field to more negative values. They reported that shift of 100 mV was found on bridge deck measured in dry and wet condition after rainfall. The potential gradients and location of the minimum potential did not change. Differences were found only in the magnitude of potential reading. More negative potentials were detected in concrete with higher degree of saturation.

Carbonation

Gu et al. (1998), concluded as carbonation process reduced the pH value of the concrete around steel reinforcement. When using half-cell potential method, potential reading will shift towards more negative values although the shift may not be very large. However, even a small shift in values can be associated with a large increase in the rate of corrosion. As carbonation process leads to an increase of concrete resistivity, potential values depend on moisture condition of concrete and resistivity. Changes in moisture content may lead to a difference of potentials up to 200 mV. Potential values become more negative as concrete moisture increases (Technical Mote NEA/CSI/R, 2003). A greater concrete cover thickness, the potential increases. For greater concrete resistance, potential shifts toward less negative half-cell potential readings. The difference between active and passive potential values diminishes, resulting on an uniform potential value at infinite. Thus, the location of small corrosion spots gets more difficult with increasing cover depth.

Effect of concrete resistivity

It is well known that concrete resistivity affects the corrosion rate of steel reinforcement (Alonso et al. 1988; Gulikers 2005; Ghods et al. 2007). With respect to half-cell potential tests, as the resistivity of concrete increases, the detection of corrosion becomes harder (Elsener, 2002). As an example from the large number of cases simulated, Fig. 2.4 illustrates the effect of concrete resistivity on the potential distribution at the steel/concrete interface and on the surface of concrete at 20°C. As can be seen in the Fig. 2.4, the increase of resistivity shifts the potential of the anodic sites to more negative values and the potential of cathodic sites to more positive values. In low resistivity concrete, as illustrated in Fig. 2.4(a), the potential distribution along the surface of the concrete closely represents the potential distribution at the interface of steel/concrete. As the resistivity of concrete increases, as shown in Figs. 2.4(b) and (c), the potential distribution at concrete surface tends to part noticeably from that of the steel/concrete interface. This difference is more obvious at sections close to the transition zone between the anode and the cathode.

Figure. 2.4(d) illustrates the potential distribution on the surface of the concrete to demonstrate that the shift in potential distribution curves with increasing concrete resistivity is not the same for anodic and cathodic surfaces: increase in resistivity affects more on the cathodic sites than on the anodic sites. At high resistivities (e.g., 5000 and 10,000 Ω.m), the change in resistivity does not affect the potential distribution of the anodic sites; however, the cathodic potentials continue increasing to more positive values, signifying smaller cathodic polarization. In Figure 2.4(d) when resistivity is not large (i.e., 50 Ω.m), cathodic section of the passive steel is polarized to more negative values, which can be interpreted as the member having higher probability of corrosion according to the standards (Elsener et al., 2003). Fig. 2.4(d) also suggests that with increasing resistivity, the potential difference between the anodic and cathodic sites increases. Thermodynamically, the tendency to corrode increases with larger potential difference; however, the corrosion rate is inversely related to concrete resistivity by Ohm's law. This implies that while carrying out half-cell measurements, potential readings should be interpreted in accordance with the resistivity of the system. Otherwise, the results can be misleading. For the same corrosion rate, one can measure different potentials at the surface of concrete, corresponding to different resistivities, and thus have more than one probability for the same state of corrosion.

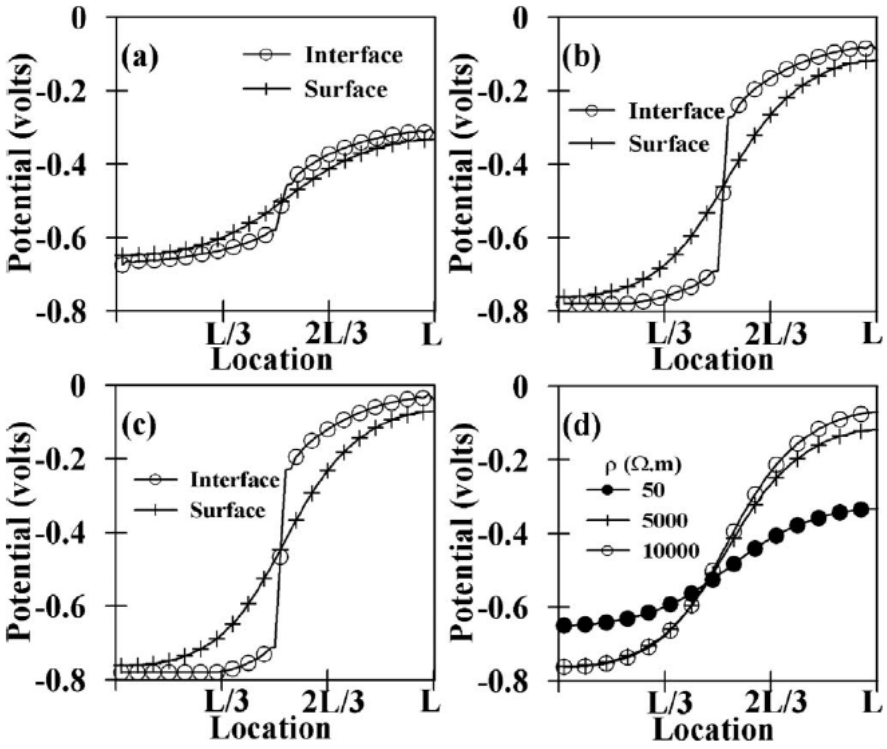

Figure 2.4 Effect of concrete resistivity on potential distributions of concrete resistance at the surface of concrete and at the steel/concrete interface: (a) ρ=50 Ω.m; (b) ρ=5000 Ω.m; (c) ρ=10000 Ω.m; and (d) Potential distribution at the surface of concrete for different values of concrete resistivity (Mohammad et.al., 2009).

Effect of Cover Thickness

The effect of cover thickness on the potential mapping and corrosion rates in simulated half-cell tests was investigated by varying the cover thickness between 20 and 140 mm. Fig. 2.5 illustrates the potential distribution at the interface of steel/concrete and on the concrete surface for d=20 mm and d=140 mm. If the cover thickness is small (e.g., 20 mm), as shown in Fig. 2.5(a), the potential distribution on the surface of concrete is almost the same as potential distribution at the interface of steel/concrete. However, such a small cover thickness is not practical, and usually thicker covers are used in practice. As cover thickness increases, the potential of the surface differs from that of interface significantly, as illustrated in Fig. 2.5(b). At these large values of cover thickness, the potential distribution on the concrete surface does not provide accurate information about the potential distribution at the steel/concrete interface. It is interesting to note that Elsener et al. (2003) has also made this observation by stating that "the potential difference between the position above the anode and a distant cathode becomes smaller with increasing cover depth." Fig. 2.5 also suggests that the increase of cover thickness results in flatter potential distribution on the steel/concrete interface, increasing the potential difference between the surface of the concrete and the steel/concrete interface considerably. This is also in agreement with Elsener's observations in Elsener (2002). As a result of these numerical observations, in half-cell potential measurements, one should also consider the effect of cover thickness on the potential distribution.

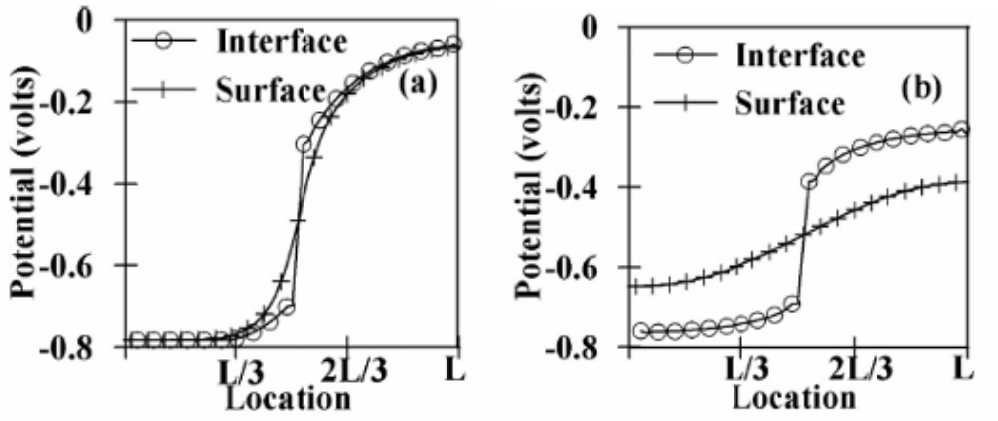

Figure 2.5 Effect of cover thickness on potential distributions at the surface of concrete and at the steel/concrete interface: (a) d=20 mm; (b) d=140 mm (Mohammad et.al., 2009).

Effect of Anode-to-Cathode Area Ratio

Fig. 2.6 illustrates the effect of Anode-to-Cathode Area Ratio (A/C) on the potential distribution on the surface of concrete and along the steel/concrete interface. For small values of A/C (i.e., 0.1), the potential distribution of anodic sites at the surface of concrete is substantially different from that of the steel/concrete interface. However, for cathodic sites the difference between the potential at the surface and steel/concrete interface is much smaller. For larger A/C, the potential difference between the surface and interface of anodic sites diminishes. This implies that accurate detection of localized corrosion (e.g., pitting), in which A/C ratio can be small, may not be feasible with half-cell potential measurement method, as also confirmed by existing standards (ASTM 1999; Elsener et al. 2003). The detection of localized corrosion becomes even harder for thick concrete covers. These observations are in line with conclusions of Elsener (2002), who experimentally studied the potential distribution at different distances above anodic and cathodic sites of rebar in physically simulated concrete solutions with different resistivities. It can be concluded from these observations that the accuracy of potential mapping in detecting the corrosion is dependent on A/C ratio.

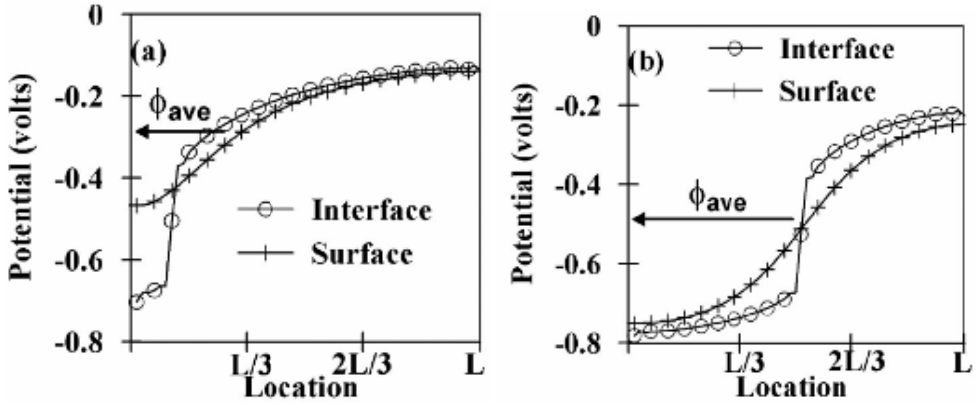

Figure 2.6 Effect of anode-to-cathode area ratio on potential distribution at the surface of concrete and at the steel/concrete interface: (a) A/C=0.1; (b) A/C=1.0

2.5.2 Macro-cell corrosion current measurement

The macro-cell corrosion current testing method is the most commonly used to predict the likelihood of corrosion of steel reinforcement in concrete. This test method is mainly used in the laboratory. However, some researchers modified this method for monitoring corrosion of reinforcing steel by installing this technique in new structures (M.Raupach, 2004).

The testing method outlined in the American Standards for Testing of Materials ASTM G 109, (1999) the Standard Test Method for Determining the Effects of Chemical Admixtures on the Corrosion of Embedded Steel Reinforcement in Concrete Exposed to Chloride Environments, was utilized. Macro-cell corrosion current was a good indicator of corrosion initiation of the reinforcing steel.

The galvanic current also called macro-cell current flow between top and bottom bars was measured by voltmeter as procedures outlined in ASTM G109. A 100 Ω resistor was placed between the top and bottom bars and the potential difference were measured. The increase in anodic current indicates the initiation of corrosion. Figure 2.7 illustrates a specimen for testing macro-cell corrosion current according to ASTM G109.

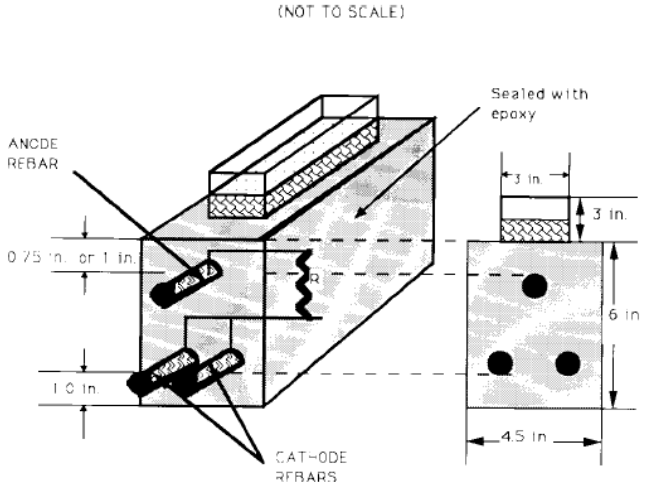

Figure 2.7 Specimen for testing macro-cell corrosion current density (ASTM G109)

2.5.3 Chloride ion content

Chloride content can be determined from powder samples removed from the concrete element at incremental depths from the exposed surface using rotary percussive drilling. The chloride contents can be determined by acid extractions of the powdered concrete, followed by a chemical determination of the chloride contents. The method is described in ASTM C 1218/C 1218M (1999). There is a probabilistic relationship between chloride concentration by weight of cement and corrosion risk. Roberts (1986) provides initial assessment of chloride content in concrete. Low corrosion risks are associated with concentration below 0.4% by weight of cement, medium risk with concentration between 0.4% and 1% and high risks above 1%. However, these values can be changed when concrete are carbonated or chloride included during of mixing (Puller, 1987). This phenomenon is presented in Table 2.3.

Table 2.3 Interpretation of chloride and carbonation test data, in terms of corrosion risk

Chloride by weight of cement	Condition of concrete adjacent to reinforcement	corrosion risk
less than 0.4%	1. Carbonated	high
	2. Uncarbonated made with cement containg less than 8%of C_3A	moderate
	3. Uncarbonated made with cement containing 8% or more C_3A in total cementitious material	low
0.4%-1%	1. as above	high
	2. as above	high
	3. as above	moderate
more than 1%	all cases	high

Source: Roberts (1986)

2.5.4 Carbonation depth measurements

The depth and extent of carbonation should be assessed either on site or in the laboratory using the technique described in Jibodee et. al., 2006. Phenolphthalein is used as an indicator to determine the depth of carbonation on freshly or drilled concrete surface. Phenolphthalein remains colorless when it is in contact with carbonated concrete but turns pink where the concrete has retained sufficient alkalinity to protect the reinforcement from surface corrosion.

Preferably, a freshly fractured surface should be used for the determination. If this is not possible, the depths of carbonation could be determined by testing dust samples removed at incremental depth from the exposed concrete surface using a percussive hammer drill. In this case it is recommended that upon commencement of the work on a structure the latter test method is calibrated at not less than three locations by comparing the results found with those obtained from testing the freshly fractured surface. Certain concretes, particularly those made with white cement or those in older structures, may contain particles of unhydrated cement which may break up upon drilling to give an apparent, but false, low depth of carbonation.

Chapter 3

Methodology

3.1 General

An experimental program was designed to study the corrosion activities of reinforcing steel in concrete. Also basic mechanical properties such as compressive strength were studied. The corrosion activities were investigated by half-cell potential measurement (HCP) and macro-cell current density measurement (i_{corr}). In addition, carbonation depth and total chloride content were applied to recheck the corrosion process.

Three different environments were selected for this study. First environment was carbon dioxide. Concrete specimens were placed in a carbonation chamber having 4% concentration of carbon dioxide, 40°C of temperatures and 55±5% of relative humidity. Second environment was chloride attack. Concrete specimens were exposed to 10% concentration of NaCl solution. For the last environment, specimens were exposed to both chloride and carbonation alternatively. In this environment, concrete specimens were exposed to cycles of carbonation and chloride. Each cycle contained 4 days of carbonation and then 3 days of chloride attack. In addition, examples of application to study corrosion activity of actual RC structures (concrete walls), which were exposed to marine environment, were also described. The concrete walls were tested by non-destructive method and destructive method. All of experimental details were presented in the following sections.

3.2 Materials

3.2.1 Ordinary Portland cement, fly ash and limestone powder

Ordinary Portland Cement ASTM Type I, manufactured in Thailand by Siam Cement Group Public Company Limited (Elephant Brand) was used for all mixtures. The fly ash obtained from Mae-Moh power plant in Thailand was used in all mixtures of the experiments. This fly ash is a product of lignite after burning process as fuel in the plant. It is classified as class 2b fly ash according to TIS 2135-2545 (calcium oxide >10%). The utilized limestone powder was supplied by Surint Omya Chemicals (Thailand) Co., ltd. The test results of chemical compositions and physical properties of these materials are shown in Table 3.1.

3.2.2 Aggregates

Natural river sand obtained from natural river, passing a ASTM C33-92a sieve No. 4 (4.75-mm openings), was used as the fine aggregate for all concrete mixes. Its specific gravity and water absorption were 2.58 g/cm^3 and 1.01%, respectively. The crushed limestone, of which maximum size is 19 mm, was used as the coarse aggregate. It was

obtained from Saraburi province with specific gravity of 2.69 g/cm^3 and water absorption of 0.25%. It was retained on the sieve No.4 (4.75-openings) and cleaned before being used.

Table 3.1 Chemical compositions and physical properties of cement, fly ash and limestone powder

Chemical compositions	**Cement**	**Fly ash**	**Limestone powder**
Silicon dioxide (%)	20.48	43.88	0.06
Aluminum oxide (%)	5.25	24.31	0.09
Iron oxide (%)	3.82	12.51	0.04
Calcium oxide (%)	65	11.18	54.80
Magnesium oxide (%)	0.95	2.73	0.57
Sulfur trioxide (%)	1.9	1.43	-
Insoluble residue (%)	0.13	-	-
Sodium oxide (%)	0.01	0.78	-
Potassium oxide (%)	0.4	2.78	-
Titanium dioxide (%)	0.25	0.47	-
Phosphorus pentaoxide (%)	0.05	0.13	-
Free Lime (%)	0.75	-	-
Gypsum Content (%)	5.6	-	-
Physical Properties			
Specific gravity (g/cm^3)	3.15	2.08	2.70
Loss on ignition (%)	1.17	0.17	44.44
Blaine Fineness (cm^2/g)	3350	3460	9260
Water requirement (%)	100	95.6	-
Bogue's potential compound compositions			
C_3S (%)	68.13		
C_2S (%)	7.41		
C_3A (%)	7.46		
C_4AF (%)	11.61		

3.2.3 Water

Ordinary tap water supplied at concrete laboratory, Sirindhorn International Institute of Technology, Thammasat University, was used for all concrete.

3.3 Mix proportion

In this study, the cementitious materials used in concrete were ordinary Portland cement, fly ash and limestone powder. The test parameters were classified by water to binder ratio, replacement ratio of fly ash and limestone powder. Different fly ash content (0, 20, 30 and 50%) and limestone powder (0, 5, 10, and 15%) with different w/b (0.4, 0.5 and 0.6) were used in this study. In addition, some mix proportions were designed by using

blended binders i.e. cement, fly ash and limestone powder. The details of mix proportions of concrete are given in Table 3.2.

The mix proportions of 27 concrete samples are shown in Table 3.2. An example of description of the mixture designation is as follow; "0.4L10F20" means the sample which has water to binder ratio of 0.4, limestone powder replacement ratio of 10% and fly ash replacement ratio of 20%.

Table 3.2 Mix proportions tested in this study

NO.	Designation	w/b	OPC	FA	LP	Water	Sand	Gravel
			(kg/m^3)	(kg/m^3)	(kg/m^3)	(kg/m^3)	(kg/m^3)	(kg/m^3)
1	0.4OPC	0.4	454	0	0	182	720	1032
2	0.4FA20	0.4	348	87	0	174	720	1032
3	0.4FA30	0.4	298	128	0	170	720	1032
4	0.4FA50	0.4	204	204	0	163	720	1032
5	0.5OPC	0.5	399	0	0	199	720	1032
6	0.5FA20	0.5	307	77	0	192	720	1032
7	0.5FA30	0.5	263	113	0	188	720	1032
8	0.5FA50	0.5	181	181	0	181	720	1032
9	0.6OPC	0.6	355	0	0	213	720	1032
10	0.6FA20	0.6	274	69	0	206	720	1032
11	0.6FA30	0.6	236	101	0	202	720	1032
12	0.6FA50	0.6	163	163	0	196	720	1032
13	0.4OPC	0.4	454	0	0	182	720	1032
14	0.4LP5	0.4	430	0	23	181	720	1032
15	0.4LP10	0.4	406	0	45	180	720	1032
16	0.4LP15	0.4	382	0	67	180	720	1032
17	0.4L10F20	0.4	306	87	44	171	720	1032
18	0.5OPC	0.5	399	0	0	199	720	1032
19	0.5LP5	0.5	378	0	20	199	720	1032
20	0.5LP10	0.5	357	0	40	198	720	1032
21	0.5LP15	0.5	336	0	59	197	720	1032
22	0.5L10F20	0.5	270	77	39	189	720	1032
23	0.6OPC	0.6	355	0	0	213	720	1032
24	0.6LP5	0.6	337	0	18	213	720	1032
25	0.6LP10	0.6	318	0	35	212	720	1032
26	0.6LP15	0.6	299	0	53	211	720	1032
27	0.6L10F20	0.6	242	69	35	203	720	1032

Note: w/b is the water to binder ratio; OPC is ordinary Portland cement, FA is fly ash and LP is of limestone powder

3.4 Specimen preparation

3.4.1 Reinforcing steel

Deformed bars having grade SD40 according to TIS 24 (Thai Industrial Standard) with diameter of 12 mm and length of 310 mm were used as reinforcing steels. They were polished by using a wire brush to remove rust shown on the surface and then degreased by acetone. All steel bars were wrapped by using insulating tape on both ends so that the 210 mm center portion of the bar was exposed. Both tape-insulated ends of the steel bars were coated again by epoxy as shown in Figure 3.1

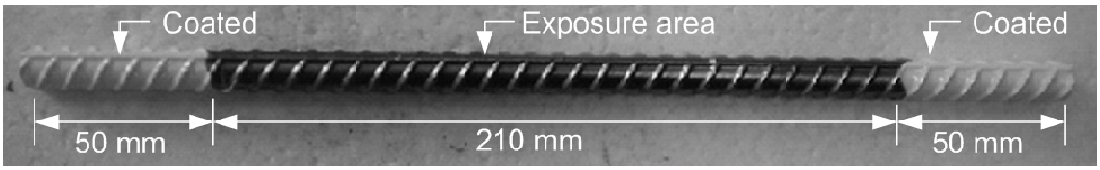

Figure 3.1 Reinforcing steel used in the specimens.

3.4.2 Specimen for chloride environment

Shape of specimens used for chloride attack was modified from ASTM G109 which was standard test method for determining the effects of chemical admixtures on the corrosion of embedded steel reinforcement in concrete exposed to chloride environments. Specimen dimensions are 95 mm × 200 mm × 250 mm. Three reinforcing steel installed in concrete which differencing cover thickness. One bar put at the top specimen. Two bars put at the bottom specimens which were placed 80 mm below the top bar. In additions, cover thickness of the top bar was varied as 30 mm and 50 mm. The top and bottom bars were electrically connected with lead wires and a 100 Ω resistor. At the top surface specimen was cleaned for installing plastic dam. The plastic dam with dimension of 150mm × 65mm was placed on the top of specimen. The plastic dam and specimen was attached by water proof silicone adhesive. The dimension details of concrete specimen are given in Figure 3.2.

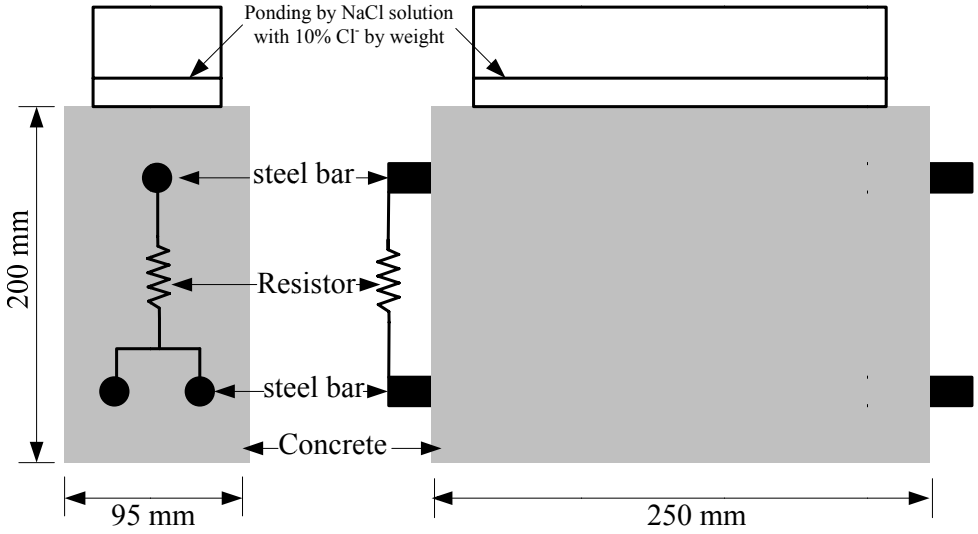

Figure 3.2 Schematic illustration of specimen exposed to chloride.

3.4.3 Specimen for carbon dioxide environment

Dimensions of prism specimens exposed to carbon dioxide are 200 mm ×200 mm ×250 mm. Concrete cover of steel was varied at 20 mm, 30 mm, 40 mm and 50 mm. At the center of each specimen, a reference bar was placed. Each reinforcing bar was electrically connected with the reference bar by using lead wires and a 100 Ω resistor as shown in Fig 3.3.

In addition, some concrete specimens were designed with 10 mm of concrete cover thickness because rate of carbonation was expected to be slow. Size of concrete specimen is similar with specimen exposed to testing chloride environment. Figure 3.4 shows schematic illustration of specimen exposed to carbonation for 10 mm of cover thickness.

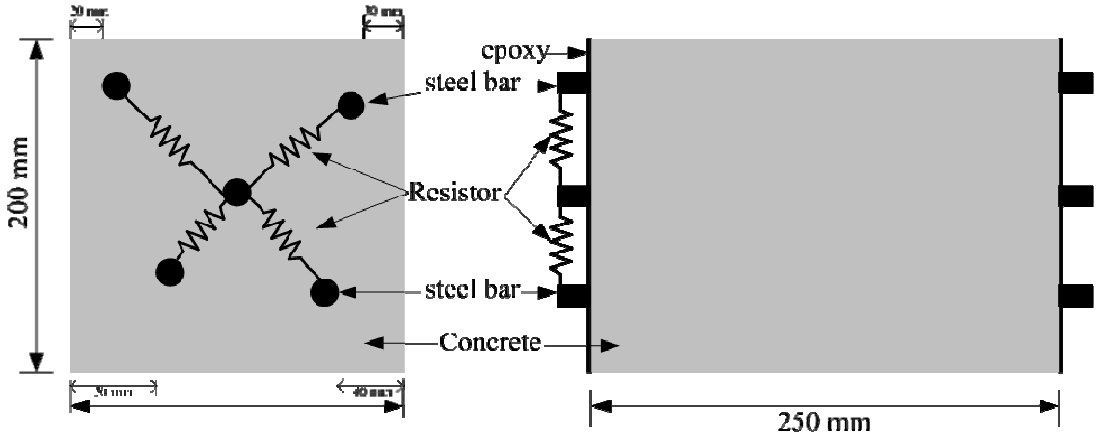

Figure 3.3 Schematic illustration of specimen with 20, 30, 40, and 50 mm steel covering thickness exposed to carbonation

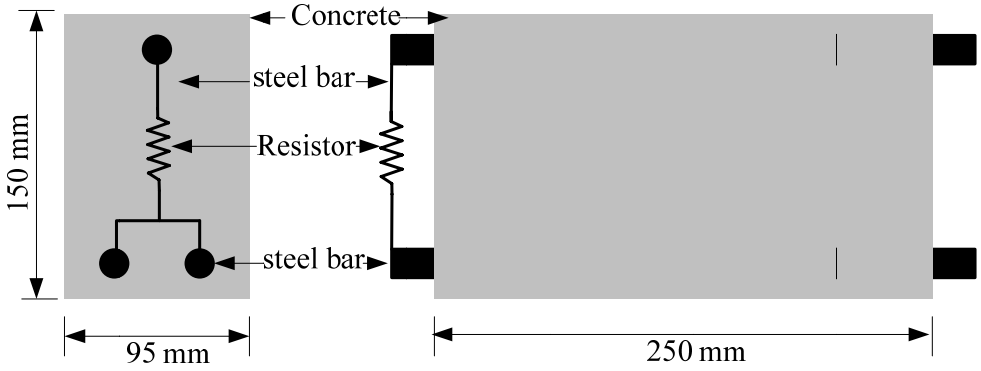

Figure 3.4 Schematic illustration of specimen with 10 mm steel covering thickness exposed to carbonation

3.4.4 Specimen for combined CO_2 and Cl^- environment

Concrete specimen for combinned CO_2 and Cl^- environment is shown in Fig 3.5. Concrete specimen exposing to both carbon dioxide and chloride was designed to be similar to the specimen for carbonation. But the only dissimilarity is the existence of plastic dam with the dimension of 150 mm × 65 mm that was placed on the top of the specimen.

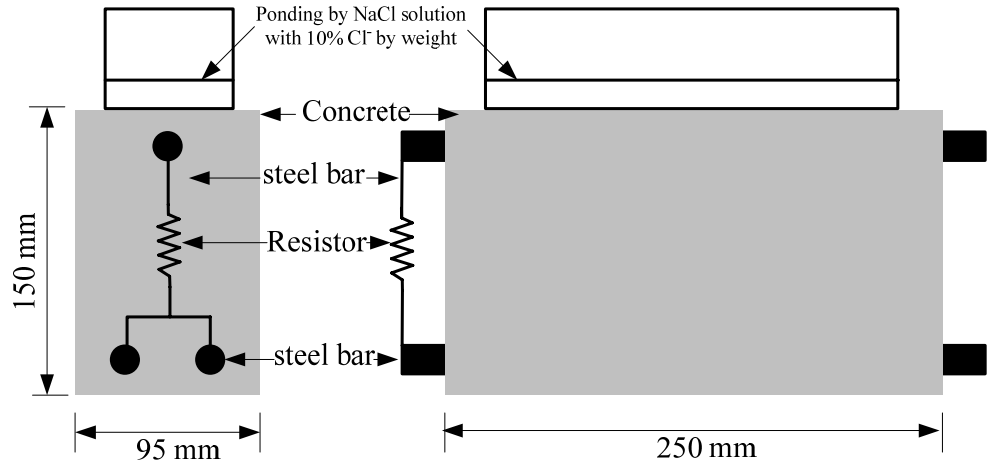

Figure 3.5 Schematic illustration of specimen with 10 mm concrete cover for combined carbonation and chloride exposure.

3.5 Exposure conditions

All specimens for testing HCP and i_{corr} in all exposure condition were demolded 24 hours after casting and were cured by covering with wet clothes for another 27 days in the laboratory atmosphere. After removing the specimens from the curing room, they were immediately exposed to the test conditions. Three major categories of exposure conditions are classified as individually ponding with solution, individually exposed to carbonation and combined cyclic exposure between ponding with chloride solution and exposure to carbonation.

(1) In case of carbon dioxide, specimens were exposed in a carbonation chamber in which the conditions were controlled at 4 % carbon dioxide concentration, 40 ^{o}C, and 55±5% RH. Figure 3.6(a) shows arrangement of specimens exposed to accelerated carbonation condition in the carbonation chamber.

(2) In case of chloride attacks, these groups of specimens were continuously ponded with solution that has concentrations of chloride of 10% NaCl by weight. This solution was used as the continuous ponding solution above the top surface of every specimen. Normal air condition was controlled at 30^{o}C and 55±5% RH. Please be noted that chloride concentration of normal sea water in Thailand is approximately 3% NaCl by weight. Figure 3.4(b) shows condition of specimens exposed to chloride solution

(3) In case of combined cyclic exposure between ponding with Cl^- solution and exposing to carbonation. Specimens were firstly placed in carbonation chamber for 4 days, and then ponded with chloride solution for 3 days to complete one cycle.


(a) Specimens in carbonation chamber (b) Ponding with chloride solution

Figure 3.6 Exposure conditions

3.6 Methods of testing

3.6.1 Compressive Strength

In this study, the cylinder specimens with the size of ϕ100x200 mm were used for testing compressive strength. This test conforms to ASTM C39/C39M-99 (Standard Test Method for Compressive Strength of Cylindrical Concrete Specimens). After the specimens were cured for a period of 7, 14, 28 and 91 days, they were tested for compressive strength. Three specimens were used for each mixture and the result was the average of the two measured values.

3.6.2 Carbonation Tests

The rate of carbonation in real environment is usually slow due to low CO_2 concentration in the environment. Accelerated carbonation test was conducted. Concrete cube specimens with the size of 100×100×100 mm were used in the accelerated carbonation test. The concrete specimens for testing carbonation depth were demolded 24 hours after casting and were water-cured for 27 days before being carbonated in the accelerated carbonation chamber invented in this study for a period of 4, 8 and 12 weeks. The temperature and relative humidity in the carbonation chamber were controlled at 40°C and 55 ± 5 %, respectively. The carbon dioxide concentration was 4% (40,000 ppm). The carbonation chamber used in this study is shown in Fig 3.7.

At the age of measurement as shown in Fig 3.8, specimens were tested for carbonation depth in the laboratory. The specimens were split and cleaned. The depths of carbonation were determined by spraying on a freshly broken surface with 1% of phenolphthalein in the solution of 70% ethyl alcohol (RILEM, 1988). The phenolphthalein solution is colorless and used as an acid-base indicator. The color of the solution changes into purple when pH is higher than the range of approximately nine. Therefore, when the solution is sprayed on a broken concrete surface, the carbonated portion is uncolored (concrete color) and non-carbonated portion is purple. The depth of carbonation is defined as the thickness of the uncolored carbonated portion. The average depths from 8 points of carbonation were measured and reported.

Figure 3.7 Carbonation chamber for carbonation depth test

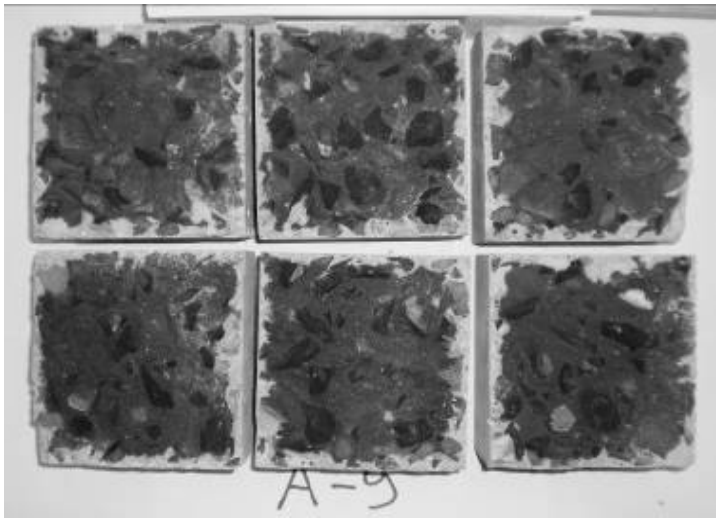

Figure 3.8 Broken surfaces of specimens after spraying with phenolphthalein

3.6.3 Determination of chloride content

Total chloride contents in concrete were determined according to ASTM C1152 after the specimens has been ponded. Five grams of powdered concrete at the surface of reinforcing bar was collected. Then, the sample of powdered concrete was dissolved in HNO_3 (nitric acid) solution, and automatically titrated against N/20 $AgNO_3$ (silver nitrate) solution as shown in Fig 3.9. Total chloride content was calculated as percentage of chloride ion by weight of the powder sample.

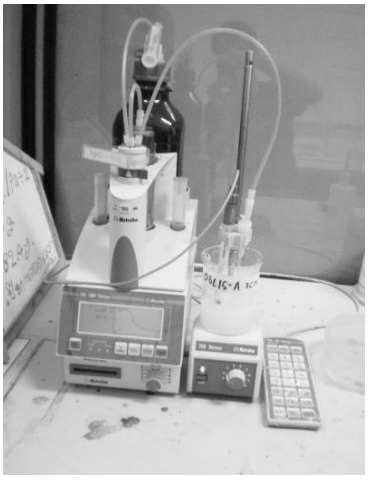

Figure 3.9 Chloride measurements (Potensiometric titration)

Figure 3.10 Half-cell potential instruments

3.6.4 Half-cell potential measurement

The corrosion potential of reinforcing steel was measured by means of HCP measurement. The HCP value indicates the probability of corrosion activity of the reinforcing steel located beneath the half cell, as described by ASTM C 876. The setup basically consists of an external copper/copper sulfate ($Cu/CuSO_4$) electrode (half cell), connecting wires and a high impedance voltmeter. The half-cell potential measurement has been widely used in the field due to its simplicity. General agreement among researchers have been reached that it effectively indicates the probability of active corrosion along the steel reinforcement in concrete. In case of chloride exposure, specimens were air-dried for 1 hour before the HCP measurement. In case of carbonation, specimens were wetted by covering with wet clothes for 12 hours to increase the moisture in concrete because environment in carbonation chamber was very dry. Measurement was conducted on the top surface at every 20 mm along the direction of top reinforcing bar. HCP was measured every day in case of chloride exposure and every week for carbon dioxide exposure.

3.6.5 Corrosion current density measurement

Actually, corrosion will be firstly initiated as micro-cell corrosion between anode and cathode within the top reinforcing bar. However, measurement of micro-cell corrosion current is very difficult. In this study, only macro-cell corrosion current was measured. Macrocell corrosion current was a good indicator of corrosion initiation of the reinforcing steel. Corrosion current (I) was measured indirectly as a voltage drop across the 100 Ω resistor connected externally between the top and bottom reinforcing bars as shown in Figure 3.11. The corrosion current is calculated based on Ohm's law as shown in Eq (1).

$$V = IR \tag{3.1}$$

where V is the voltage drop across the resistor (μV), I is the current due to corrosion (μA), R is a resistor (100Ω in this study). Voltmeter is a high impedance type with a resolution of 0.01 mV as recommended by ASTM G109. Then, corrosion current density (i_{corr}) was calculated as shown in Eq (2).

$$i_{corr} = \frac{I}{A} \tag{3.2}$$

where i_{corr} is the corrosion current density (μA/cm^2), and A is the surface area of exposed reinforcing steel. In this study, exposed steel has the surface area of 79.168 cm^2 (surface area of the center portion without epoxy coat).

Figure 3.11 Schematic illustrations were testing the voltage.

3.7 On site half-cell potential measurement of reinforced concrete structures

This section describes an experimental investigation on a reinforced concrete to compare half-cell potential measurement carried out from wetting condition to those obtained from drying condition. Three measured building locations, all reinforced concrete

wall members, were investigated. First location (SD2-R) is a part of concrete wall which was repaired by concrete. Second location (SD2-C) is the existing unrepaired wall (same as that of the first location but without repair). Final location (SP3-L) is a newly built concrete wall. Three walls are located 12 km from sea. The three measured walls are shown in Figs 4.12 and 4.13

Half-cell potential values, concrete cover thickness and chloride content were determined to indicate states of corrosion. Covering meter was used to determine concrete cover thickness and locations of steel bars inside the concrete. Half-cell potential testing (HCP) was used to determine the corrosion activity of steel bars. However, HCP testing was conducted after wetting for 12 hours and 1 hour (duration of wetting was a test parameter). In addition, reinforced concrete wall members were drilled by a drill gimlet. The depth of drilling to take concrete powder samples for chloride content analysis is every 10 mm up to 50 mm from the exposed surface.

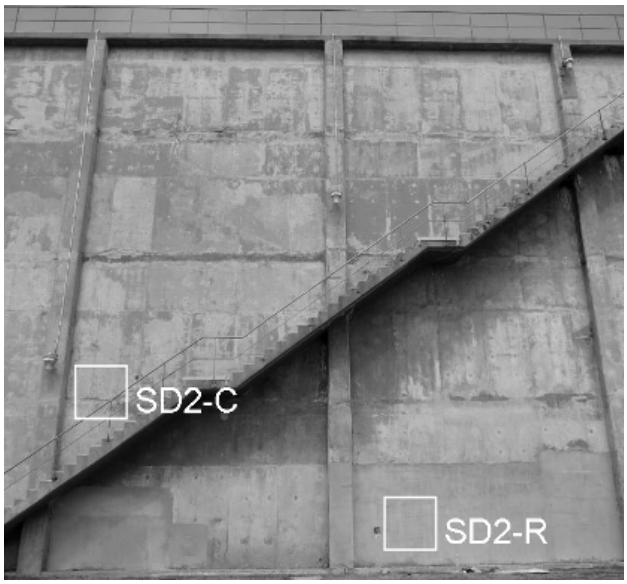

Figure 3.12 Locations of SD2-C and SD2-R

Figure 3.13 Locations of SP3-L

Chapter 4

Results and discussions

4.1 General

This chapter presented the results and discussions of mechanical properties of concrete specimens and corrosion activities of concrete specimens, which were exposed to three environments. Compressive strength development of concrete with varied ratios of cement, fly ash and limestone powder is presented in section 4.2. The corrosion activity of concrete specimens which were exposed to carbon dioxide environment is presented in section 4.3. The corrosion activity of concrete specimens exposed to chloride environment is presented in section 4.4 and 4.5. Section 4.6 presents results and discussions on the corrosion activity of concrete specimens exposed to combined cyclic environment. In addition an example of, the inspection results of actual reinforced concrete structures are also presented in the last section. The results and discussions are presented in the following sections.

4.2 Compressive strength development

4.2.1 Effect of replacement ratio of fly ash on compressive strength

The compressive strength of each mixture was determined. Figure 4.1 shows the compressive strength of concrete specimens with varied w/b ratios and percentages of fly ash (FA) replacement. As expected, the compressive strength of all concrete specimens increases with the time of curing. In addition, generally, when percentage of FA was increased, compressive strength of concrete specimens decreased. For instance, Figure 4.1(a) shows the results of compressive strength of concrete specimens with w/b=0.4 with varied percentages of FA. Concrete specimens with 0.4FA50, 0.4FA30 and 0.4FA20 showed lower compressive strength than that of 0.4OPC. Figure 4.1(b) and Figure 4.1(c) for concrete specimens with w/b=0.5 and w/b=0.6, respectively, also show similar tendency with those in Fig. 4.1(a) for w/b=0.4.

4.2.2 Effect of replacement ratio of limestone powder on compressive strength

The compressive strength at 7, 14, 28 and 91 days of limestone powder (LP) concrete are presented in Fig. 4.2. It was found that at optimum content of LP, compressive strength of concrete increased. Figure 4.2(a) presented compressive strength of concrete with w/b=0.4. It was discovered that, in 7, 14 and 28 days, 0.4LP5 has higher compressive strength than 0.4OPC. However, at 91 days compressive strength of 0.4LP5 was lower than that of 0.4OPC. Therefore, LP had adverse effect on compressive strength of concrete if high replacement was added in the concrete especially with high w/b ratio. This result can be seen in Fig. 4.2(b) and Fig. 4.2(c) which show that OPC tends to had higher compressive strength than 5%, 10%, and 15% of LP replacements. So, at high w/b ratios,

concrete tends to more severely encounter the problem of strength drop when incorporating high LP content.

In this study, the use of FA and LP in concrete has effect on the compressive strength. The result of compressive strength of concrete with combined FA (20%) and LP (10%) are shown in Fig. 4.2(a). The 0.4L10F20 had lower compressive strength than 0.4OPC, 0.4LP5, 0.4LP10 and 0.4LP15.

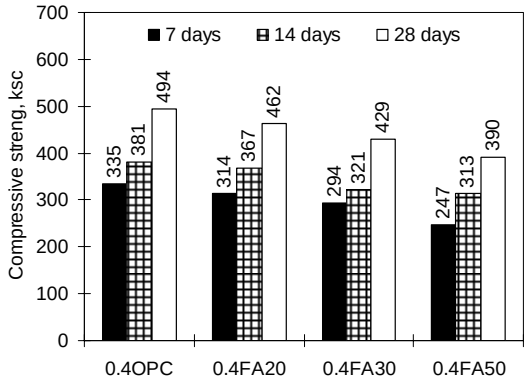

(a) w/b=0.4

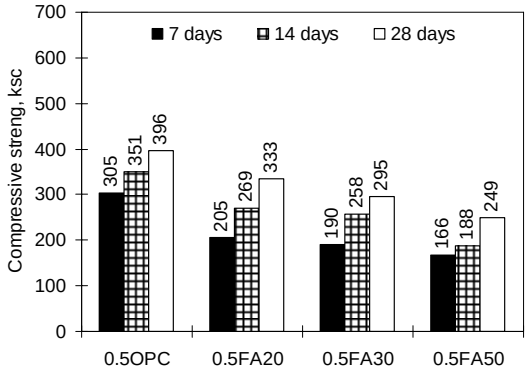

(b) w/b=0.5

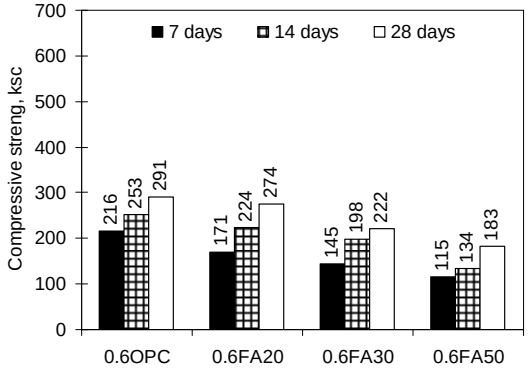

(c) w/b=0.6

Figure 4.1 Compressive strengths of FA concrete at different ages.

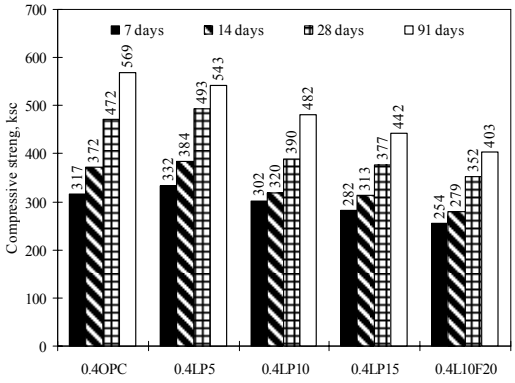

(a) w/b=0.4

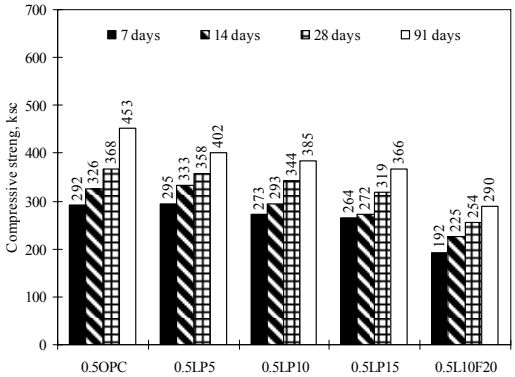

(b) w/b=0.5

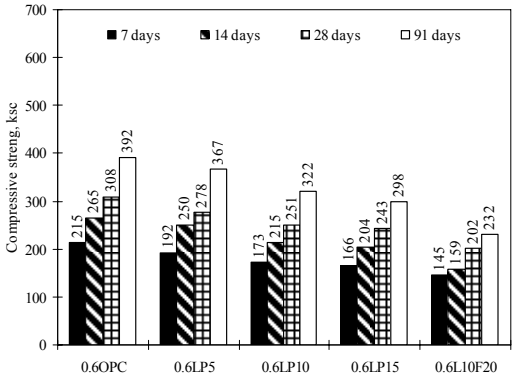

(c) w/b=0.6

Figure 4.2 Compressive strengths of LP concrete at different ages.

4.3 Corrosion activity of concrete specimens exposed to carbon dioxide environment

Concrete specimens were prepared by varying mix proportions, concrete cover thickness and then exposed to carbon dioxide environment. The corrosion activities of concrete specimens were monitored by half-cell potential measurement, corrosion current density method and carbonation depth measurement. The results and discussions are presented in the following sections.

4.3.1 Carbonation depth

Carbonation depth of specimens measured by spraying phenolphthalein solution on freshly broken surface of specimens after exposure are presented and discussed. Unchanged color zone shows carbonated portion of concrete, while purple portion shows non-carbonated zone. Carbonation depths were measured at three different points from four exposed surfaces. The average values were determined and presented separately.

Specimens were mixed with four different fly ash replacement percentages 0%, 10%, 20% and 50% in order to see the effect of replacing amount of FA on rate of carbonation. Examples of results of carbonation depth of specimens with different FA replacement ratios are shown in Fig. 4.3(a), 4.3(b) and 4.3(c) for w/b equal to 0.4, 0.5 and 0.6 respectively. The three figures show that concrete with 20% and 50% FA replacement ratios have larger carbonation depth than 0% FA replacement. In other words, order of resistance against carbonation is 0%>20%>50%. Because a produced amount of $Ca(OH)_2$ (calcium hydroxide) by cement hydration of FA concrete is less than that of OPC concrete. FA also consumes $Ca(OH)_2$ for its pozzolanic reaction (Jibodee et al., 2005). Therefore, rate of carbonation of FA concrete is faster than that of OPC concrete.

The effect of water to binder ratio (w/b) on the carbonation depth is also presented in Fig. 4.3. It is shown that for a given FA content, a lower w/b leads to a lower carbonation depth. This is due to denser pore structure. This is in agreement with Jibodee et al. (2005) and many other researchers (Balayssaca, 1992; Cahyadi, 1993 and Chi, 2002) that a lower w/b led to lower porosity of mixture.

In addition, many researchers recommended that, if carbonated front extended near surface of steel bar, corrosion of reinforcing steel started. From these criteria, if carbonation front extended deeper than the concrete cover thickness (10 mm), reinforcing steel at the top bar would start to corrode. Then, concrete specimens with w/b of 0.6, and 50%, 20% and 0% of fly ash replacement ratios corroded on 5, 11 and 44 days, respectively (see Fig. 4.3c). The corrosion time of other specimens are shown in Table 4.1.

Table 4.1 Corrosion starting time of concrete specimens in case of carbonation, days

Binder	w/b=0.4	w/b=0.5	w/b=0.6
OPC	74	67	44
FA20	41	12	11
FA50	24	9	5

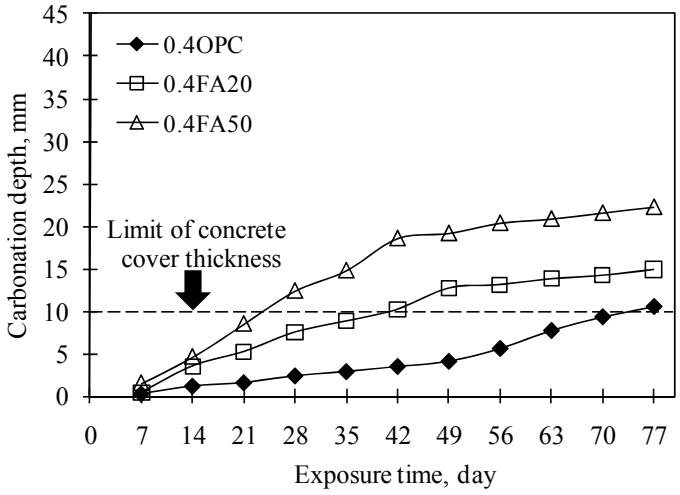

(a) w/b = 0.4

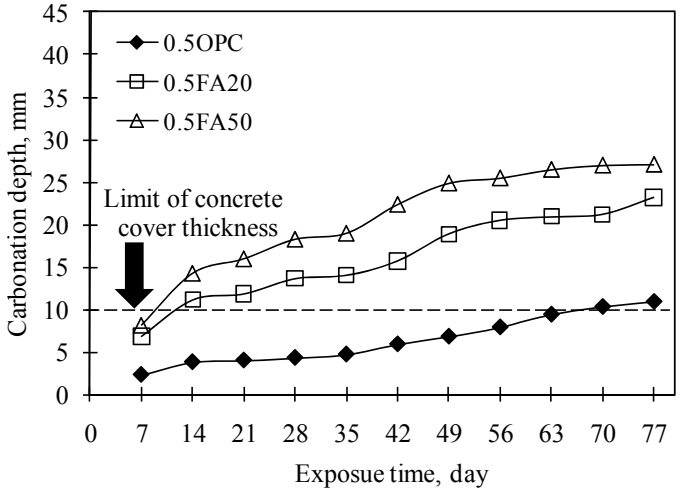

(b) w/b = 0.5

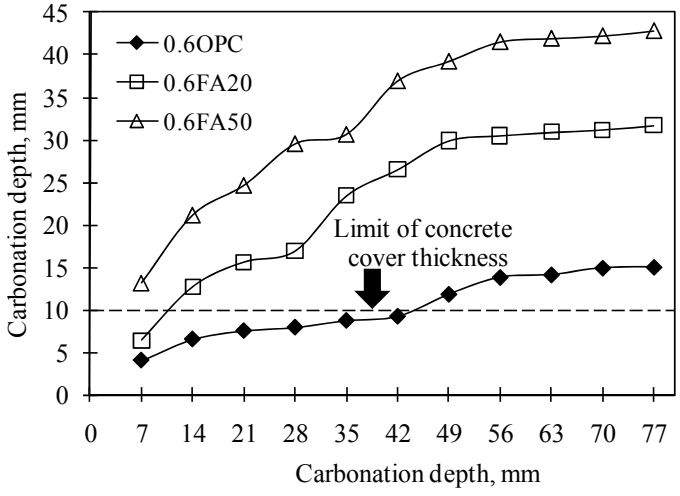

(c) w/b = 0.6

Figure 4.3 Carbonation depths of concrete specimens

4.3.2 Half-cell potential measurement (carbonation specimens)

After 77 days of exposure to carbonation all concrete specimens were monitored by using the half-cell potential method to determine the corrosion initiation time. The results of half-cell potential measurement were obtained every 7 days. Figure 4.4 shows the half-cell potential values of concrete specimens having 10 mm covering. Figure 4.4(c) shows that half-cell potential values of all specimens with w/b=0.6 showed not different values at 0 day of exposure. After that, half-cell potential showed values ranging from -50 to -200 mV when time of exposure increased. At 7 days of exposure, specimens 0.6FA50 shown higher negative potential values than specimens 0.6FA20 and 0.6OPC. But the specimens 0.6OPC showed higher negative potential value than 0.6FA20. After 7 days of exposure, half-cell potential of all specimens showed stable values when exposure times increased. In the same way, concrete specimens with w/b=0.5 (Fig 4.4(b)) had similar tendency of HCP value with w/b=0.6 (Fig 4.4(c)). However, both w/b=0.5 and w/b=0.6 was differently trended with w/b=0.4 (Fig 4.4(a). Fig 4.4(a) shows constant value of HCP reading. This indicated no severe corrosion of the reinforcing steel when the numerical criteria of ASTM C876 were used.

4.3.3 Corrosion current measurement (carbonation specimens)

Macro-cell corrosion current was measured and then converted to corrosion current density for monitoring corrosion activities. Figure 4.5 shows the results of corrosion current density under exposure to carbon dioxide. From Fig. 4.5(c), it was observed that at 0 days of exposure no current flowed between top bar and bottom bars in all specimens. After 7 days of exposure, 0.6FA50 showed high corrosion current density of 0.05 $\mu A/cm^2$. But the 0.6FA20 and 0.6OPC still showed unchanged of corrosion current density values. After 14 days of exposure, corrosion current density of 0.6FA20 was higher than that 0.6OPC. After that, 0.6OPC started to show rising values at exposure time of 49 days. The i_{corr} values in case of carbonation show only small jump in all specimens. This is because, the corrosion of steel bars in concrete due to carbonation is micro-cell corrosion (uniform corrosion). The ratio between area of anode and cathode are equal and also very small. The criteria for determining corrosion starting time in case of carbonation are therefore the jumping of i_{corr} value. The results of corrosion starting time get along well with results of carbonation depth in Table 4.1. At the end of the exposure period, the jumping of corrosion current density for different specimens started by the order: 50% before 20% before 0%.

From the presented results, it was observed that half-cell potential was not good for being used to detect corrosion in case of carbonation. This is because the half-cell potential values did not change even carbonation front had already reached the steel. From Fig. 4.3(c), at 7 days of exposure, specimens with water to binder ratio of 0.6 and 50% fly ash replacement showed larger carbonation depths when compared to the thickness of concrete cover (10 mm). At the same time, half-cell potential only indicated the value of -156 mV as seen in Figure 4.5(c). After that, half-cell potential showed rather constant values. This indicated that the reinforcing steel was already ready to start corrosion by carbonation when refer to depth of carbonation. However, half-cell potential value still showed passive condition when referring to ASTM C876.

In addition, half-cell potential and corrosion current density showed different tendencies. When carbonated front extended to reach the reinforcing steel, corrosion current density showed value increase. After that, corrosion current density continuously

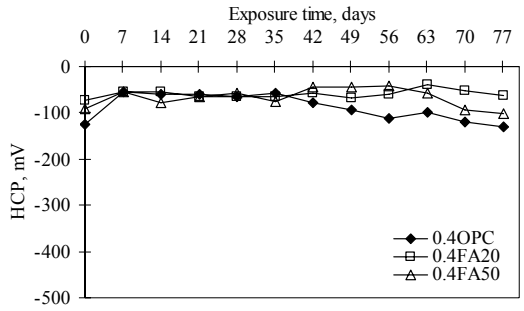

(a) w/b=0.4

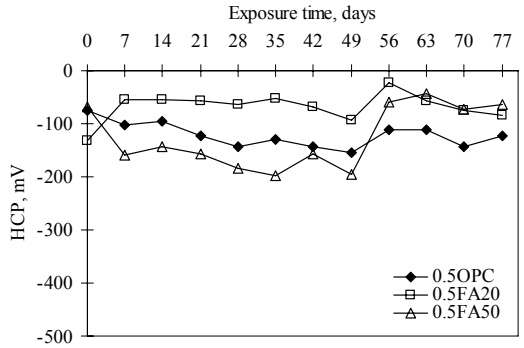

(b) w/b=0.5

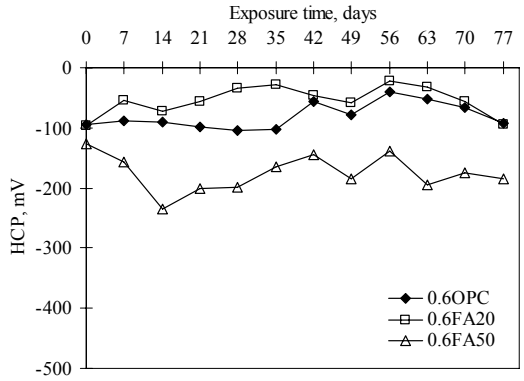

(c) w/b=0.6

Figure 4.4 Half-cell potential value of concrete exposed to CO_2

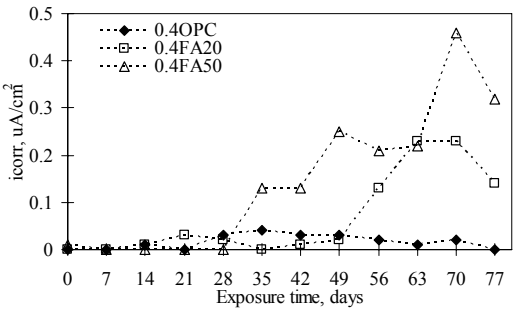

(a) w/b=0.4

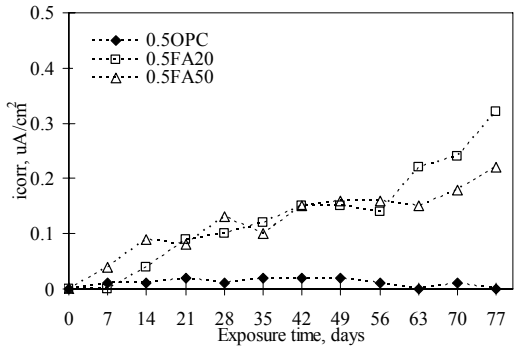

(b) w/b=0.5

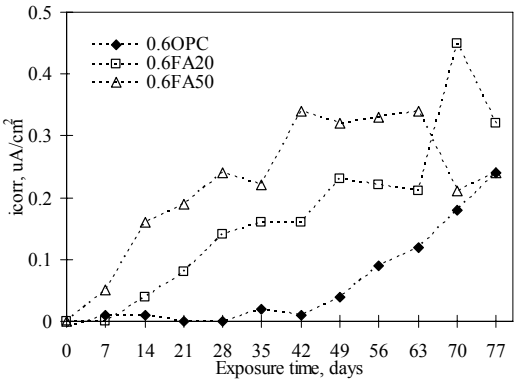

(c) w/b=0.6

Figure 4.5 Corrosion current density of concrete exposed to CO_2

increased when exposure time increased. Nevertheless, half-cell potential showed constant value when carbonated front extended to reach the reinforcing steel. The measured half-cell potential is likely to be affected by the high resistivity and lower porosity of the carbonated concrete.

4.4 Corrosion activity of fly ash concrete specimens exposed to chloride environment

The corrosion activity of laboratory concrete specimens which has been exposed to chloride environment is presented in this section. Concrete specimens were marked with different mix proportions and different concrete cover thickness. The details of mix proportions are shown in Table 3.2. The curing period of fly ash concrete specimens was 28 days. After that, 10% NaCl solution was used as the ponding solution at the top surface of the specimens. The details of specimens are shown in Fig. 3.2. The corrosion activities

of concrete specimens are monitored by measuring half-cell potential (HCP) and corrosion current density (i_{corr}). In addition, total chloride content was also measured for being compared with the HCP and i_{corr} values. All of the results are presented in the following sections.

4.4.1 Half-cell potential measurement (chloride specimens)

After 28 days of curing and then start exposure to chloride on the 29th days, half-cell potential (HCP) was measured every day. The HCP results of specimens with 30 mm of covering thickness are demonstrated in Fig. 4.6. In the same way, the HCP results of specimens with 50 mm of cover thickness are demonstrated in Fig. 4.7. From both Fig.4.6 and Fig. 4.7, the HCP showed constant value at early period. After that, HCP values immediately decreased depending on concrete mix proportions and concrete covering thickness. This phenomenon was explained using Fig. 4.6(a) as an example. Specimen 0.4FA50 showed stable HCP value during the first 14 days of exposure. After that, it changed to more negative values at the 15th days and then remain rather constant until 68 days (end of test). Other mix proportions also showed similar tendency when compared with 0.4FA50 except that the day the HCP values started to drop were different. The summary of the time the HCP value started to decrease for each mix proportion is presented in Table 4.2. In addition, at the end of testing (68days), HCP value of all concrete specimen had more negative than -350 mV, which identifies that steel bars in concrete had probability 90% corrosion (refer to ASTM C876). As expected, time of HCP value dropping is different when concrete cover thickness of concrete specimen increased. Large concrete cover thickness had longer time until HCP value dropped. For Fig. 4.6(a) and 4.7(a), HCP value of 0.4FA50 with 30 mm concrete cover thickness at 21 days was -543 mV but the HCP value at 21 days of exposure of 0.4FA50 with 50 mm concrete cover thickness was only -320 mV. However, at the long time of exposure (after HCP immediately decreased), both cases of 30 mm and 50 mm concrete cover thickness had similar HCP values. Taweechai (2007) reported that fly ash could improve resistance against chloride ion penetration. The reasons are because pozzolanic reaction of fly ash causes denser pore structure in concrete and provides higher chloride binding capacity when compared to mixture with cement only. However, the HCP results obtained in this study showed the opposite trend. The reasons are explained in the following paragraph. At the end of exposure (62 days), Table 4.2, the HCP values of all concrete specimens are more negative than -350 mV. For example, the HCP values of 0.5OPC, 0.5FA20, 0.5FA30 and 0.5FA50 are -509, -564, -487 and -673 mV, respectively. These results illustrate that, the concrete specimens with high FA replacement (FA50) show more negative value of HCP than FA30, FA20 and OPC concrete at the end of exposure. It can be explained that FA50 concrete had more moisture than OPC due to its higher porosity at the tested age and then caused low electrical resistance of the concrete.

Corrosion of specimen with of 50% fly ash replacement was earlier than that of the OPC specimen because the specimen was exposed to chloride at an early age. Pozzolanic reaction of fly ash in the concrete had not much proceeded yet especially when fly ash was used in a large content. So the porosity of the concrete with 50% fly ash replacement could be higher than those of other specimens at the early ages (Maruya et al., 2003; Sumranwanich and Tangtermsirikul, 2004). This explanation is supported by the results of chloride content in Fig. 4.8. As shown in the figure, the total chloride content near the surface of steel in the 50% fly ash replacement specimen after exposure for 36 days is the highest. In case of specimen with 0.6 of w/b ratio and 50% replacement of fly ash, total

chloride content was 0.12% by weight of concrete, which is higher than chloride content threshold to initiate corrosion. The chloride threshold which causes steel corrosion is specified according to EIT 1014 (Standard of Engineering Institute of Thailand) to be 0.4% of total binder which is approximately 0.05% by weight of the tested concrete sample. Chloride content of specimens with 0% fly ash replacement was higher than the chloride threshold but HCP at 36 days as shown in Fig. 4.6(c) still show no corrosion. This may be due to effect of Cl^-/OH^- ratio. In case of OPC concrete, the amount of OH^- is higher than that of the fly ash concrete. When compared to fly ash concrete, the pH of the OPC concrete was higher, it requires higher Cl^- content to depassivate the steel. Then, the steel bar might not yet start to corrode (Thangavel and Rengaswamy, 1998). Therefore, chloride threshold of OPC concrete can be higher than those of fly ash concrete. Future studies are needed to verify the effect of alkalinity on the chloride threshold.

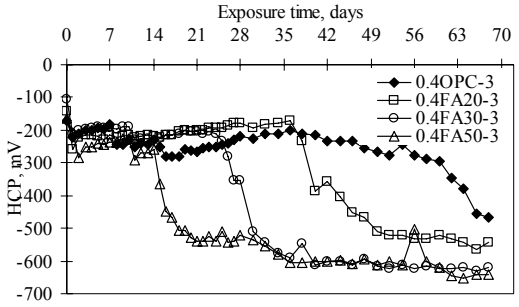

(a) w/b=0.4

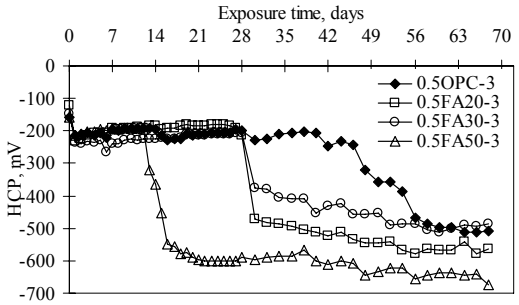

(b) w/b=0.5

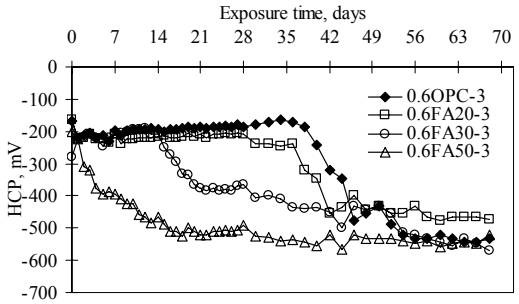

(c) w/b=0.6

Figure 4.6 HCP values of fly ash concrete specimens with 30 mm steel covering depth exposed to chloride environment.

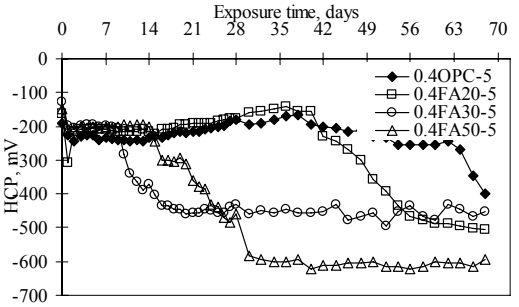

(a) w/b=0.4

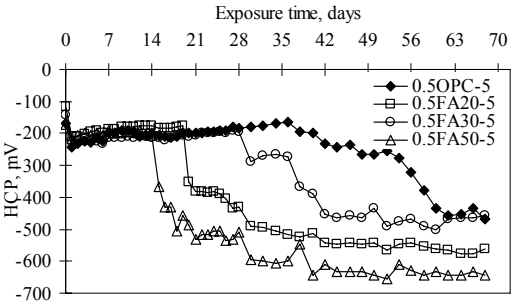

(b) w/b=0.5

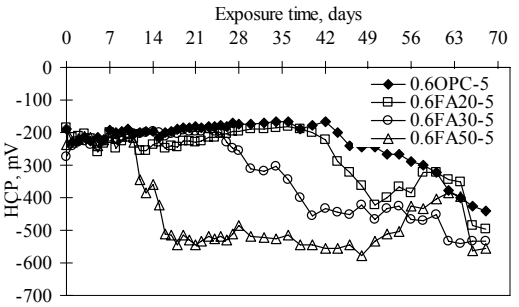

(c) w/b=0.6

Figure 4.7 HCP values of fly ash concrete specimens with 50 mm steel covering depth exposed to chloride environment.

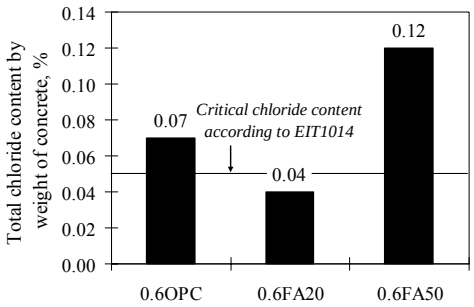

Figure 4.8 Total chloride content at the steel surface of fly ash concrete specimen after exposed to chloride environment for 36 days

Table 4.2 Comparison of corrosion starting times using HCP measurement (for Fly ash concrete specimens exposed to chloride)

	Concrete cover thickness (3 cm)				Concrete cover thickness (5 cm)			
	Initial period (0 day of exposure)	Corrosion starting		End of exposure, 68 days	Initial period (0 day of exposure)	Corrosion starting		End of exposure, 68 days
Name	HCP, mV	Time, day	HCP, mV	HCP, mV	HCP, mV	Time, day	HCP, mV	HCP, mV
0.4OPC	-171	64	-378	-466	-191	68	-398	-398
0.4FA20	-144	40	-387	-543	-163	50	-357	-504
0.4FA30	-106	27	-353	-619	-126	32	-365	-453
0.4FA50	-164	15	-364	-643	-149	21	-360	-593
0.5OPC	-160	50	-358	-509	-170	58	-378	-467
0.5FA20	-122	39	-470	-564	-116	42	-350	-563
0.5FA30	-147	36	-375	-487	-142	38	-367	-456
0.5FA50	-157	14	-365	-673	-174	15	-365	-644
0.6OPC	-166	46	-476	-534	-188	62	-378	-439
0.6FA20	-163	42	-453	-472	-186	48	-362	-498
0.6FA30	-280	20	-365	-568	-275	38	-400	-534
0.6FA50	-202	4	-375	-523	-238	13	-386	-555

Figure 4.9(a) and Figure 4.9(b) demonstrate the effect of w/b ratio on the HCP values in concrete mixes made with OPC and FA50. The HCP values of OPC concrete with w/b=0.6 were more negative than those of w/b=0.5 and 0.4, respectively. In addition, HCP values of each mix proportions with different w/b showed good correlation with severity of rust at steel surface. The severity of rust was investigated by visual inspection. For example, concrete made with w/b=0.6 showed more negative of HCP than concrete made with w/b=0.5 and 0.4, respectively, and the extent of rust was also the most severe in 0.6OPC than in 0.5OPC and 0.4OPC. This may be explained that for concrete specimen made with w/b=0.6, corrosion of steel bars started sooner when compared to the concrete made with w/b=0.5 and 0.4, respectively. So, concrete with w/b=0.6 showed more severe rusting at the steel surface than that of w/b=0.5 and 0.4, respectively. For concrete made with OPC, the effect of w/b ratio may be attributed to increase porosity due to an increase the w/b ratio and reduction in the volume of cement. Increase of porosity can facilitate water penetration, decreasing the electrical resistance of covering concrete. Another reason is that the chloride fixing ability and resistance against chloride penetration are reduced due to lower amount of cement in case of higher w/b ratio. Therefore, chloride content at steel surface of high w/b ratio specimen is higher than that of low w/b ratio at the same time. This summary was supported by visual inspection which showed more severe corrosion in w/b=0.6 than that of w/b=0.4. From the Figure 4.9(b) it was found that for concrete with 50% fly ash replacement, the HCP values showed unclear correlation with severity of rust at steel bars. This because concrete with FA50 has high porosity. It should be noted that higher porosity of FA concrete when compared to OPC concrete is due to the effect of curing method used in this study.

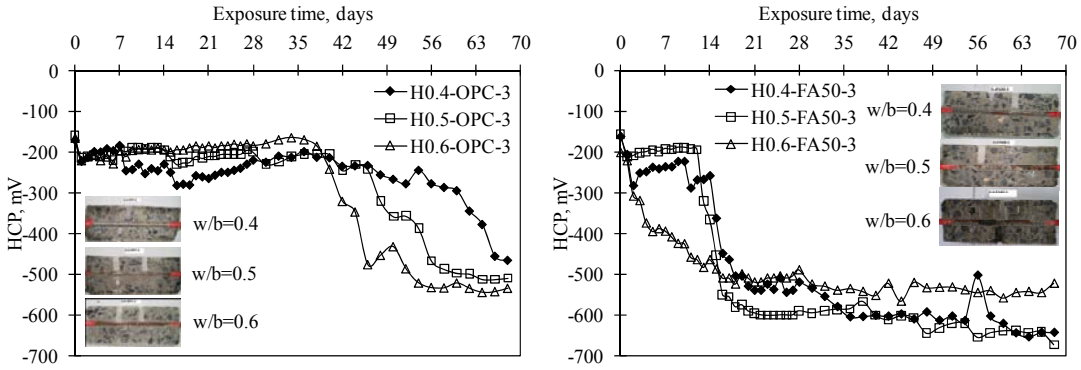

(a) OPC (b) FA50

Figure 4.9 Effects of w/b ratio of concrete specimen with 3 cm of covering depth on HCP values

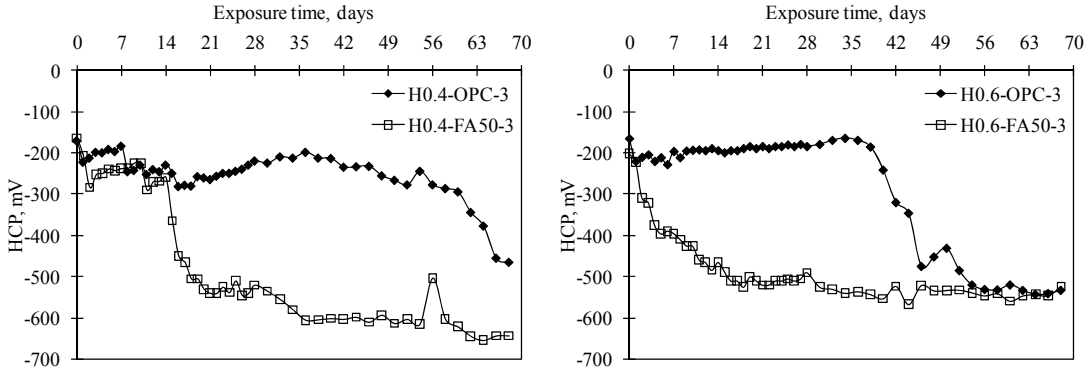

(a) w/b=0.4 (b) w/b=0.6

Figure 4.10 Effects of FA replacement of concrete specimen with 3 cm of covering depth on HCP values

Figure 4.10 shows the effect of FA replacement ratio on HCP values. The HCP value of 0.4FA50 (Fig. 4.10 (a)) showed more negative values than 0.4OPC. However, for w/b=0.6(Fig. 4.10b), the HCP values of concrete mix 0.6FA50 showed same HCP value to 0.6OPC. This means that, an increasing of FA replacement may influence HCP values only for concrete made with low w/b ratio. A decreasing to more negative values of concrete made with high volume of FA content may be attributed to increase porosity which has been explained previously. In case of high w/b ratio specimen, the effect of increasing of porosity due to FA replacement is not clearly seen. This is because the OPC concrete with high w/b ratio also has high porosity. According to these results, influence of FA replacement ratio on HCP measurement should be studied more in the future.

4.4.2 Corrosion current density (chloride specimens)

It is well known that corrosion current measurement (i_{corr}) according to ASTM G109 can be used to investigate corrosion initiation of steel effectively but it is difficult to be used in the field. In contrast, half-cell potential measurement (HCP) is popular for the field measurement. However, there are many parameters which affect HCP reading according to ASTM C876. In this study, the results of HCP values were compared with i_{corr} values. The corrosion current density can be used to identify steel corrosion from the increasing of current flowing between anode (top bar) and cathode (bottom bars). Figure 4.11 and Figure 4.12 demonstrate the i_{corr} values of the specimens with 30 mm and 50 mm

concrete cover thicknesses which were exposed to chloride environment. Rilem TC 154-EMC (2004) recommends that, if corrosion current density value is higher than 0.2 $\mu A/cm^2$ (chloride environment), corrosion of reinforcing steel is regarded to be started. From these criteria when i_{corr} of each specimen is higher than 0.2 $\mu A/cm^2$, the top bar will be considered corroded. Figure 4.11(c) shows the results of concrete with w/b=0.6. It was found that i_{corr} of 0.6FA50 increased to 0.20 $\mu A/cm^2$ at the end of 6 days. In the case of 0.6FA30, i_{corr} increased to 0.21 $\mu A/cm^2$ at the end of 18 days and for 0.6FA20, i_{corr} increased to 0.9 $\mu A/cm^2$ at the end of 38 days. Whereas in the case of 0.6OPC i_{corr} increased to 0.6 $\mu A/cm^2$ at the end of 45 days. These results had similar tendencies with the results of HCP which showed corrosion starting time in the order of 0.6FA50, 0.6FA30, 0.6FA20, and 0.6OPC, respectively. Figures 4.11(a) and 4.11(b) show i_{corr} of concrete specimens with w/b=0.4 and 0.5, respectively. Both w/b=0.4 and 0.5 showed similar tendency in order of corrosion starting time to w/b=0.6. As expected, corrosion starting time of w/b=0.5 was faster than that of w/b=0.4 because higher w/b ratio caused higher porosity of concrete. Then, chloride ion can easily penetrate to reach the steel bars in case of larger w/b ratio. The summary of starting time of i_{corr} values increasing of each mix proportion is presented in Table 4.3. In additions, it also founded that, i_{corr} values showed fluctuation after steel bars in concrete depassivated already. Because, the electrons moved inconstant current between top bar and bottom bars.

At the time when i_{corr} started to increase, HCP also dropped immediately. For instance, Figure 4.11 and 4.12 show that HCP value of concrete specimen with w/b=0.6 and 30 mm cover thickness suddenly drop at 4 days. At the same time, i_{corr} values softly increase. It means that half-cell potential method is effective for detecting corrosion initiation of steel bars exposure to chloride according to ASTM C876. Moreover, half-cell potential method is better than corrosion current density method for investigation of corrosion starting time in laboratory because the change of HCP values at the corrosion starting time is more obvious when compared to change of i_{corr}. The comparison between corrosion starting times obtained from both techniques is given in Table 4.4.

Table 4.3 Comparison of corrosion starting times using i_{corr} measurement (for fly ash concrete specimens exposed to chloride)

	Concrete cover thickness (3 cm)				Concrete cover thickness (5 cm)			
	Initial period (0 day of exposure)	Corrosion starting		End of exposure, 68 days	Initial period (0 day of exposure)	Corrosion starting		End of exposure, 68 days
Name	icorr, $\mu A/cm^2$	Time, day	icorr, $\mu A/cm^2$	icorr, $\mu A/cm^2$	icorr, $\mu A/cm^2$	Time, day	icorr, $\mu A/cm^2$	icorr, $\mu A/cm^2$
0.4OPC	0.01	64	0.45	0.56	0.01	68	0.24	0.24
0.4FA20	0.05	40	0.35	0.22	0.03	50	0.45	0.35
0.4FA30	0.01	27	0.32	0.45	0.00	32	0.60	0.43
0.4FA50	0.04	22	0.21	0.11	0.03	27	0.20	0.22
0.5OPC	0.00	48	0.56	0.35	0.01	56	0.66	0.45
0.5FA20	0.02	42	1.77	0.27	0.04	46	0.89	0.34
0.5FA30	0.04	38	0.57	0.45	0.05	40	0.56	0.34
0.5FA50	0.01	13	0.27	0.44	0.01	17	0.53	0.67
0.6OPC	0.03	44	0.60	0.56	0.03	64	0.78	0.65
0.6FA20	0.04	38	0.90	0.60	0.01	48	0.56	0.11
0.6FA30	0.02	18	0.21	0.21	0.09	38	0.20	0.22
0.6FA50	0.03	6	0.20	0.54	0.01	12	0.26	0.98

Table 4.4 Comparison of corrosion times obtained from HCP and i_{corr} techniques (for fly ash concrete specimens with 3 cm exposed to chloride)

Corrosion starting time, days	w/b=0.4				w/b=0.5				w/b=0.6			
	OPC	FA20	FA30	FA50	OPC	FA20	FA30	FA50	OPC	FA20	FA30	FA50
HCP	64	40	27	15	50	39	36	14	46	42	20	4
icorr	64	40	27	22	48	42	38	13	44	38	18	6

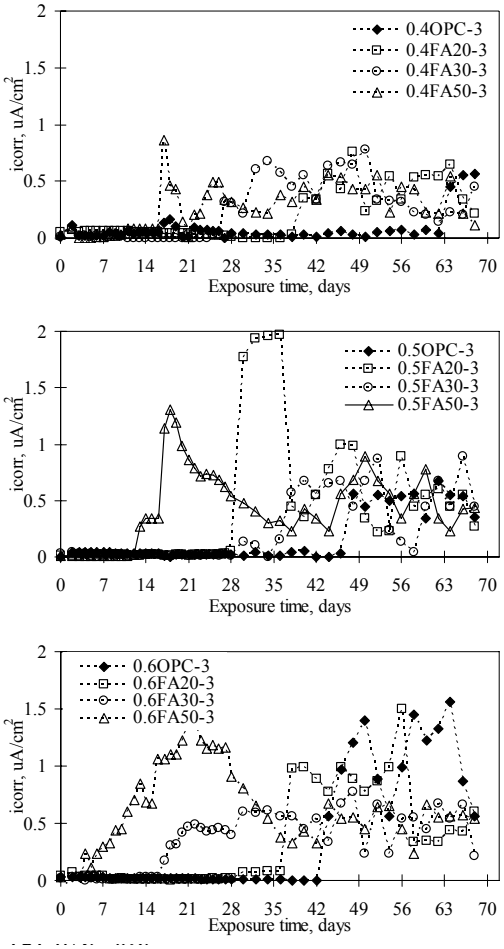

Figure 4.11 Corrosion current density of fly ash concrete with 30 mm steel covering exposure to chloride environment.

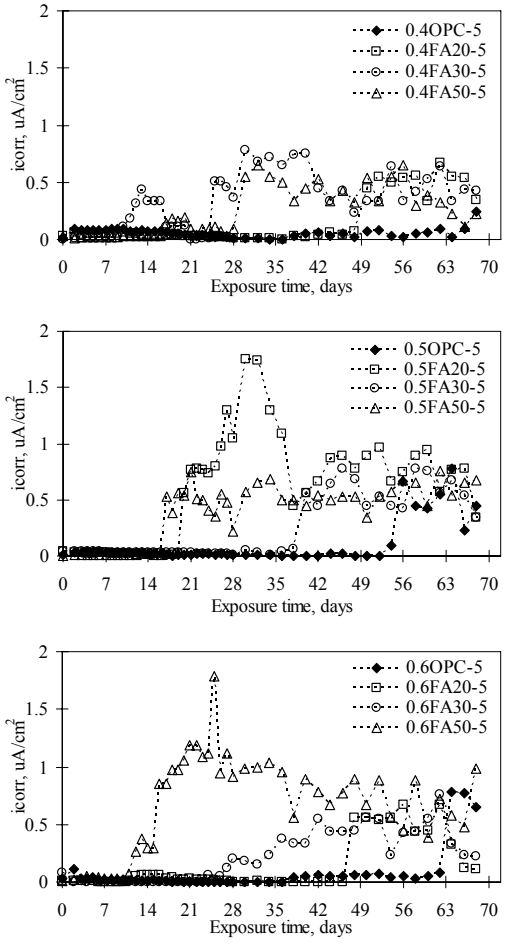

Figure 4.12 Corrosion current density of fly ash concrete with 50 mm steel covering exposure to chloride environment.

4.4.3 Visual inspection (chloride specimens)

Figure 4.13 shows the extent of rust on the steel surface (for specimens with 30 mm of concrete cover thickness) after the end of testing HCP and i_{corr}. Summary photos of rusting are given in Appendix A. The extent of rust was the most severe on the steel surface in 0.6OPC. In addition, 0.6FA50 had higher degree of rusting on the steel surface than 0.6FA30, 0.6FA20 and 0.6OPC, respectively. Similar tendency can be seen for w/b=0.5 and w/b=0.4. If comparing the results of visual inspection with half-cell potential values (Table 4.2) at the end of exposure (68 days), half-cell potential values at the time before breaking specimens showed more negative than -350 mV for all concrete specimens. It indicated that, half-cell potential is useful for monitoring corrosion level of steel bars in the tested concrete.

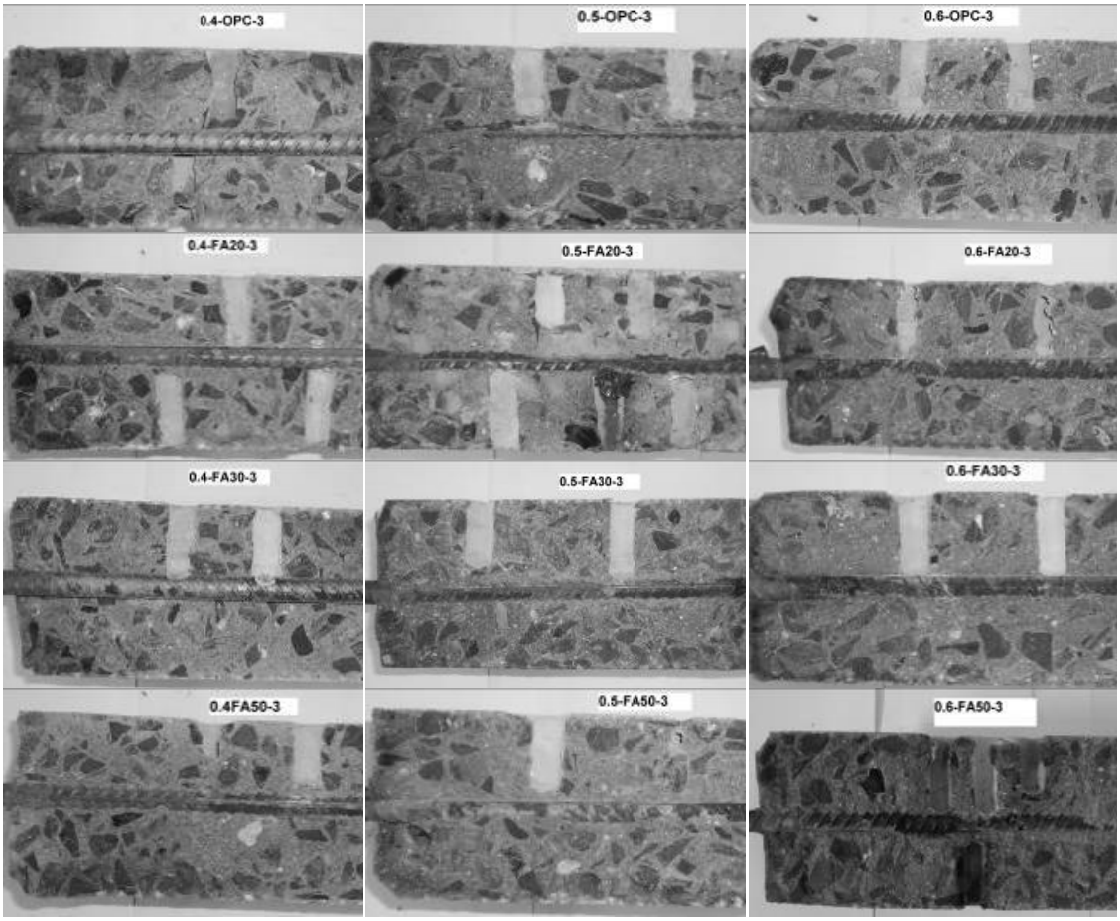

Figure 4.13 Visual examination of rust on rebars in concrete with 30 mm of concrete cover thickness after 68 days of chloride exposure.
(for fly ash concrete specimens exposed to chloride)

4.5 Corrosion activity of limestone powder concrete specimens exposed to chloride environment

Similarly specimens to those of the fly ash concrete specimens were prepared for testing the limestone powder concrete. But curing period of limestone powder concrete specimens was longer (56 days) than that of the fly ash concrete specimens (28 days). The results and discussions of this study are presented in the following section.

4.5.1 Half-cell potential measurement (chloride specimens)

After curing, concrete specimens were exposed to chloride solution. Half-cell potential measurement was used to monitor corrosion of steel bars in concrete. The test results are as given in Figs. 4.14 and 4.15. In concrete with w/b=0.4 (Fig.4.14 (a)), the steel bars of 0.4LP15 concrete showed an initial potential value of -180 mV and became more negative with time. It showed more negative potential than -350 mV at the end of 42 days. In the case of 0.4LP10 concrete, it showed -85 mV initially and decreased to be more negative than -350 mV at the end of 44 days. In case of 0.4L10F20, the initial value was -145 mV and it reached -365 mV at the end of 60 days. In the case of 0.4LP5, it showed -180 mV initially and reached more negative potential than -350 mV at the end of 56 days.

For 0.4OPC, the initial value was -100 mV and reached more negative potential of -356 mV at the end of 70 days. At the end of 92 days (end of testing), the potential values are -458, -489, -544, -463 and -436 mV in 0.4LP15, 0.4LP10, 0.4L10F20, 0.4LP5 and 0.4OPC concrete, respectively. From the results, the effect of LP on HCP values at the end of exposure is still unclear. The corrosion starting time of concrete specimens with 50 mm of concrete cover thickness which shown in Fig 4.15 has similarly tendency when compared to the case of 30 mm of concreter cover thickness. In addition, at the end of testing (92days), HCP value of all concrete specimen had more negative than -350 mV, which identifies that steel bars in concrete had probability 90% corrosion (refer to ASTM C876). The comparisons of corrosion starting times and HCP result at the end testing of all specimens are given in Table 4.5.

Table 4.5 Comparison of corrosion starting times using HCP measurement (for limestone powder concrete specimens exposed to chloride).

	Concrete cover thickness (3 cm)				Concrete cover thickness (5 cm)			
	Initial period (0 day of exposure)	Corrosion starting		End of exposure, 92 days	Initial period (0 day of exposure)	Corrosion starting		End of exposure, 92 days
Name	HCP, mV	Time, day	HCP, mV	HCP, mV	HCP, mV	Time, day	HCP, mV	HCP, mV
0.4OPC	-100	70	-356	-436	-220	84	-432	-452
0.4LP5	-180	56	-354	-436	-205	66	-398	-548
0.4LP10	-85	44	-386	-489	-80	60	-403	-578
0.4LP15	-180	42	-389	-458	-180	56	-399	-458
0.4L10F20	-145	60	-365	-544	-150	80	-468	-453
0.5OPC	-215	62	-365	-478	-135	76	-398	-418
0.5LP5	-150	46	-356	-524	-135	58	-389	-463
0.5LP10	-195	38	-389	-458	-175	52	-405	-458
0.5LP15	-165	30	-389	-523	-110	46	-399	-452
0.5L10F20	-165	40	-359	-425	-130	50	-403	-582
0.6OPC	-120	54	-399	-459	-125	62	-389	-425
0.6LP5	-120	26	-377	-562	-155	38	-396	-425
0.6LP10	-165	14	-355	-582	-140	18	-369	-459
0.6LP15	-90	18	-401	-425	-125	28	-399	-458
0.6L10F20	-130	22	-366	-478	-150	30	-399	-496

Table 4.6 Comparison of corrosion starting times using i_{corr} measurement (for limestone powder concrete specimens exposed to chloride).

	Concrete cover thickness (3 cm)				Concrete cover thickness (5 cm)			
	Initial period (0 day of exposure)	Corrosion starting		End of exposure, 92 days	Initial period (0 day of exposure)	Corrosion starting		End of exposure, 92 days
Name	icorr, $\mu A/cm^2$	Time, day	icorr, $\mu A/cm^2$	icorr, $\mu A/cm^2$	icorr, $\mu A/cm^2$	Time, day	icorr, $\mu A/cm^2$	icorr, $\mu A/cm^2$
0.4OPC	0.01	70	0.23	0.66	0.08	84	0.20	0.68
0.4LP5	0.00	56	0.50	3.85	0.00	66	0.30	0.55
0.4LP10	0.02	44	0.23	1.90	0.00	60	0.30	1.99
0.4LP15	0.00	42	0.23	0.99	0.00	56	0.40	3.99
0.4L10F20	0.00	60	0.60	1.90	0.00	80	0.36	1.26
0.5OPC	0.00	62	0.20	3.46	0.00	76	0.99	2.76
0.5LP5	0.02	46	0.34	1.90	0.00	60	0.90	1.99
0.5LP10	0.00	38	0.35	2.78	0.00	52	0.70	2.45
0.5LP15	0.00	30	0.25	2.65	0.04	46	0.44	0.99
0.5L10F20	0.00	42	0.44	2.10	0.03	50	0.33	2.45
0.6OPC	0.02	54	0.40	0.33	0.00	62	0.30	1.20
0.6LP5	0.00	26	0.36	2.10	0.00	38	0.39	2.85
0.6LP10	0.00	14	0.24	3.69	0.00	18	0.28	0.99
0.6LP15	0.00	18	0.27	3.12	0.00	28	0.31	3.99
0.6L10F20	0.00	22	0.34	2.22	0.00	30	0.45	2.10

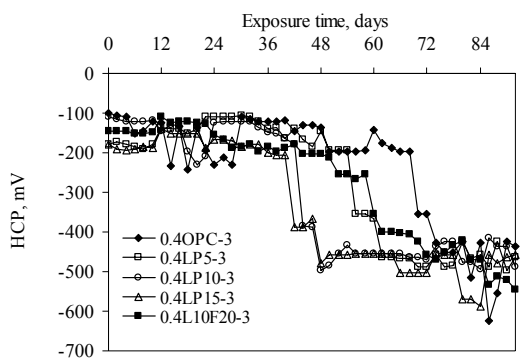

(a) w/b=0.4 and covering 30 mm

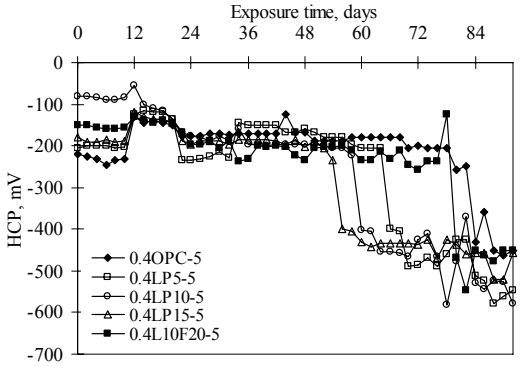

(a) w/b=0.4 and covering 50 mm

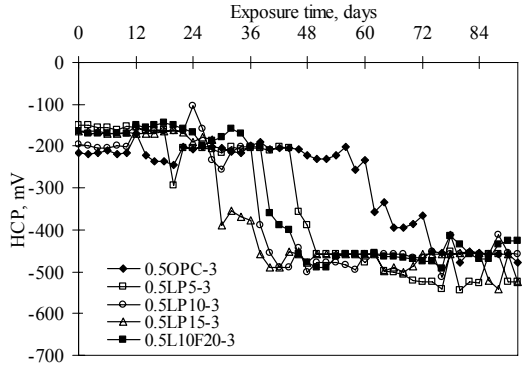

(b) w/b=0.5 and covering 30 mm

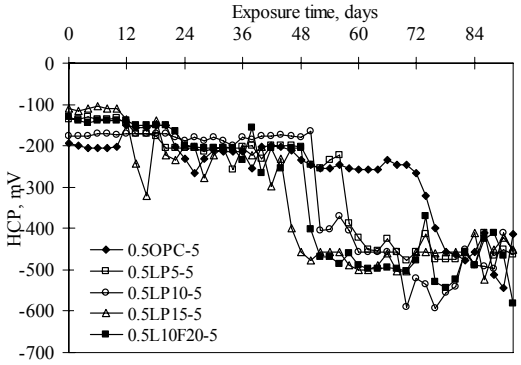

(b) w/b=0.5 and covering 50 mm

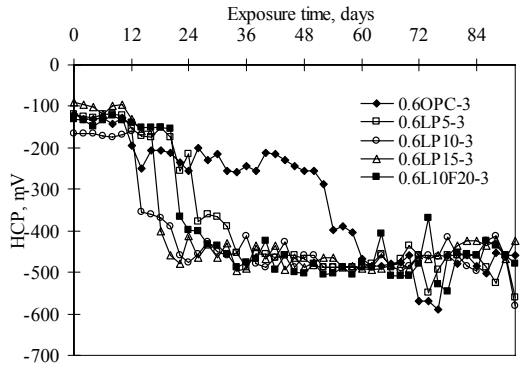

(c) w/b=0.6 and covering 30 mm

Figure 4.14 HCP of limestone powder concrete with 30 mm covering exposed to chloride environment

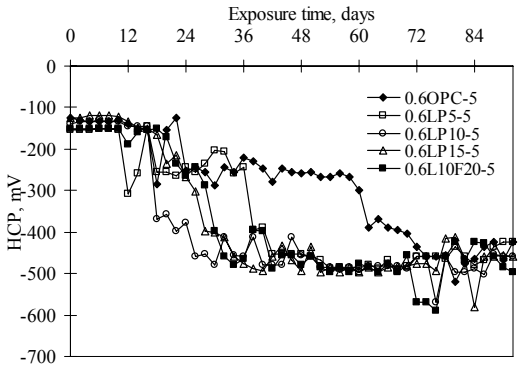

(c) w/b=0.6 and covering 50 mm

Figure 4.15 HCP of limestone powder concrete with 50 mm covering exposed to chloride environment

4.5.2 Corrosion current density (chloride specimens)

It is recommended that corrosion of steel bars in concrete will start when corrosion current density (i_{corr}) is over of 0.2 μA/cm^2 (Rilem TC 154-EMC, 2004). This criterion is applied in this study. In 0.4LP15 concrete with w/b=0.4 (Fig. 4.16(a)), i_{corr} increased to 0.23 μA/cm^2 suddenly at the end of 42 days and after that the i_{corr} show variation until the end of 92 days of exposure. In 0.4LP10 concrete, the i_{corr} increased with time and reached a value of 0.23 μA/cm^2 at the end of 44 days. In the case of 0.4L10F20 concrete, the i_{corr} increased with time and reached a value of 0.6 μA/cm^2 at the end of 60 days. In the case of

0.4LP5 concrete, the i_{corr} increased with time and reached a value of 0.5 μA/cm^2 at the end of 56 days. For 0.4OPC concrete, the steel bar attained a shift of i_{corr} to 0.23 μA/cm^2 at the end of 70 days. In the same way, the HCP and i_{corr} in case of LP concrete exposed to chloride have the same tendency as those of FA concrete for the aspect of corrosion starting time. Corrosion starting times of steel bars in concrete with 50 mm of concrete cover thickness were longer than those with concrete covering thickness of 30 mm. In addition, the order of staring corrosion time of concrete covering thickness of 50 mm had similar tendency to the case of 30 mm cover thickness. The corrosion starting times of all tested mix proportions were summarized in Table 4.6.

The results indicate that OPC concrete has the latest corrosion starting time when compared with LP concretes and L10F20 concretes. At the end of exposure period, the corrosion starting time for concrete with w/b=0.4 started by the order: 0.4LP15 before 0.4LP10 before 0.4L10F20 before 0.4LP5 before 0.4OPC. This order of corrosion starting time has similar trend with those of w/b=0.5 and w/b=0.6, with a reversing pair of test results in w/b=0.6 (0.6LP10 before 0.6LP15). Many researchers (Hien, 2010; Hussain, 1995) reported that for concrete with small w/b ratio, the reduction of permeation of chloride and water causes the reduction of corrosion. For this reason, the corrosion starting time of concrete with high w/b ration occurred before low of w/b ratio. Ghrici (2007) demonstrated that the penetration of chloride ion increased in concretes containing 15% limestone powder. Also, Bonavetti (2000) reported that the penetration of chloride ion increased from 43% to 114% for concretes containing 10% and 20% of limestone powder, respectively. Similar results were confirmed in this study that the corrosion starting times of concrete with LP replacement occurred before OPC. However, corrosion starting time of L10F20 was in the middle between LP10 and OPC. It means that, the penetration of chloride ion was decreased when adding FA in LP concrete due to pozzolanic reaction which was explained already in section 4.4.

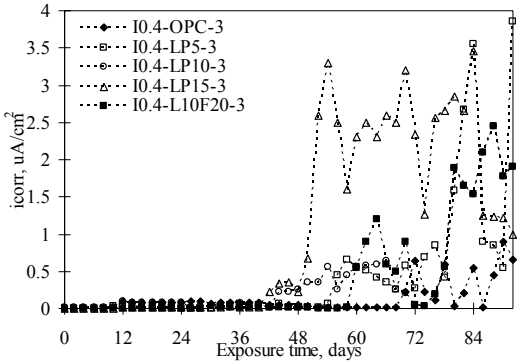

(a) w/b=0.4 and covering 30 mm

Figure 4.16 i_{corr} of LP concrete with 30 mm covering exposed to chloride environment

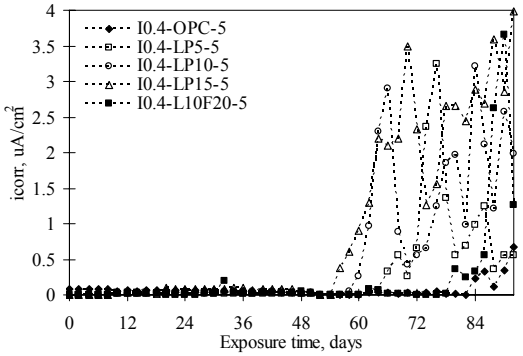

(a) w/b=0.4 and covering 50 mm

Figure 4.17 i_{corr} of LP concrete with 50 mm covering exposed to chloride environment

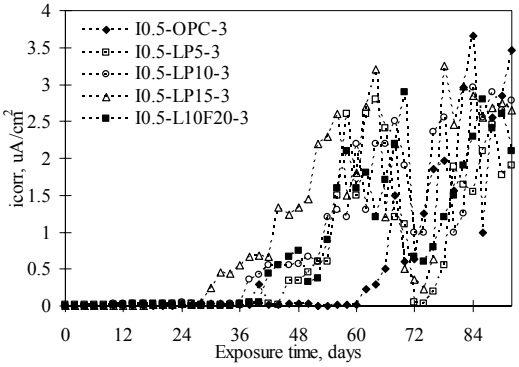

(b) w/b=0.5 and covering 30 mm

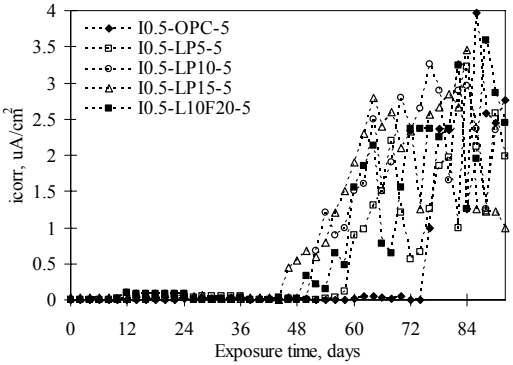

(b) w/b=0.5 and covering 50 mm

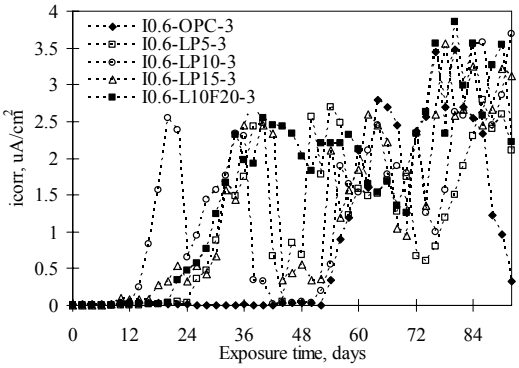

(c) w/b=0.6 and covering 30 mm

Figure 4.16 i_{corr} of LP concrete with 30 mm covering exposed to chloride environment

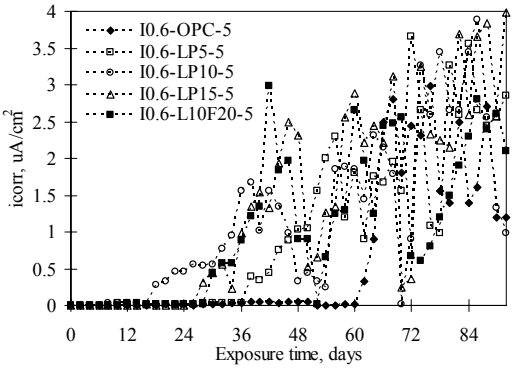

(c) w/b=0.6 and covering 50 mm

Figure 4.17 i_{corr} of LP concrete with 50 mm covering exposed to chloride environment

4.5.3 Total chloride content (chloride specimens)

To verify whether HCP measurement can be used to detect the corrosion starting time of steel bars in concrete, chloride content near the top steel bars in the specimens were also measured in the tests. Concrete powder was collected and tested for the amount of total chloride in concrete. EIT 1014 recommends that, steel bars in concrete depassivates when its surrounding concrete has total chloride content higher than 0.4% by weight of the cement. In this test, the timing of concrete powder sample collection is important. Since the concept was to collect the powder sample when steel bars had already depassivated, the concrete powder samples were collected when HCP values decreased to be more negative than -350 mV. After passing this criterion for 6 day, concrete specimens were drilled to collect concrete powder samples.

The results of the measured chloride content are discussed in Fig. 4.18. It can be seen that 62% of total samples have higher chloride content than the critical chloride content according to EIT 1014. However, 32% of total samples still have total chloride lower than this criterion. This indicates that, after HCP values were more negative than -350 mV, chloride content in majority of the samples at the steel surface was higher than the limit of EIT 1014 (0.4% by weight of cement). Then, half-cell potential measurement is considered to have potential to detect the corrosion starting time or depassivation of steel bars in reinforced concrete which is exposed to chloride in the laboratory.

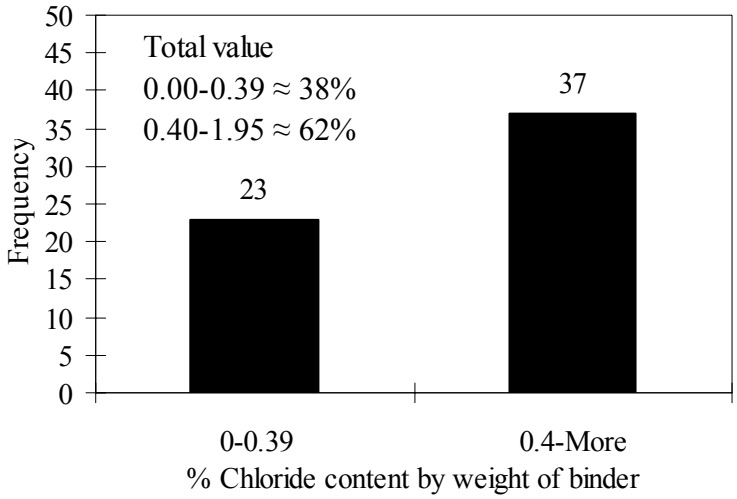

Figure 4.18 Frequency of data of total chloride content by weight of binder collected from the specimens showing HCP values more negative than -350 mV

4.6 Corrosion activities of concrete specimens exposed to combined chloride and carbon dioxide environments

Effect of different exposure conditions between exposure to NaCl solution and exposure to carbonation was also studied. Concrete specimens were subjected to cyclically alternative environments by exposing to NaCl for 3 days and then exposing to CO_2 for 4 days for 1 cycle. Corrosion activities of steel bars were monitored by HCP and i_{corr}. The results of this study are presented as follows.

4.6.1 Half-cell potential measurement

Figure 4.19(a), 4.19(b), and 4.19(c) show results of specimens exposed to the combined chloride and carbonation cycles. It shows that HCP values are more negative with increasing exposure time. From Fig. 4.19(a), in the case of 0.4FA50, HCP value was -124 mV at the initial period and then became more negative than -368 mV at the end of 49 days. At the end of 63 days, the HCP values of 0.4FA20 and 0.4OPC were -134 and -232 mV at the initial period and decreased rapidly to -365 and -382 mV, respectively. In the case of w/b=0.5, Fig. 4.19(b), 0.5FA50 showed -124 mV at the initial period and then reached a more negative value of -443 mV at the end of 7 days. In the case of 0.5FA20 concrete, the initial value was -242 mV but suddenly decreased to -396 mV at the end of 21 days. For 0.5OPC concrete, it was initially -145 mV and reached a potential of -403 mV at the end of 28 days. Whereas in the case of 0.6FA20 and 0.6OPC concrete, the specimens showed -134 and -164 mV initially and showed more negative potential values of -396 and -403 mV at the end of 21 and 28 days, respectively. The summary of corrosion starting times identified by HCP of concrete specimens in this test series is given in Table 4.7. The results indicated that combined environments affected corrosion starting time of concrete specimens.

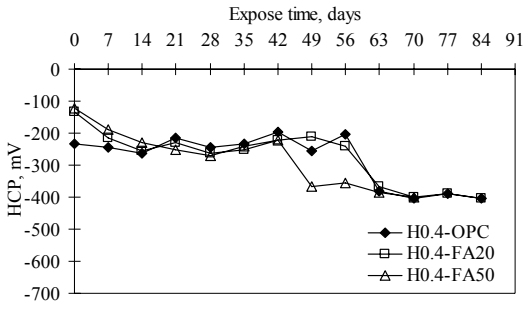

(a) w/b=0.4

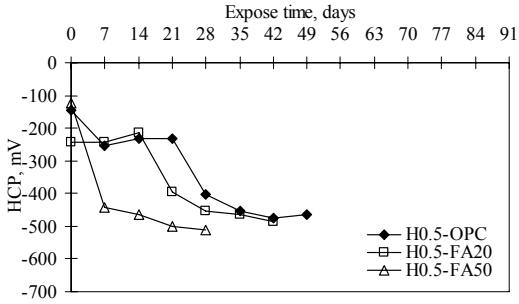

(b) w/b=0.5

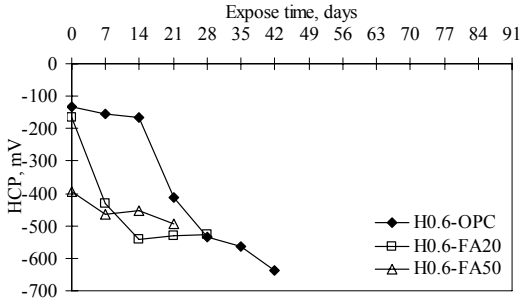

(c) w/b=0.6

Figure 4.19 Half-cell potential value of concrete exposed to combined chloride and carbonation

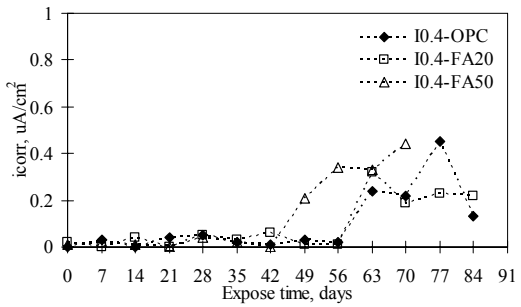

(a) w/b=0.4

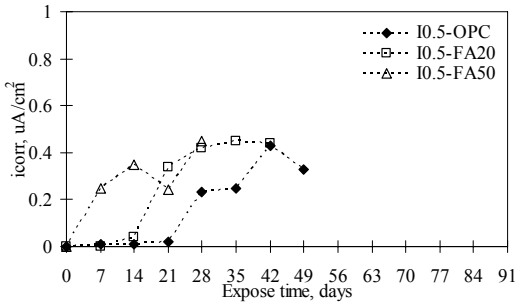

(b) w/b=0.5

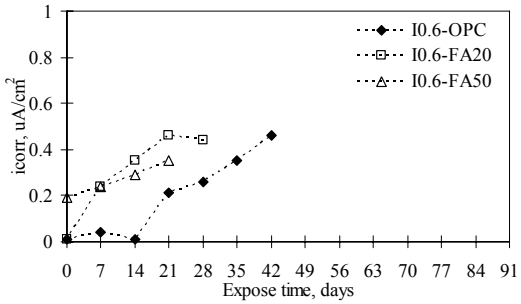

(c) w/b=0.6

Figure 4.20 Corrosion current density of concrete exposed to combined chloride and carbonation

Table 4.7 Corrosion starting times of concrete specimens in case of combined chloride attack and carbonation

	Results of HCP measurement			Results of icorr measurement		
	Initial	Corrosion starting		Initial	Corrosion starting	
Name	HCP, mV	Time, day	HCP, mV	icorr, μA/cm^2	Time, day	icorr, μA/cm^2
0.4OPC	-232	63	-382	0.00	63	0.24
0.4FA20	-134	63	-365	0.02	63	0.32
0.4FA50	-124	49	-368	0.01	49	0.21
0.5OPC	-145	28	-403	0.00	28	0.23
0.5FA20	-242	21	-396	0.00	21	0.34
0.5FA50	-124	7	-443	0.00	7	0.25
0.6OPC	-134	28	-413	0.01	28	0.21
0.6FA20	-164	7	-432	0.01	7	0.24
0.6FA50	-394	0	-394	0.19	0	0.19

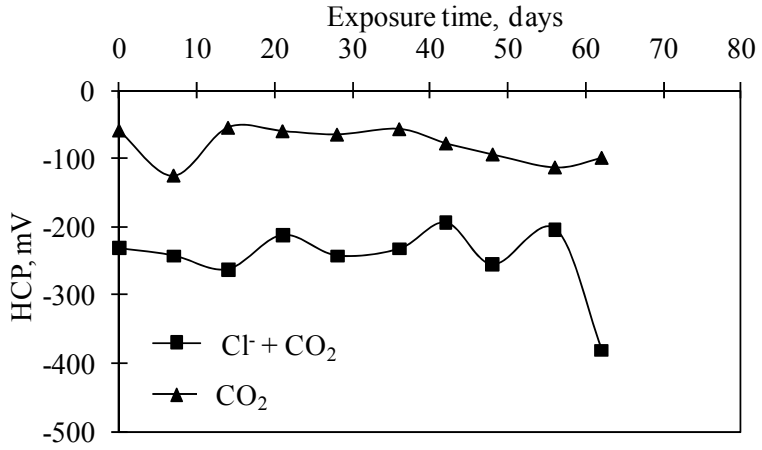

(a) w/b=0.4

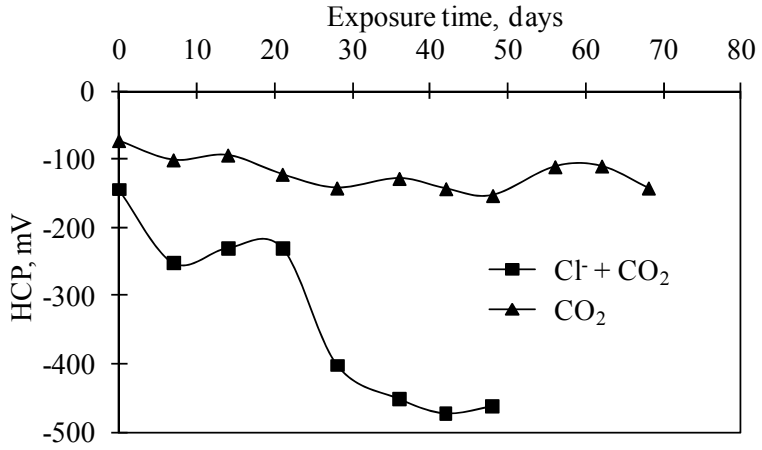

(b) w/b=0.5

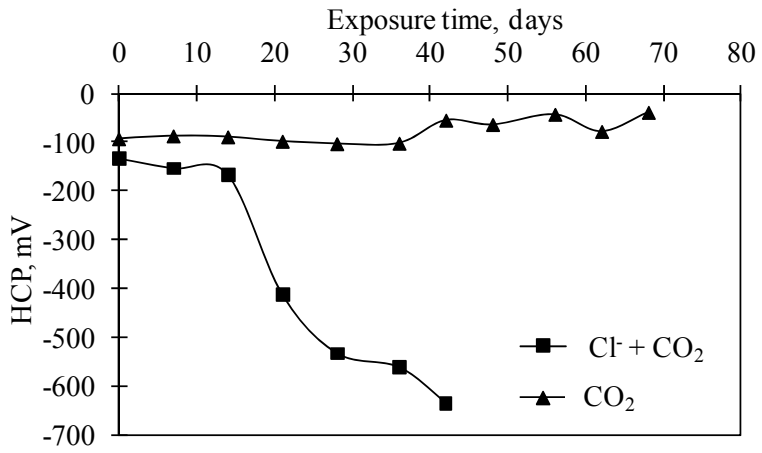

(c) w/b=0.6

Fig 4.21 Comparison of HCP results of specimen OPC exposed to carbonation and combined chloride and carbonation environments

Table 4.8 Comparison of corrosion starting time of concrete specimens exposed to combined $Cl^- + CO_2$ and CO_2

Corrosion starting time, days									
Name	0.4OPC	0.4FA20	0.4FA50	0.5OPC	0.5FA20	0.5FA50	0.6OPC	0.6FA20	0.6FA50
CO_2+Cl^-	63	63	49	28	21	7	28	7	0
CO_2	74	41	24	67	12	9	44	11	5

Experimental comparisons of HCP results of concrete specimens, with 10 mm cover thickness, exposed to carbonation (CO_2) and combined chloride and carbonation ($Cl^- + CO_2$) are demonstrated in Fig. 4.21 and comparisons of corrosion starting times of these environments are given in Table 4.8. The results showed that for concrete specimens which were exposed to $Cl^- + CO_2$, corrosion of steel bars started sooner when compared to the case of CO_2 only (section 4.3). For instance, corrosion starting time of 0.5OPC in case of exposure to $Cl^- + CO_2$ was 28 days, whereas the corrosion starting time in case of exposure to CO_2 was 67 days. Concrete specimens with w/b=0.4 and w/b=0.5 have the same tendency of corrosion starting time as the specimen with w/b=0.5 as demonstrated in Fig 4.21. It is generally known that reaction of carbonation takes long time. Then, corrosion starting time in case of carbonation was longer than the case of exposure to $Cl^- + CO_2$. However, carbonated concrete had influence on the HCP values after steel bars had corroded already (carbonation depth larger than concrete cover thickness). HCP still showed constant values even though carbonation had reached the steel bars in concrete. This was because carbonation increased electrical resistance of the concrete (filling pores in concrete by $CaCO_3$) causing low flow of current through the concrete cover. Another reason is the low porosity of concrete causing lower moisture content during measuring HCP. In addition, these was no chloride in the specimens in the carbonation series. These are the reasons that HCP readings in case of carbonation still showed constant values when steel bars in concrete had been depassivated. In this study, the comparison of results of HCP values between the cases of $Cl^- + CO_2$ and Cl^- only was not made because concrete specimens of both cases had different concrete cover thickness ($Cl^- + CO_2$=10 mm but Cl^- =30mm). The comparison of the results of HCP values between $Cl^- + CO_2$ and Cl^- only is left for future study.

After a specimen was exposed to CO_2 and Cl^-, carbonation, occurring at front surface of concrete, caused dissolution of fixed chloride (Sancharoen, 2004). Fixed chloride ability of concrete was reduced. Mechanisms of effect of carbonation on chloride diffusion are simply shown in Fig. 4.22. As shown in Fig. 4.22(b), 4.22(d) and 4.22(e), a portion of fixed chloride is changed to free chloride during carbonation and can diffuse further into the concrete, although it was not subjected to chloride solution from outside. When specimens are resubjected to chloride solution, more chloride diffuses into the concrete if free chloride concentration in pore solution is still less than the concentration of the exposed solution as shown in Fig. 4.22(C). Another reason is due to effect of wetting and drying. When specimens were exposed to carbonation (CO_2), water in pore solution can evaporate, but chloride ion was still in the pore solution near the surface of concrete specimens. After resubjection to wetting period (Cl^-), chloride ion from outside solution moved to inside concrete by capillary suction process which is a very quick process. This increased the concentration of Cl^- ion near the surface of concrete especially when the concrete was subjected to many wetting and drying cycles. This is one more reason that make corrosion starting time of $Cl^- + CO_2$ sooner than Cl^- only.

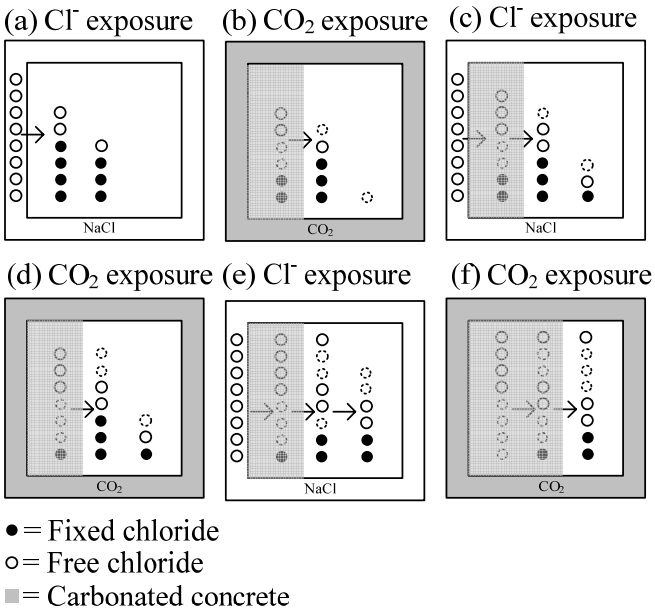

Figure 4.22 Mechanisms of effect of carbonation on chloride diffusion

4.6.2 Corrosion current density

Figure 4.20 shows results of the measured i_{corr} of steel bars in concrete specimens in the combined environments. In the case of 0.4FA50, 0.4FA20 and 0.4OPC, Fig. 4.20(a) shows corrosion current density of 0.21, 0.32 and 0.24 μA/cm^2 at the end of 49, 63 and 63 days, respectively. The results for 0.5FA50, 0.5FA20 and 0.5OPC in Fig. 4.20(b) illustrate that these concrete reach corrosion current density of 0.25, 0.34 and 0.23 μA/cm^2 at the end of 7, 21 and 28 days, respectively. Whereas in the case of 0.6FA50, 0.6FA20 and 0.6OPC concrete, the specimens show 0.19, 0.24 and 0.21 μA/cm^2 at the end of 0, 7 and 21 days, respectively. The summary of corrosion starting times of concrete specimens in this series is shown in Table 4.7. All i_{corr} results have relationship with HCP values. When the i_{corr} values start to increase, HCP values decrease. Then results indicate that both i_{corr} and HCP are effective to be used to detect initiation of corrosion of reinforcement in laboratory testing.

4.7 Half-cell potential test on reinforced concrete structures on site

4.7.1 Effect of wetting and drying condition

The HCP tests were carried out on walls of RC structures. Three locations were tested i.e. SD2-R, SR2-C located on the east side of a 10-year old RC structure and SP3-L located on the west of a 2-year old RC structure. Table 4.9 shows main characteristics of these RC walls. Figure 4.23, 4.24 and 4.25, ((a) is for the case of applying moisture for 12 hours and (b) is for the case of applying moisture for 1 hour) show the HCP results. The results are expressed in the grey scale maps indicating the values of HCP measurement in 3 different ranges according to ASTM C876: the white zones correspond to areas of which the HCP values are more positive than -200 mV, the gray zones correspond to areas of which the HCP values are -200 mV to -350 mV, the black zones correspond to areas of which the HCP values are more negative than -350 mV.

Figure 4.24(a) show the measurements taken from surface with 12 hours of moisture application while Fig. 4.24(b) shows results for 1 hour of moisture application. HCP values are more negative when moisture has been applied. This is also illustrated by more black area in Fig. 4.23(a) and Fig. 4.24(a) than in Fig 4.23(b) and Fig. 4.24(b). This result can be explained by the electrical conductivity between steel bar inside concrete and reference electrode used in HCP measurement. When applying moisture to the concrete, concrete has low electrical resistance which increases electrical current flow between the steel bar and the reference electrode causing HCP value more negative.

Table 4.9 Characteristics of the measured concrete walls.

Wall	fc', ksc	Cover depth, cm	Distance between rebars, cm	Age, year
SD2-R	616	6.14	20	2 (after repaired)
SD2-C	161	6.14	20	10
SP3-L	529	4.54	20	2

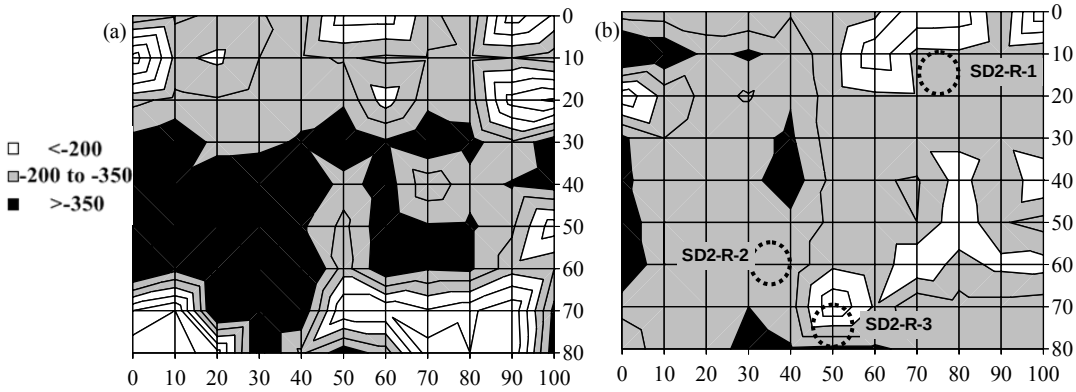

Figure 4.23 Results of the HCP measurement of SD2-R: (a) W-SD2-R (applying moisture for 12 hours), (b) D-SD2-R (applying moisture for 1 hour)

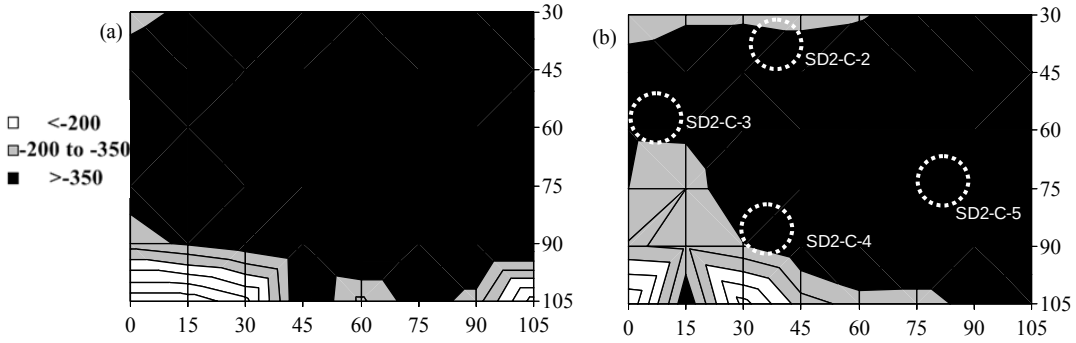

Figure 4.24 Results of the HCP measurement of SD2-C: (a) W-SD2-C (applying moisture for 12 hours), (b) D-SD2-C (applying moisture for 1 hour)

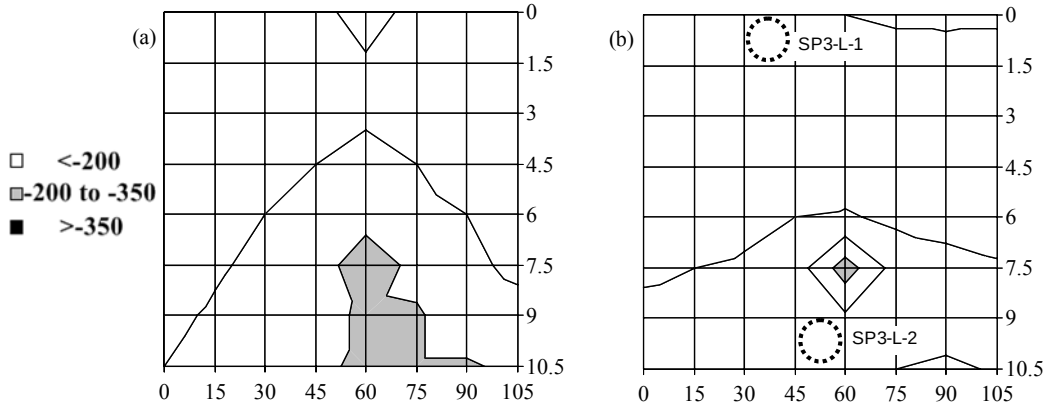

Figure 4.25 Results of the HCP measurement of SP3-L: (a) W-SP3-L (applying moisture for 12 hours), (b) D-SP3-L (applying moisture for 1 hour)

4.7.2 Total chloride content

EIT 1014 specifies critical chloride content to initiate corrosion at approximately 0.05% by weight of concrete. The ASTM standard C876 provides general guidelines for the interpretation of the HCP data. According to these guidelines, the probability of corrosion of the rebars is less than 10% if the potential is greater than -200 mV, whereas potential values lower than -350 mV indicate a high probability (> 90%) that corrosion is active. The HCP values between -200 mV and -350 mV indicate areas where the corrosion activity is uncertain. Figure 4.23, 4.24 and 4.25 give the HCP results of the wall members. The results are plotted in the grey scale maps indicating the probability of corrosion of the reinforcements: the white zones correspond to areas where the probability of corrosion is lower than 10%, the gray zones correspond to areas where the probability of corrosion is uncertain, and the black zones correspond to areas where the probability of corrosion is higher than 90%.

The HCP value and total chloride content by weight of concrete at different locations are shown in Table 4.10. All samples which have HCP values more negative than -350 mV showed chloride content much higher than 0.05%. For example, sample SD2-C-5 has HCP value more negative than -350 mV and has total chloride content of 0.23% by weight of concrete at the layer 50 mm from concrete surface. The results indicate that the numerical criteria of ASTM C876 get along, to a certain extent, with the results of total chloride content observed in this study.

However, at SD2-C-2 and SD2-C-3 showed chloride content of concrete at depth of 5 cm of 0.08% and 0.09% by weight of concrete. It means that steel bars in concrete would be corroded when compared with EIT 1014. However, HCP of both locations showed the values less than -350 mV. It is considered that concrete ingredients and mix proportions have influence on critical chloride content to initiate corrosion of steel bars in concrete. More studies are needed to verify the effect of concrete ingredients mix proportions and deterioration of concrete on the chloride threshold. In addition both SD2-C-2 and SD2-C-3 showed constant distribution of chloride content. This may be due to effect of rain which causes chloride to diffuse out of the concrete.

Table 4.10 Total chloride content by weight of concrete

Name	HCP value (applying moisture for 1 hour), mV	HCP value (applying moisture for 12 hour), mV	Total chloride content in each layer, % by weight of concrete				
			1 cm	2 cm	3 cm	4 cm	5 cm
SD2-R-1	-200 to -350	-200 to -350	0.07	0.02	0.02	0.02	0.03
SD2-R-2	-200 to -350	> -350	0.10	0.02	0.02	0.02	0.01
SD2-R-3	-200 to -350	-200 to -350	0.07	0.01	0.01	0.01	0.01
SD2-C-2	-200 to -350	> -350	0.07	0.03	0.06	0.07	0.08
SD2-C-3	-200 to -350	> -350	0.09	0.08	0.13	0.13	0.09
SD2-C-4	> -350	> -350	0.24	0.19	0.14	0.17	0.11
SD2-C-5	> -350	> -350	0.16	0.38	0.26	0.23	0.23
SP3-L-1	< -200	< -200	0.03	0.01	0.01	0.01	0.01
SP3-L-2	< -200	< -200	0.04	0.01	0.01	0.01	0.01

Chapter 5

Conclusion

Based on the findings obtained from the experimental results, the following conclusions can be drawn:

1. The half-cell potential values depended on concrete exposure conditions. For chloride condition, half-cell potential values were constant before corrosion initiation time. After steel was depassivated, half-cell potential rapidly decreased to more negative values. However, for carbonation, half-cell potential values increased to be less negative due to increasing resistance of carbonated concrete. This indicates that half-cell potential is not appropriate for detecting the corrosion activity of reinforcing bars in concrete exposed to carbonation. On the other hand, HCP is more efficient than i_{corr} to be used for detecting depassivation of steel bars in concrete in the laboratory.

2. Water to binder ratio had influence on corrosion starting time of steel bars in concrete. The corrosion starting time of high w/b ratio concrete started sooner than low w/b ratio concrete.

3. After rebars was depassivated, high volume of FA replacement tended to decrease the HCP values to be more negative, especially for specimen made with low w/b ratio. However, the influences of FA replacement on HCP value cannot be clearly seen in case of FA concrete made with high w/b ratio.

4. The LP concrete had earlier corrosion starting time than OPC concrete. However, corrosion starting time of LP concrete become longer when 20% of FA was included in the LP concrete.

5. HCP measurement was more efficient to be applied to inspect corrosion starting time than corrosion current density method in Cl^- exposure condition. The half-cell potential values suddenly decreased to more negative values while corrosion current density gradually increased at the depassivation of the steel bars. HCP measurement is considered to have potential to detect the corrosion starting time of steel bars in reinforced concrete which is exposed to Cl^- and combined $Cl^- + CO_2$ in the laboratory.

6. Actual corrosion surveys showed that the half-cell potential shifted to more negative values when longer moisture period was applied to the concrete. The more negative potential area on the potential contour map corresponded to the area with higher chloride content.

REFERENCES

Alonso, C., Andrade, C., Castellote, M., and Castro, P., 2000. Chloride threshold values to depassivate reinforcing bars embedded in a standardized OPC mortar, *Cement and Concrete Research* 30:1047–1055.

A. Poursaee and C.M Hanson, 2007. Reinforcing steel passivetion in mortar and pore solution. *Cement and Concrete Research* 37:1127-1133.

ACI Committee 222, 2001. *Protection of Metals in Concrete Against Corrosion.* American Concrete Institute.

ACI Committee 318, 1995. *Building Code Requirement for Reinforce concrete*. American Concrete Institute.

ASTM G109, 2005. Standard test method for determining the effects of chemical admixtures on the corrosion of embedded steel reinforcement in concrete exposed to chloride environments. *Annual Book of ASTM Standards* 03.02:11-16.

ASTM C 876-91, 2006. Standard Test Method for Half-cell Potentials of Uncoated Reinforcing Steel in Concrete. *Annual Book of ASTM Standards* 03.02:11-16.

Atis, C.D., 2003. Accelerated Carbonation and Testing of Concrete Made with Fly Ash. *Construction and Building Materials* 17(3):147-152.

Bonavetti V, Donza H, Rahhal V, Irassar E., 2000. Influence of initial curing on the properties of concrete containing limestone blended cement. *Cement Concrete Research* 30(5):703–708.

B.Elsener, 2002. Macrocell corrosion of steel in concrete-implications for corrosion monitoring. *Cement & Concrete Composites* 24:65-72.

Balayssaca, J.P., Détrichéa, C.H., and Grandet J., 1992. Effects of curing upon carbonation of concrete. *Construction and Building Materials* 9:91-95.

Broomfield, John P., 1997. *Corrosion of Steel in Concrete,* E.& F.N. Spon, London, UK.

Bertolini., L, Elsener., B, Pedeferri., P, and Polder.,R. *Corrosion of Steel in Concrete*.Wiley, Weinheim.

Cahyadi, J.H., and Uomoto, T., 1993. *Influence of Environmental Relative Humidity on carbonation of concrete (Mathematical Modeling)*, Durability of Building Materials and Components 6. Edited by Nagataki, S., Nireki, T., and Tomosawa, F., E & FN SPON, pp. 1142-1151.

Chi, M.J., Huang, R., and Yang, C.C., 2002. Effects of Carbonation of Mechanical Properties and Durability of Concrete Using Accelerated Test Method, *Journal of Marine Science and Technology* 10:14-20.

C. Andrade, C. Alonso, 2001. On-site measurements of corrosion rate of reinforcements, *Construction and Building Materials* 15:141-145.

C.andrade and I.Martinez, 2005. Calibration by gravimetric losses of electrochemical corrosion rate measurement using modulated confinement of the current. *Materials and Structures* 38:833-841.

Cahyadi, J.H., and Uomoto, T., 1993. Influence of Environmental Relative Humidity on carbonation of concrete (Mathematical Modeling). *Durability of Building Materials and Components* 6. Edited by Nagataki, S., Nireki, T., and Tomosawa, F., E & FN SPON, pp. 1142-1151.

Cengiz Duran Atis, 2003. Accelerated carbonation and testing of concrete made with fly ash. *Construction and Building Materials* 17:147–152.

Evans.U.R., 1960. The Corrosion and Oxidation of Metals. Prentice-Hall,Inc.

Ghrici M, Kenai S, Said Mansour M., 2007. Mechanical properties and durability of mortar and concrete containing natural pozzolana and limestone blended cements. *Cement Concrete Comp* 29:542–549.

Glass, G. K., and Buenfeld, N. R., 1997. The presentation of the chloride threshold level for corrosion of steel in concrete. *Corrosion Science* 39:1001–1013.

Gu, P., and J. J. Beaudoin 1998. Obtaining Effective Half-Cell Potential Measurements in Reinforced Concrete Structures. *Construction Technology Update No. 18.* National Research Council of Canada, Ottawa, Ontario, Canada, July.

Hieu T. Cam., N. Neithalath, 2010. Moisture and ionic transport in concretes containing coarse limestone powder. *Cement and Concrete Composites* 22:345-355.

Hussain, S. E., Rasheeduzzafar, Al-Musallam, A., and Al-Gahtani, A. S., 1995. Factors affecting threshold chloride for reinforcement corrosion in concrete. *Cement and Concrete Research* 25:1543–1555.

J. Khunthongkeaw , S. Tangtermsirikul , T. Leelawat, 2006, A study on carbonation depth prediction for fly ash concrete, *Construction and Building Materials* 20:744–753.

Japan Society of Civil Engineers, 2004. Environmental impact evaluation of concrete.! Concrete Engineering Series 62.

K. Sakr., 2004. Effect of cement type on the corrosion of reinforcing steel bars exposed to acidic media using electrochemical techniques. *Cement and Concrete Research* 35:1820–1826.

K. Wang, P.R.L. Helene and P.J.M. Monteiro., 2007. Potential use of zinc in the repair of corroded reinforced concrete. *Cement & Concrete Composites* 28:707-715.

K. Kaewmanee, S. Tangtermsirikul,and and R. Kasemchaisiri, 2006. Effect of Prticle Size of Limestone Powder on Properties of Normal Concrete and Special Concrete. *Proceedings of the 11th National Convention on Civil Engineering*, Engineering Institute of Thailand, Phuket, 20-22.

Luca Betolini, B Elsener, P Pedeferri and R Polder 2004, *Corrosion of steel in concrete*, Wiley-vch.

Ministry of Industry, 1985, *Standard for Concrete Aggregate*, TIS 566.

Ministry of Industry, 1989. *Standard for Portland Cement, Part 1, Specifications*, TIS 15.

Neville, A.M, 1995. *Properties of Concrete*, Longman.

Neville, A.M. and Brooks J.J., 1997. *Concrete Technology*. Longman.

Oh, B. H., Jang, S. Y., and Shin, Y. S., 2003. Experimental investigation of the threshold chloride concentration for corrosion initiation in reinforced concrete structures. *Magazine of. Concrete Research* 55(2):117–124.

Raupach, M., 1996. Chloride-induce macrocell corrosion of steel in concrete-theoretical background and practical consequences. *Construction and Building Materials* 10(5), 329–338.

RILEM TC 154-EMC, "Electrochemical Techniques for Measuring Metallic Corrosion" Recommendations, "Half-cell potential measurements – Potential mapping on reinforced concrete structures," *Materials and Structures*. 36 August - September (2003):461-471.

RILEM Technical Committee CPC-18, 1988. Measurement of Hardened Concrete Carbonation Depth, TC14-CPC, RILEM.

RILEM Technical Committee, 2007. Electrochemical techniques for measuring corrosion in concrete-measurements with embedded probes, TC 154-EMC, RILEM.

M H Roberts., 1986. *Determination of the chloride and cement contents of hardened concrete. Building Research Establishment*, England:BREPress.

Sancharoen, P. 2004. Corrosion of reinforcing steel due to cyclic exposure of chloride and carbonation. Ph.D. dissertation. Department of Civil Engineering, The University of Tokyo, Tokyo, Japan, September.

Technical Note NEA/CSI/R(2002). Electrochemical Techniques to Detect Corrosion in Concrete Structures in Nuclear Installations. *Nuclear Energy Agency*, Paris, France, July 2002.

Trejo, D., and Pillai, R.G., 2003. Accelerated chloride threshold testing: Part 1—ASTM A615 and A706 reinforcement. *ACI Materials. J.* 100:519–527.

Thad Marshall Pinkerton, 2007. Sensitivity of half-cell potential measurements to properties of concrete bridge deck, *Master thesis*, Department of Civil and Environmental Engineering, Brigham Young University, USA.

V Zivica, 2003, Corrosion of reinforcement induced by environment containing chloride and carbon dioxide. *Build Material Science* 26:605-608.

Appendix A

Visual inspection

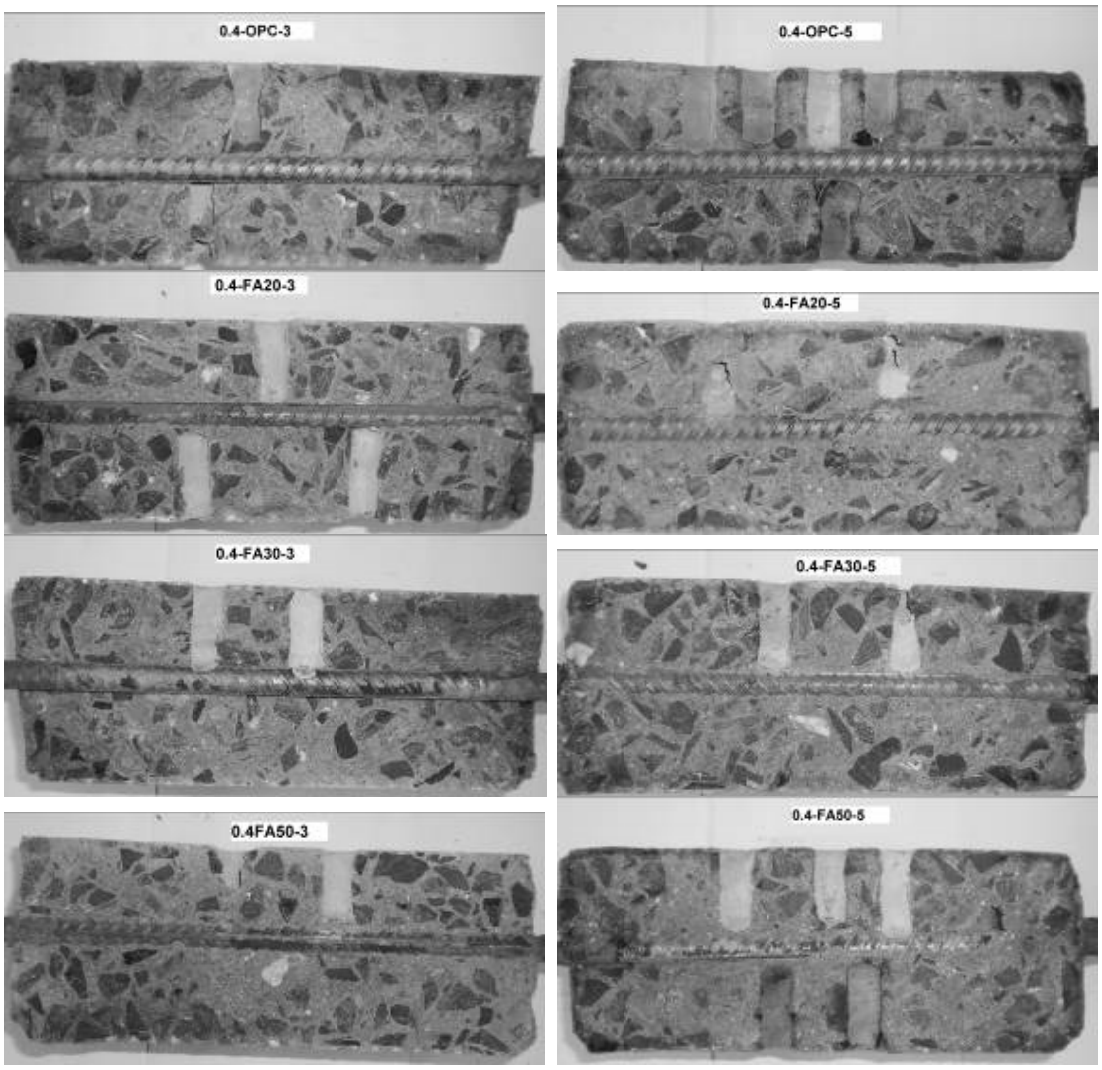

Figure A-1 Extent of rust on rebars in fly ash concrete with 0.4 of w/b ratio
at the end of the test

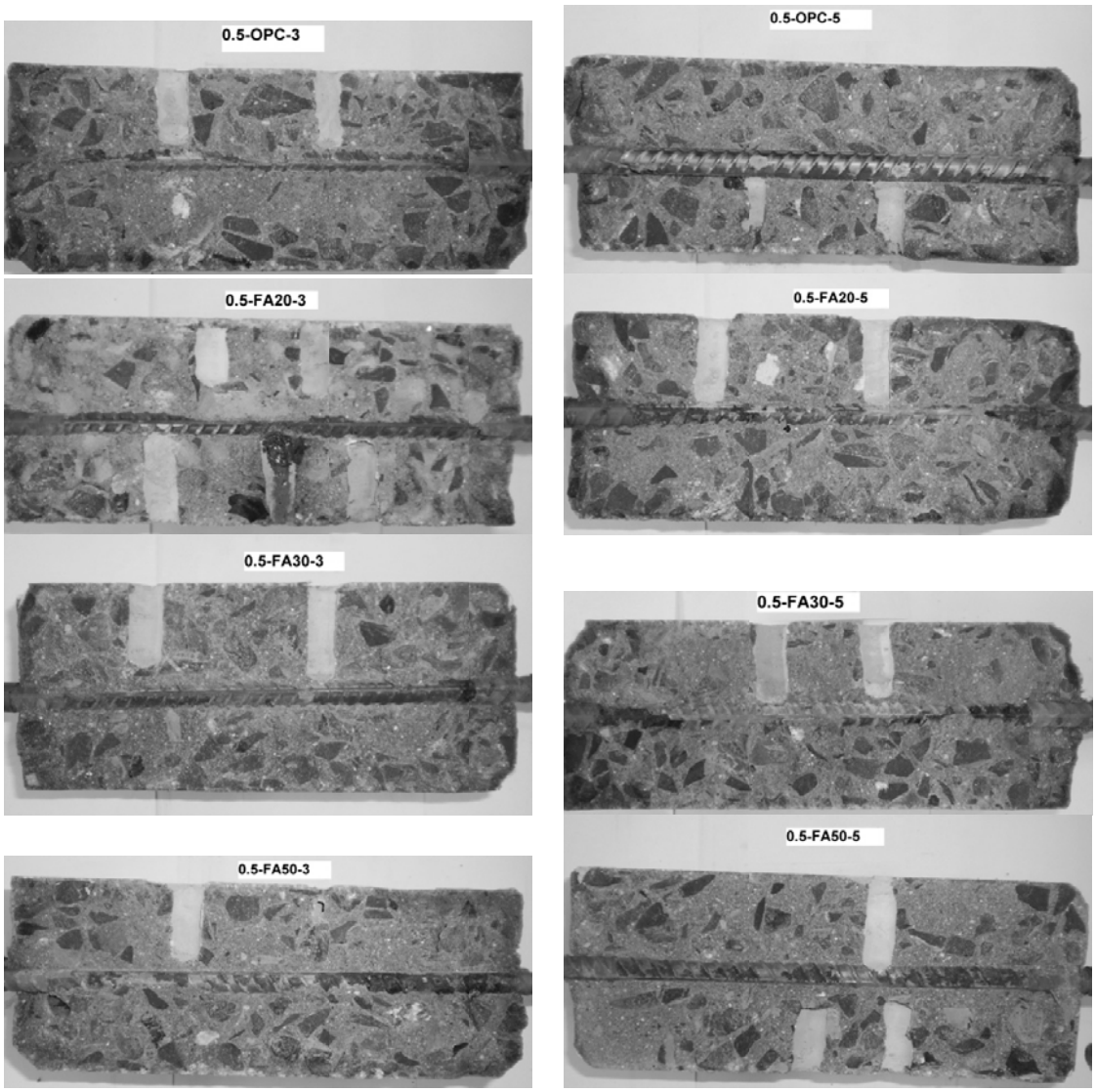

Figure A-2 Extent of rust on rebars in fly ash concrete with 0.5 of w/b ratio at the end of the test

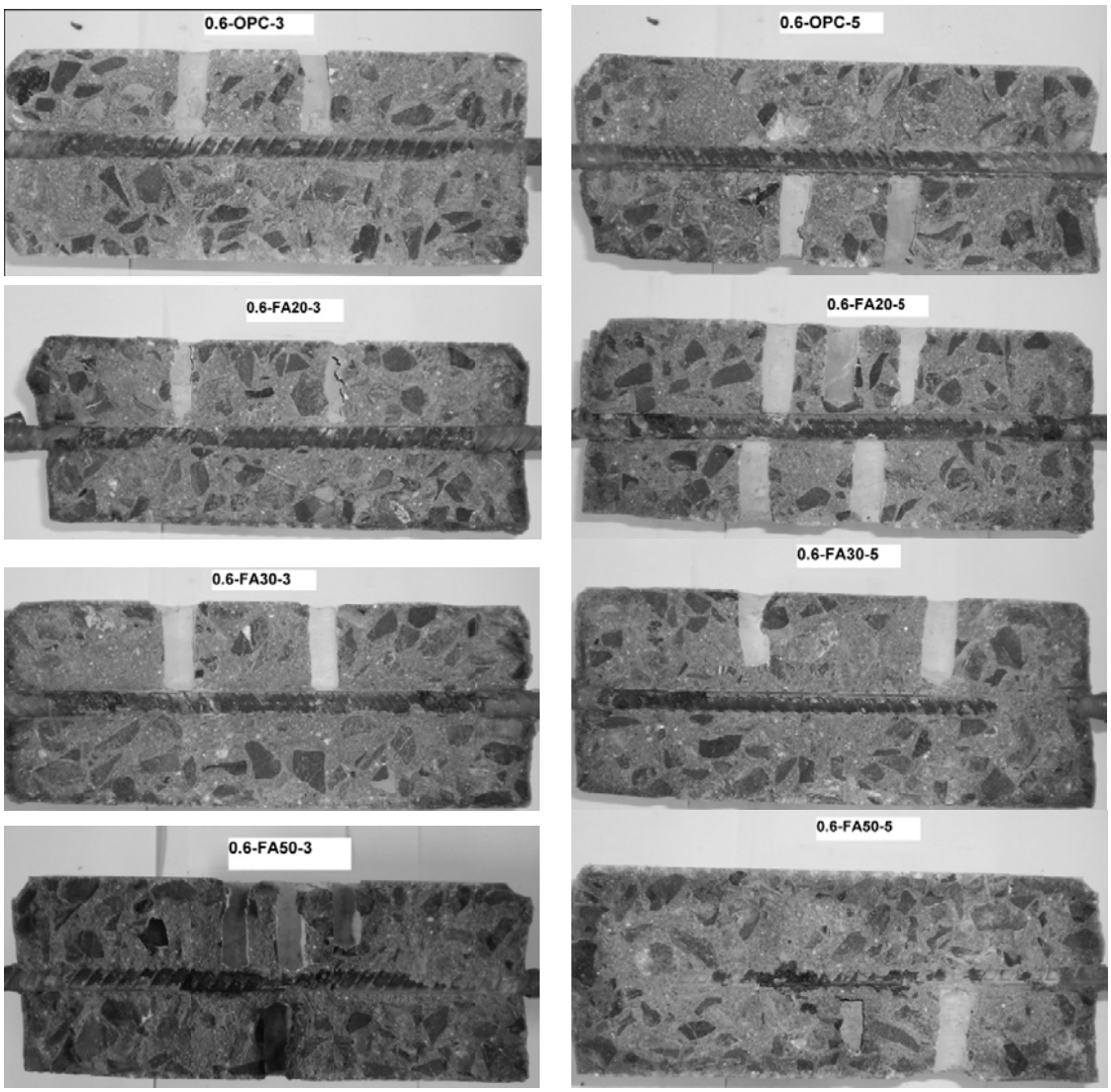

Figure A-3 Extent of rust on rebars in fly ash concrete with 0.6 of w/b ratio
at the end of the test

Appendix B

Half-cell potential test data

Table B.1 Average half-cell potential values of concrete exposed to CO_2

Mix \ Days	0	7	14	21	28	35	42	49	56	63	70	77
H0.4-OPC	-125	-55	-59	-60	-65	-57	-78	-94	-113	-99	-119	-129
H0.4-FA20	-73	-55	-55	-66	-64	-64	-56	-69	-60	-40	-53	-62
H0.4-FA50	-92	-55	-77	-64	-56	-76	-45	-44	-42	-57	-93	-102
H0.5-OPC	-74	-102	-95	-123	-143	-129	-144	-154	-112	-111	-143	-123
H0.5-FA20	-131	-55	-55	-57	-64	-53	-68	-94	-22	-56	-75	-84
H0.5-FA50	-69	-158	-143	-156	-184	-198	-156	-195	-60	-43	-73	-64
H0.6-OPC	-94	-88	-90	-99	-104	-103	-56	-79	-40	-53	-67	-93
H0.6-FA20	-97	-55	-72	-56	-35	-29	-47	-59	-22	-33	-56	-94
H0.6-FA50	-126	-156	-234	-201	-198	-165	-145	-184	-138	-194	-175	-185

Table B.2 Average half-cell potential values of concrete exposed to combined cyclic CO_2 and NaCl

Mix \ Days	0	7	14	21	28	35	42	49	56	63	70	77	84
H0.4-OPC	-232	-243	-263	-213	-243	-233	-195	-256	-204	-382	-402	-389	-402
H0.4-FA20	-134	-214	-254	-231	-264	-253	-222	-212	-242	-365	-399	-389	-403
H0.4-FA50	-124	-189	-231	-253	-272	-241	-222	-368	-357	-385	-399	-	-
H0.5-OPC	-145	-253	-231	-231	-403	-453	-474	-463	-	-	-	-	-
H0.5-FA20	-242	-243	-213	-396	-453	-464	-486	-	-	-	-	-	-
H0.5-FA50	-124	-443	-465	-502	-512	-	-	-	-	-	-	-	-
H0.6-OPC	-134	-154	-167	-413	-534	-563	-636	-	-	-	-	-	-
H0.6-FA20	-164	-432	-543	-529	-528	-	-	-	-	-	-	-	-
H0.6-FA50	-394	-465	-453	-493		-	-	-	-	-	-	-	-

Table B.3 Average half-cell potential values of fly-ash concrete exposed to NaCl solution

HCP, mV	0	1	2	3	4	5	6	7	8	9	10	11	12	13	14	15	16	17	18	19	20	21	22	23
H0.4-OPC-3	-171	-223	-213	-199	-200	-192	-197	-184	-246	-243	-230	-253	-241	-246	-230	-250	-282	-279	-281	-258	-261	-265	-257	-250
H0.4-OPC-5	-191	-227	-243	-230	-227	-228	-240	-235	-238	-240	-240	-243	-240	-245	-235	-230	-235	-225	-220	-215	-220	-215	-215	-210
H0.4-FA20-3	-144	-258	-222	-215	-214	-219	-228	-215	-223	-220	-216	-221	-220	-215	-220	-224	-215	-214	-203	-200	-205	-200	-200	-192
H0.4-FA20-5	-163	-306	-215	-209	-208	-205	-210	-208	-213	-215	-215	-215	-215	-210	-215	-221	-210	-210	-205	-195	-195	-192	-190	-190
H0.4-FA30-3	-106	-213	-200	-197	-192	-189	-195	-193	-196	-190	-190	-228	-225	-225	-220	-225	-215	-215	-211	-200	-205	-205	-210	-205
H0.4-FA30-5	-126	-199	-205	-198	-194	-194	-201	-197	-203	-204	-282	-338	-365	-389	-372	-403	-435	-435	-445	-445	-460	-455	-456	-445
H0.4-FA50-3	-164	-208	-284	-253	-250	-239	-243	-238	-238	-225	-225	-290	-270	-269	-260	-364	-450	-465	-505	-505	-530	-540	-540	-525
H0.4-FA50-5	-149	-208	-209	-203	-204	-201	-206	-203	-204	-200	-195	-198	-195	-195	-200	-243	-300	-300	-305	-295	-310	-360	-380	-385
H0.5-OPC-3	-160	-215	-211	-208	-213	-206	-220	-196	-198	-190	-190	-192	-190	-190	-195	-213	-230	-226	-225	-210	-215	-210	-210	-205
H0.5-OPC-5	-170	-243	-232	-223	-227	-215	-225	-197	-198	-190	-190	-193	-210	-205	-198	-205	-210	-215	-210	-200	-200	-200	-200	-195
H0.5-FA20-3	-122	-231	-225	-214	-208	-205	-205	-193	-195	-190	-190	-188	-190	-185	-185	-195	-190	-190	-185	-180	-185	-185	-185	-181
H0.5-FA20-5	-116	-210	-210	-203	-195	-191	-198	-188	-189	-180	-180	-178	-175	-175	-175	-184	-185	-185	-180	-175	-350	-380	-380	-385
H0.5-FA30-3	-147	-235	-240	-233	-235	-229	-264	-240	-241	-230	-225	-228	-225	-225	-225	-222	-225	-225	-220	-210	-215	-215	-215	-210
H0.5-FA30-5	-142	-226	-227	-224	-225	-226	-232	-213	-215	-215	-210	-213	-210	-210	-215	-214	-220	-215	-210	-205	-210	-205	-200	-200
H0.5-FA50-3	-157	-213	-210	-203	-201	-195	-200	-193	-195	-190	-190	-193	-195	-321	-365	-453	-550	-555	-580	-575	-590	-595	-600	-601
H0.5-FA50-5	-174	-218	-205	-200	-205	-198	-207	-191	-198	-195	-195	-193	-190	-204	-205	-365	-430	-429	-505	-455	-485	-530	-515	-515
H0.6-OPC-3	-166	-221	-211	-205	-221	-212	-229	-197	-212	-196	-194	-193	-195	-190	-195	-200	-195	-195	-190	-185	-190	-185	-190	-185
H0.6-OPC-5	-188	-230	-225	-213	-225	-214	-224	-194	-201	-195	-189	-203	-200	-195	-195	-214	-200	-195	-190	-185	-185	-180	-185	-180
H0.6-FA20-3	-163	-225	-218	-210	-224	-222	-235	-208	-240	-225	-222	-219	-220	-219	-215	-213	-220	-220	-215	-206	-215	-210	-220	-210
H0.6-FA20-5	-186	-215	-210	-204	-220	-260	-233	-201	-247	-225	-215	-218	-255	-255	-236	-230	-250	-240	-245	-225	-225	-230	-225	-216
H0.6-FA30-3	-280	-225	-220	-210	-219	-246	-218	-207	-204	-200	-195	-193	-190	-210	-210	-250	-270	-295	-331	-335	-365	-375	-385	-377
H0.6-FA30-5	-275	-242	-228	-225	-236	-240	-226	-213	-218	-210	-205	-203	-205	-200	-195	-201	-210	-205	-205	-191	-195	-195	-195	-190
H0.6-FA50-3	-202	-222	-309	-320	-375	-396	-389	-395	-409	-425	-426	-459	-465	-484	-465	-488	-510	-510	-525	-500	-510	-520	-520	-510
H0.6-FA50-5	-238	-230	-218	-210	-215	-239	-224	-214	-216	-210	-205	-230	-345	-386	-360	-424	-510	-514	-545	-515	-530	-545	-535	-520

Table B.3 Average half-cell potential values of fly-ash concrete exposed to NaCl solution

HCP, mV	24	25	26	27	28	30	32	34	36	38	40	42	44	46	48	50	52	54	56	58	60	62	64	66	68
H0.4-OPC-3	-250	-245	-240	-230	-220	-225	-210	-213	-199	-213	-214	-235	-234	-233	-256	-267	-278	-245	-278	-287	-295	-345	-378	-456	-466
H0.4-OPC-5	-205	-200	-199	-185	-180	-195	-190	-180	-169	-166	-195	-203	-205	-214	-211	-231	-234	-254	-253	-253	-255	-243	-267	-345	-398
H0.4-FA20-3	-195	-195	-185	-180	-180	-195	-184	-180	-170	-234	-387	-356	-403	-453	-468	-512	-523	-522	-534	-533	-521	-534	-544	-565	-543
H0.4-FA20-5	-190	-185	-180	-175	-175	-160	-154	-150	-140	-156	-157	-231	-245	-267	-302	-357	-394	-435	-465	-478	-489	-488	-494	-502	-504
H0.4-FA30-3	-210	-235	-280	-353	-355	-510	-545	-575	-590	-546	-612	-602	-602	-612	-594	-615	-622	-612	-623	-617	-622	-622	-618	-629	-619
H0.4-FA30-5	-450	-455	-455	-439	-430	-460	-450	-455	-445	-456	-455	-452	-432	-476	-465	-455	-494	-453	-435	-465	-476	-432	-444	-467	-453
H0.4-FA50-3	-538	-510	-545	-540	-520	-535	-555	-580	-605	-604	-601	-603	-598	-610	-593	-613	-603	-614	-503	-603	-621	-644	-654	-643	-643
H0.4-FA50-5	-430	-440	-470	-485	-460	-585	-595	-600	-600	-594	-621	-611	-612	-603	-604	-602	-614	-615	-622	-616	-601	-603	-603	-614	-593
H0.5-OPC-3	-205	-205	-205	-195	-200	-230	-225	-211	-205	-204	-206	-245	-231	-243	-321	-358	-357	-387	-467	-487	-497	-499	-512	-512	-509
H0.5-OPC-5	-195	-190	-190	-180	-185	-180	-175	-168	-165	-193	-199	-231	-243	-234	-267	-267	-256	-278	-321	-378	-435	-455	-453	-435	-467
H0.5-FA20-3	-181	-180	-185	-190	-215	-470	-483	-486	-495	-504	-512	-522	-513	-534	-547	-546	-541	-567	-578	-565	-566	-567	-543	-578	-564
H0.5-FA20-5	-380	-390	-405	-435	-430	-490	-495	-505	-515	-523	-514	-543	-548	-542	-548	-541	-564	-547	-543	-554	-561	-567	-578	-576	-563
H0.5-FA30-3	-210	-210	-210	-205	-205	-375	-380	-405	-410	-409	-453	-432	-423	-456	-455	-452	-489	-486	-486	-503	-513	-501	-489	-492	-487
H0.5-FA30-5	-200	-195	-199	-192	-195	-290	-270	-265	-275	-367	-389	-453	-466	-456	-465	-435	-489	-476	-467	-489	-500	-467	-465	-466	-456
H0.5-FA50-3	-601	-600	-600	-600	-590	-595	-590	-586	-585	-567	-601	-612	-602	-607	-645	-632	-621	-621	-655	-644	-639	-639	-644	-641	-673
H0.5-FA50-5	-505	-505	-535	-531	-510	-595	-600	-605	-600	-546	-645	-612	-632	-634	-634	-645	-654	-611	-629	-643	-633	-644	-645	-632	-644
H0.6-OPC-3	-185	-181	-185	-180	-185	-180	-170	-165	-170	-186	-242	-321	-347	-476	-453	-432	-486	-521	-532	-533	-521	-534	-544	-542	-534
H0.6-OPC-5	-180	-176	-180	-170	-175	-175	-170	-165	-165	-189	-178	-168	-199	-239	-243	-246	-267	-265	-289	-299	-321	-378	-399	-425	-439
H0.6-FA20-3	-210	-205	-210	-205	-210	-240	-240	-245	-240	-321	-345	-453	-435	-400	-444	-432	-453	-455	-432	-465	-478	-465	-464	-467	-472
H0.6-FA20-5	-215	-205	-205	-195	-195	-190	-190	-185	-180	-190	-199	-221	-289	-321	-362	-423	-401	-368	-385	-324	-322	-345	-352	-485	-498
H0.6-FA30-3	-385	-380	-385	-370	-365	-406	-400	-410	-436	-440	-434	-449	-500	-432	-443	-432	-453	-512	-523	-532	-545	-554	-534	-547	-568
H0.6-FA30-5	-195	-200	-231	-250	-255	-310	-320	-305	-344	-400	-454	-435	-443	-453	-423	-467	-435	-426	-467	-470	-452	-532	-542	-534	-534
H0.6-FA50-3	-510	-505	-510	-505	-490	-525	-530	-540	-536	-543	-553	-523	-567	-521	-534	-533	-532	-539	-546	-541	-559	-546	-543	-546	-523
H0.6-FA50-5	-525	-520	-530	-510	-485	-520	-522	-525	-515	-543	-543	-556	-554	-543	-576	-532	-512	-502	-426	-435	-402	-386	-398	-563	-555

Table B.4 Average half-cell potential values of LP concrete with w/b=0.4 exposed to NaCl solution

HCP, mV	0	2	4	6	8	10	12	14	16	18	20	22	24	26	28	30	32	34	36	38	40	42	44	46
H0.4-OPC-3	-100	-105	-110	-150	-145	-122	-123	-234	-132	-243	-135	-194	-231	-212	-231	-110	-115	-120	-120	-120	-117	-145	-130	-132
H0.4-OPC-3	-165	-170	-160	-170	-180	-169	-134	-243	-213	-193	-265	-145	-145	-145	-150	-150	-147	-110	-125	-120	-120	-125	-234	-123
H0.4-OPC-5	-220	-225	-230	-245	-235	-231	-129	-145	-140	-145	-150	-175	-175	-175	-170	-170	-173	-170	-170	-170	-170	-170	-125	-169
H0.4-OPC-5	-160	-165	-165	-165	-160	-163	-222	-201	-265	-203	-205	-235	-235	-230	-225	-215	-228	-145	-150	-150	-150	-150	-189	-178
H0.4-LP5-3	-180	-173	-180	-185	-190	-180	-135	-140	-140	-150	-140	-110	-110	-110	-110	-105	-109	-120	-140	-135	-165	-140	-168	-186
H0.4-LP5-3	-190	-190	-190	-190	-190	-190	-115	-125	-125	-130	-130	-180	-190	-195	-190	-185	-188	-140	-150	-150	-150	-150	-168	-159
H0.4-LP5-5	-205	-200	-200	-200	-205	-202	-125	-115	-120	-120	-135	-235	-235	-230	-225	-215	-228	-145	-150	-150	-150	-150	-168	-168
H0.4-LP5-5	-190	-190	-190	-190	-190	-190	-110	-115	-115	-120	-120	-140	-140	-145	-145	-140	-142	-135	-145	-145	-245	-145	-189	-168
H0.4-LP10-3	-110	-115	-120	-120	-120	-117	-145	-130	-132	-197	-230	-210	-125	-120	-120	-120	-122	-135	-148	-150	-165	-178	-386	-389
H0.4-LP10-3	-120	-120	-120	-130	-120	-122	-96	-125	-130	-135	-140	-156	-168	-189	-175	-185	-189	-196	-175	-254	-389	-399	-457	-457
H0.4-LP10-5	-80	-80	-85	-90	-90	-85	-55	-100	-110	-115	-135	-168	-175	-178	-189	-175	-189	-158	-198	-198	-199	-197	-197	-196
H0.4-LP10-5	-85	-85	-85	-80	-80	-83	-75	-110	-115	-115	-130	-189	-189	-189	-197	-198	-189	-196	-189	-198	-189	-199	-178	-197
H0.4-LP15-3	-180	-190	-195	-190	-185	-188	-140	-150	-150	-150	-150	-189	-168	-168	-169	-185	-178	-179	-199	-206	-205	-389	-389	-366
H0.4-LP15-3	-175	-175	-175	-170	-175	-174	-145	-155	-160	-155	-150	-156	-189	-175	-169	-155	-189	-203	-201	-205	-206	-208	-203	-202
H0.4-LP15-5	-180	-190	-190	-185	-190	-187	-120	-130	-135	-135	-145	-188	-198	-187	-187	-187	-198	-185	-186	-185	-186	-189	-198	-185
H0.4-LP15-5	-185	-180	-185	-180	-175	-181	-137	-155	-155	-155	-170	-178	-189	-198	-196	-185	-203	-205	-205	-206	-207	-215	-214	-199
H0.4-L10F20-3	-145	-145	-145	-150	-150	-147	-110	-125	-120	-120	-125	-126	-156	-168	-189	-185	-178	-196	-185	-196	-189	-178	-203	-204
H0.4-L10F20-3	-140	-135	-135	-140	-145	-139	-230	-165	-170	-185	-220	-206	-203	-204	-205	-211	-206	-205	-206	-213	-214	-222	-231	-210
H0.4-L10F20-5	-150	-150	-155	-160	-160	-155	-130	-140	-145	-140	-145	-168	-198	-198	-189	-205	-187	-236	-231	-201	-203	-201	-202	-222
H0.4-L10F20-5	-130	-130	-135	-140	-140	-135	-100	-120	-120	-120	-130	-135	-158	-198	-158	-203	-201	-189	-198	-199	-206	-205	-204	-206

Table B.4 Average half-cell potential values of LP concrete with w/b=0.4 exposed to NaCl solution

HCP, mV	48	50	52	54	56	58	60	62	64	66	68	70	72	74	76	78	80	82	84	86	88	90	92
H0.4-OPC-3	-135	-198	-196	-198	-198	-195	-143	-175	-189	-198	-198	-356	-356	-426	-452	-452	-423	-515	-426	-625	-555	-425	-436
H0.4-OPC-3	-123	-145	-156	-156	-167	-167	-167	-167	-187	-179	-356	-432	-452	-458	-465	-485	-458	-457	-512	-498	-468	-412	-456
H0.4-OPC-5	-168	-189	-189	-189	-189	-178	-178	-178	-178	-178	-178	-204	-201	-206	-204	-205	-256	-248	-432	-359	-452	-462	-452
H0.4-OPC-5	-169	-198	-189	-189	-189	-179	-198	-197	-198	-198	-198	-204	-205	-204	-235	-245	-206	-265	-320	-385	-369	-458	-478
H0.4-LP5-3	-145	-195	-195	-195	-354	-354	-367	-465	-465	-467	-468	-487	-489	-458	-489	-486	-425	-467	-458	-489	-425	-498	-463
H0.4-LP5-3	-198	-197	-192	-194	-194	-194	-365	-478	-543	-543	-544	-544	-569	-458	-459	-469	-478	-598	-458	-589	-578	-578	-562
H0.4-LP5-5	-159	-167	-178	-178	-178	-198	-204	-205	-204	-398	-405	-489	-487	-469	-489	-459	-426	-426	-512	-523	-578	-562	-548
H0.4-LP5-5	-198	-167	-199	-199	-199	-199	-204	-204	-356	-405	-405	-455	-458	-548	-495	-458	-465	-458	-478	-425	-423	-452	-418
H0.4-LP10-3	-496	-486	-455	-433	-455	-455	-455	-455	-455	-455	-465	-465	-469	-436	-425	-425	-475	-475	-494	-415	-436	-436	-489
H0.4-LP10-3	-478	-498	-498	-498	-498	-498	-497	-499	-497	-504	-503	-503	-458	-458	-459	-465	-489	-475	-458	-469	-458	-458	-468
H0.4-LP10-5	-198	-196	-199	-205	-206	-222	-403	-405	-455	-455	-456	-465	-425	-412	-465	-582	-478	-369	-528	-545	-524	-526	-578
H0.4-LP10-5	-207	-208	-205	-206	-207	-256	-403	-444	-432	-467	-477	-476	-458	-458	-462	-415	-489	-526	-458	-562	-548	-548	-569
H0.4-LP15-3	-478	-458	-458	-458	-456	-455	-456	-455	-455	-504	-504	-503	-503	-452	-458	-459	-569	-569	-589	-458	-478	-465	-458
H0.4-LP15-3	-245	-204	-204	-205	-205	-203	-211	-367	-356	-367	-405	-455	-458	-459	-569	-458	-478	-426	-435	-425	-468	-525	-458
H0.4-LP15-5	-203	-189	-205	-233	-399	-405	-432	-444	-433	-434	-435	-435	-436	-425	-468	-425	-436	-459	-458	-457	-521	-521	-457
H0.4-LP15-5	-205	-208	-205	-205	-356	-366	-366	-366	-389	-385	-389	-356	-458	-469	-459	-462	-459	-457	-458	-489	-524	-514	-458
H0.4-L10F20-3	-203	-211	-255	-255	-266	-256	-356	-399	-399	-402	-405	-425	-458	-469	-452	-432	-421	-469	-469	-532	-512	-521	-544
H0.4-L10F20-3	-215	-206	-203	-366	-356	-59	-395	-405	-422	-435	-436	-455	-562	-425	-459	-587	-562	-548	-523	-562	-541	-521	-452
H0.4-L10F20-5	-235	-205	-203	-203	-201	-211	-233	-233	-214	-231	-211	-245	-256	-236	-236	-125	-468	-548	-452	-462	-478	-452	-452
H0.4-L10F20-5	-208	-203	-203	-222	-201	-211	-233	-254	-245	-222	-236	-255	-236	-256	-125	-233	-462	-413	-458	-412	-432	-478	-488

Table B.5 Average half-cell potential values of LP concrete with w/b=0.5 exposed to NaCl solution

HCP, mV	0	2	4	6	8	10	12	14	16	18	20	22	24	26	28	30	32	34	36	38	40	42	44	46
H0.5-OPC-3	-215	-220	-215	-210	-220	-216	-170	-222	-236	-236	-245	-201	-206	-203	-201	-205	-212	-215	-198	-189	-206	-205	-204	-208
H0.5-OPC-3	-195	-195	-195	-195	-200	-196	-165	-180	-173	-180	-175	-189	-203	-201	-205	-222	-231	-212	-245	-232	-256	-198	-187	-185
H0.5-OPC-5	-195	-200	-205	-205	-205	-202	-150	-155	-155	-150	-150	-203	-230	-265	-230	-212	-214	-213	-215	-255	-203	-201	-203	-212
H0.5-OPC-5	-235	-235	-230	-225	-215	-228	-145	-150	-150	-150	-150	-204	-189	-125	-195	-189	-198	-197	-189	-196	-193	-178	-196	-201
H0.5-LP5-3	-150	-150	-155	-155	-160	-154	-155	-160	-160	-160	-295	-204	-205	-204	-206	-215	-201	-206	-204	-205	-209	-201	-205	-356
H0.5-LP5-3	-150	-150	-150	-150	-150	-150	-190	-236	-214	-215	-231	-205	-206	-245	-235	-203	-201	-205	-213	-215	-201	-245	-359	-389
H0.5-LP5-5	-135	-135	-130	-135	-135	-134	-145	-170	-170	-175	-205	-205	-204	-206	-213	-204	-205	-256	-203	-201	-230	-201	-201	-201
H0.5-LP5-5	-200	-200	-200	-195	-190	-197	-175	-175	-175	-260	-222	-230	-215	-215	-230	-256	-230	-215	-207	-289	-203	-204	-245	-236
H0.5-LP10-3	-195	-200	-205	-205	-200	-201	-155	-165	-165	-165	-165	-165	-105	-159	-233	-256	-212	-203	-201	-389	-455	-489	-489	-444
H0.5-LP10-3	-165	-165	-160	-160	-165	-163	-180	-185	-190	-185	-190	-156	-203	-205	-204	-205	-222	-359	-458	-478	-489	-499	-489	-425
H0.5-LP10-5	-175	-175	-175	-170	-170	-173	-170	-170	-170	-170	-170	-178	-189	-178	-189	-178	-188	-199	-178	-185	-176	-175	-174	-175
H0.5-LP10-5	-150	-150	-150	-145	-140	-147	-145	-230	-190	-222	-230	-214	-201	-215	-203	-256	-205	-203	-204	-205	-205	-205	-206	-257
H0.5-LP15-3	-165	-165	-165	-170	-170	-167	-170	-170	-170	-165	-160	-168	-189	-178	-185	-389	-355	-369	-378	-457	-489	-489	-452	-457
H0.5-LP15-3	-110	-110	-110	-110	-105	-109	-120	-140	-135	-165	-140	-201	-201	-200	-203	-201	-322	-389	-378	-399	-458	-489	-499	-474
H0.5-LP15-5	-110	-115	-110	-105	-110	-110	-135	-243	-320	-140	-222	-235	-201	-202	-278	-222	-203	-205	-204	-222	-203	-298	-230	-399
H0.5-LP15-5	-85	-80	-80	-85	-85	-83	-105	-130	-140	-295	-150	-201	-230	-205	-245	-213	-233	-201	-233	-256	-212	-245	-278	-222
H0.5-L10F20-3	-165	-170	-170	-170	-170	-169	-151	-155	-150	-145	-150	-158	-168	-199	-186	-178	-159	-169	-202	-203	-359	-389	-399	-458
H0.5-L10F20-3	-90	-95	-95	-95	-90	-93	-110	-135	-140	-145	-160	-189	-156	-189	-199	-203	-206	-256	-210	-230	-215	-245	-388	-378
H0.5-L10F20-5	-130	-140	-145	-140	-140	-139	-140	-150	-150	-150	-150	-165	-199	-203	-204	-206	-205	-204	-233	-156	-266	-204	-255	-205
H0.5-L10F20-5	-160	-160	-160	-160	-160	-160	-229	-242	-230	-150	-250	-205	-206	-256	-230	-212	-212	-213	-230	-245	-201	-230	-222	-201

Table B.5 Average half-cell potential values of LP concrete with w/b=0.5 exposed to NaCl solution

HCP, mV	48	50	52	54	56	58	60	62	64	66	68	70	72	74	76	78	80	82	84	86	88	90	92
H0.5-OPC-3	-222	-230	-230	-222	-201	-256	-233	-356	-333	-396	-396	-386	-365	-452	-456	-412	-478	-451	-456	-458	-458	-457	-478
H0.5-OPC-3	-157	-198	-233	-245	-245	-212	-233	-233	-256	-245	-396	-405	-455	-412	-421	-412	-436	-258	-536	-529	-425	-462	-469
H0.5-OPC-5	-235	-245	-255	-255	-245	-255	-256	-256	-256	-233	-245	-245	-265	-321	-398	-458	-462	-478	-456	-412	-512	-545	-415
H0.5-OPC-5	-203	-204	-233	-212	-212	-233	-256	-233	-233	-212	-254	-345	-356	-456	-458	-475	-451	-412	-478	-451	-462	-512	-532
H0.5-LP5-3	-389	-457	-457	-457	-457	-458	-477	-456	-499	-502	-506	-522	-525	-523	-542	-452	-545	-523	-526	-458	-459	-523	-524
H0.5-LP5-3	-458	-477	-455	-458	-502	-502	-458	-503	-504	-503	-488	-459	-458	-458	-459	-58	-456	-452	-455	-412	-541	-512	-532
H0.5-LP5-5	-203	-245	-255	-233	-222	-389	-422	-450	-455	-426	-458	-478	-458	-415	-475	-475	-475	-457	-489	-412	-465	-452	-463
H0.5-LP5-5	-215	-235	-255	-245	-245	-366	-366	-359	-399	-402	-405	-455	-455	-455	-462	-458	-469	-412	-458	-512	-523	-458	-465
H0.5-LP10-3	-501	-477	-477	-477	-485	-495	-458	-458	-459	-459	-458	-466	-466	-451	-512	-458	-459	-456	-458	-457	-412	-456	-458
H0.5-LP10-3	-477	-475	-488	-488	-489	-478	-489	-458	-458	-458	-469	-423	-512	-422	-452	-412	-452	-522	-452	-412	-478	-452	-155
H0.5-LP10-5	-179	-165	-405	-402	-369	-405	-458	-456	-456	-457	-458	-589	-522	-536	-593	-555	-541	-452	-489	-492	-498	-412	-458
H0.5-LP10-5	-205	-206	-203	-399	-399	-389	-405	-423	-456	-458	-456	-458	-455	-458	-456	-457	-452	-458	-412	-456	-432	-468	-495
H0.5-LP15-3	-478	-459	-458	-459	-458	-458	-458	-458	-498	-489	-502	-487	-458	-459	-459	-458	-456	-452	-456	-521	-541	-458	-523
H0.5-LP15-3	-458	-478	-589	-458	-459	-465	-457	-458	-459	-456	-458	-478	-458	-589	-459	-569	-524	-415	-455	-458	-458	-452	-465
H0.5-LP15-5	-458	-478	-458	-458	-458	-489	-499	-499	-489	-459	-502	-502	-458	-458	-459	-458	-458	-457	-412	-523	-452	-423	-452
H0.5-LP15-5	-246	-359	-458	-458	-458	-459	-465	-425	-435	-458	-478	-498	-465	-458	-478	-425	-423	-459	-458	-458	-548	-495	-458
H0.5-L10F20-3	-478	-489	-489	-465	-458	-458	-459	-459	-465	-465	-468	-469	-475	-475	-494	-415	-436	-458	-469	-469	-436	-425	-425
H0.5-L10F20-3	-399	-458	-489	-489	-489	-498	-478	-426	-458	-486	-496	-436	-489	-475	-458	-469	-458	-455	-489	-458	-458	-459	-465
H0.5-L10F20-5	-204	-403	-469	-469	-485	-459	-489	-498	-498	-496	-498	-503	-478	-369	-528	-545	-524	-458	-488	-425	-412	-465	-582
H0.5-L10F20-5	-201	-355	-455	-458	-478	-305	-489	-358	-498	-498	-489	-465	-489	-526	-458	-562	-548	-435	-485	-458	-458	-462	-415

Table B.6 Average half-cell potential values of LP concrete with w/b=0.6 exposed to NaCl solution

HCP, mV	0	2	4	6	8	10	12	14	16	18	20	22	24	26	28	30	32	34	36	38	40	42	44	46
H0.6-OPC-3	-120	-130	-132	-127	-141	-128	-195	-250	-206	-205	-211	-235	-256	-201	-230	-214	-256	-258	-245	-255	-211	-215	-230	-245
H0.6-OPC-3	-140	-140	-145	-145	-140	-142	-135	-145	-145	-245	-145	-154	-156	-158	-198	-201	-203	-205	-204	-206	-205	-255	-233	-201
H0.6-OPC-5	-125	-130	-135	-135	-135	-132	-140	-150	-153	-285	-155	-125	-254	-245	-256	-289	-245	-256	-222	-230	-248	-278	-248	-256
H0.6-OPC-5	-115	-115	-115	-115	-120	-116	-150	-222	-236	-255	-222	-245	-245	-258	-258	-259	-258	-258	-258	-233	-231	-215	-248	-256
H0.6-LP5-3	-120	-125	-128	-119	-120	-123	-155	-170	-175	-150	-175	-255	-215	-377	-359	-366	-389	-452	-488	-455	-455	-465	-458	-459
H0.6-LP5-3	-150	-155	-150	-145	-135	-147	-155	-160	-165	-270	-333	-359	-489	-485	-478	-458	-455	-452	-469	-485	-478	-489	-458	-458
H0.6-LP5-5	-155	-155	-155	-150	-150	-153	-309	-258	-145	-255	-255	-265	-245	-255	-235	-204	-205	-259	-244	-396	-389	-452	-452	-452
H0.6-LP5-5	-150	-150	-150	-150	-150	-150	-145	-150	-150	-165	-160	-201	-233	-201	-203	-212	-219	-208	-269	-245	-369	-377	-421	-412
H0.6-LP10-3	-165	-165	-165	-170	-175	-168	-160	-355	-359	-369	-389	-458	-477	-455	-426	-451	-458	-453	-412	-478	-489	-465	-426	-487
H0.6-LP10-3	-165	-165	-160	-155	-150	-159	-160	-160	-165	-369	-401	-399	-398	-412	-458	-478	-459	-489	-499	-452	-412	-399	-458	-478
H0.6-LP10-5	-140	-135	-135	-130	-135	-135	-145	-145	-145	-369	-358	-399	-378	-458	-452	-478	-412	-456	-458	-412	-478	-478	-478	-412
H0.6-LP10-5	-155	-160	-155	-160	-155	-157	-150	-162	-165	-387	-458	-412	-456	-423	-459	-456	-421	-412	-478	-412	-412	-452	-412	-423
H0.6-LP15-3	-90	-96	-102	-120	-100	-95	-130	-160	-160	-401	-458	-478	-412	-465	-432	-465	-431	-498	-491	-435	-468	-435	-495	-465
H0.6-LP15-3	-115	-110	-110	-110	-110	-111	-120	-140	-147	-165	-369	-359	-399	-402	-412	-412	-412	-419	-432	-468	-457	-489	-503	-457
H0.6-LP15-5	-125	-125	-120	-120	-120	-122	-135	-148	-150	-165	-236	-215	-268	-301	-399	-402	-412	-458	-477	-488	-495	-458	-432	-467
H0.6-LP15-5	-150	-150	-150	-150	-145	-149	-145	-150	-150	-150	-155	-256	-222	-399	-452	-489	-475	-455	-412	-469	-489	-476	-452	-498
H0.6-L10F20-3	-130	-135	-148	-134	-122	-134	-140	-150	-150	-150	-155	-366	-399	-402	-432	-436	-455	-489	-477	-469	-423	-495	-458	-499
H0.6-L10F20-3	-145	-145	-140	-140	-140	-142	-145	-150	-150	-150	-205	-324	-399	-458	-469	-458	-422	-456	-477	-431	-496	-485	-476	-416
H0.6-L10F20-5	-150	-150	-150	-150	-150	-150	-190	-160	-155	-150	-170	-236	-265	-245	-288	-399	-458	-478	-465	-396	-398	-489	-456	-457
H0.6-L10F20-5	-100	-105	-105	-105	-100	-103	-120	-135	-137	-150	-145	-222	-245	-278	-222	-387	-399	-406	-421	-456	-478	-444	-458	-468

Table B.6 Average half-cell potential values of LP concrete with w/b=0.6 exposed to NaCl solution

HCP, mV	48	50	52	54	56	58	60	62	64	66	68	70	72	74	76	78	80	82	84	86	88	90	92
H0.6-OPC-3	-255	-256	-289	-399	-388	-405	-469	-485	-485	-478	-475	-458	-569	-569	-589	-458	-478	-459	-485	-503	-452	-458	-459
H0.6-OPC-3	-201	-203	-389	-458	-458	-458	-478	-425	-462	-488	-463	-488	-478	-426	-435	-425	-468	-498	-485	-458	-459	-569	-458
H0.6-OPC-5	-259	-256	-268	-266	-259	-266	-299	-389	-369	-389	-396	-405	-436	-459	-458	-457	-521	-477	-465	-436	-425	-468	-425
H0.6-OPC-5	-278	-259	-269	-268	-269	-265	-236	-202	-256	-425	-366	-425	-498	-496	-485	-489	-493	-477	-498	-458	-469	-459	-462
H0.6-LP5-3	-469	-485	-489	-489	-489	-489	-489	-478	-456	-489	-469	-436	-458	-548	-495	-458	-459	-456	-458	-489	-526	-458	-562
H0.6-LP5-3	-459	-459	-458	-499	-502	-458	-489	-478	-479	-498	-489	-469	-469	-436	-425	-425	-489	-459	-502	-458	-548	-495	-458
H0.6-LP5-5	-453	-458	-469	-489	-489	-489	-498	-478	-489	-469	-493	-482	-458	-458	-459	-465	-435	-458	-478	-469	-436	-425	-425
H0.6-LP5-5	-425	-455	-489	-489	-496	-496	-436	-492	-491	-482	-493	-506	-425	-412	-465	-582	-465	-465	-468	-458	-458	-459	-465
H0.6-LP10-3	-459	-458	-488	-488	-488	-488	-488	-488	-458	-485	-496	-485	-458	-458	-462	-415	-458	-486	-496	-425	-412	-465	-582
H0.6-LP10-3	-412	-435	-485	-496	-485	-485	-485	-478	-485	-496	-485	-489	-503	-452	-458	-459	-498	-496	-498	-458	-458	-462	-415
H0.6-LP10-5	-456	-459	-485	-485	-485	-485	-486	-482	-482	-482	-481	-489	-458	-459	-569	-458	-498	-498	-489	-503	-452	-458	-459
H0.6-LP10-5	-465	-498	-485	-485	-485	-496	-495	-489	-493	-472	-493	-465	-436	-425	-468	-425	-548	-495	-458	-458	-459	-569	-458
H0.6-LP15-3	-488	-477	-465	-465	-489	-485	-492	-493	-491	-482	-478	-492	-458	-469	-459	-462	-436	-425	-425	-436	-425	-468	-425
H0.6-LP15-3	-462	-477	-498	-496	-485	-489	-493	-506	-506	-509	-507	-509	-465	-458	-478	-425	-458	-459	-465	-458	-469	-459	-462
H0.6-LP15-5	-495	-435	-496	-485	-496	-485	-496	-485	-496	-485	-482	-482	-475	-475	-494	-415	-412	-465	-582	-458	-459	-456	-458
H0.6-LP15-5	-493	-476	-496	-485	-485	-485	-485	-485	-475	-496	-475	-478	-489	-475	-458	-469	-458	-462	-415	-499	-489	-459	-502
H0.6-L10F20-3	-503	-478	-506	-503	-489	-504	-475	-489	-407	-509	-508	-507	-478	-369	-528	-545	-452	-458	-459	-425	-435	-458	-478
H0.6-L10F20-3	-489	-468	-496	-466	-489	-489	-478	-485	-486	-485	-485	-478	-489	-526	-458	-562	-459	-569	-458	-459	-465	-465	-468
H0.6-L10F20-5	-478	-459	-485	-498	-485	-496	-475	-485	-496	-475	-496	-455	-569	-569	-589	-458	-425	-468	-425	-426	-458	-486	-496
H0.6-L10F20-5	-478	-468	-469	-485	-478	-495	-485	-485	-485	-495	-478	-488	-478	-426	-435	-425	-469	-459	-462	-498	-498	-496	-498

Appendix C

Corrosion current density test data

Table C.1 Average corrosion current density values of concrete exposed to CO_2

Mix \ Days	0	7	14	21	28	35	42	49	56	63	70	77
I0.4-OPC	0	0	0.01	0	0.03	0.04	0.03	0.03	0.02	0.01	0.02	0
I0.4-FA20	0	0	0.01	0.03	0.02	0	0.01	0.02	0.13	0.23	0.23	0.14
I0.4-FA50	0.01	0	0	0	0	0.13	0.13	0.25	0.21	0.22	0.46	0.32
I0.5-OPC	0	0.01	0.01	0.02	0.01	0.02	0.02	0.02	0.01	0	0.01	0
I0.5-FA20	0	0	0.04	0.09	0.1	0.12	0.15	0.15	0.14	0.22	0.24	0.32
I0.5-FA50	0	0.04	0.09	0.08	0.13	0.1	0.15	0.16	0.16	0.15	0.18	0.22
I0.6-OPC	-0	0.01	0.01	0	0	0.02	0.01	0.04	0.09	0.12	0.18	0.24
I0.6-FA20	0	0	0.04	0.08	0.14	0.16	0.16	0.23	0.22	0.21	0.45	0.32
I0.6-FA50	0	0.05	0.16	0.19	0.24	0.22	0.34	0.32	0.33	0.34	0.21	0.24

Table C.2 Average corrosion current density values of concrete exposed to combined cyclic CO_2 and NaCl

Mix \ Days	0	7	14	21	28	35	42	49	56	63	70	77	84
I0.4-OPC	0	0.03	0	0.04	0.05	0.02	0.01	0.03	0.02	0.24	0.22	0.45	0.13
I0.4-FA20	0.02	0	0.04	0	0.05	0.03	0.06	0.01	0.01	0.32	0.19	0.23	0.22
I0.4-FA50	0.01	0.02	0.01	0	0.04	0.02	0	0.21	0.34	0.33	0.44	-	-
I0.5-OPC	0	0.01	0.01	0.02	0.23	0.25	0.43	0.33	-	-	-	-	-
I0.5-FA20	0	0	0.04	0.34	0.42	0.45	0.44	-	-	-	-	-	-
I0.5-FA50	0	0.25	0.35	0.24	0.45	-	-	-	-	-	-	-	-
I0.6-OPC	0.01	0.04	0.01	0.21	0.26	0.35	0.46	-	-	-	-	-	-
I0.6-FA20	0.01	0.24	0.35	0.46	0.44	-	-	-	-	-	-	-	-
I0.6-FA50	0.19	0.24	0.29	0.35	-	-	-	-	-	-	-	-	-

Table C.3 Average corrosion current density values of fly-ash concrete exposed to NaCl solution

uA/cm^2	0	2	3	4	5	6	7	8	9	10	11	12	13	14	15	16	17	18	19	20	21	22	23	24
I0.4-OPC-3	0.01	0.12	0.02	0.02	0.02	0.02	0.02	0.05	0.05	0.02	0.06	0.04	0.05	0.05	0.05	0.05	0.14	0.17	0.10	0.01	0.01	0.09	0.07	0.08
I0.4-OPC-5	0.01	0.09	0.08	0.09	0.08	0.08	0.08	0.09	0.09	0.10	0.07	0.08	0.08	0.08	0.08	0.08	0.06	0.05	0.05	0.04	0.04	0.03	0.04	0.03
I0.4-FA20-3	0.05	0.07	0.05	0.07	0.06	0.06	0.06	0.06	0.06	0.06	0.06	0.06	0.05	0.05	0.05	0.05	0.05	0.04	0.04	0.04	0.04	0.03	0.03	0.03
I0.4-FA20-5	0.03	0.06	0.04	0.05	0.05	0.05	0.05	0.05	0.06	0.06	0.05	0.05	0.04	0.05	0.05	0.05	0.04	0.04	0.04	0.03	0.03	0.03	0.03	0.02
I0.4-FA30-3	0.01	0.10	0.02	0.02	0.02	0.02	0.02	0.02	0.02	0.02	0.00	0.00	0.00	0.00	0.00	0.00	0.00	0.00	0.00	0.00	0.04	0.00	0.01	0.00
I0.4-FA30-5	0.00	0.02	0.02	0.02	0.02	0.02	0.02	0.02	0.03	0.11	0.19	0.32	0.43	0.34	0.34	0.34	0.11	0.12	0.12	0.12	0.01	0.01	0.01	0.01
I0.4-FA50-3	0.04	0.09	0.00	0.00	0.00	0.01	0.01	0.02	0.02	0.03	0.08	0.08	0.08	0.08	0.08	0.08	0.87	0.46	0.44	0.14	0.01	0.21	0.22	0.38
I0.4-FA50-5	0.03	0.01	0.02	0.02	0.02	0.02	0.02	0.02	0.02	0.03	0.03	0.03	0.03	0.03	0.03	0.03	0.15	0.18	0.16	0.19	0.09	0.04	0.09	0.09
I0.5-OPC-3	0.00	0.04	0.04	0.04	0.04	0.04	0.04	0.04	0.04	0.03	0.03	0.03	0.03	0.03	0.03	0.03	0.01	0.00	0.02	0.02	0.02	0.02	0.03	0.02
I0.5-OPC-5	0.01	0.03	0.04	0.04	0.04	0.04	0.03	0.04	0.03	0.03	0.03	0.03	0.03	0.02	0.02	0.02	0.01	0.00	0.01	0.01	0.01	0.02	0.02	0.02
I0.5-FA20-3	0.02	0.01	0.01	0.02	0.02	0.02	0.02	0.02	0.02	0.02	0.02	0.01	0.01	0.02	0.02	0.02	0.02	0.01	0.02	0.02	0.02	0.02	0.02	0.02
I0.5-FA20-5	0.04	0.03	0.03	0.02	0.02	0.03	0.03	0.02	0.02	0.02	0.02	0.01	0.02	0.02	0.02	0.02	0.01	0.01	0.02	0.56	0.77	0.78	0.76	0.73
I0.5-FA30-3	0.04	0.04	0.03	0.03	0.03	0.00	0.01	0.00	0.01	0.02	0.02	0.02	0.01	0.02	0.02	0.02	0.01	0.01	0.02	0.02	0.01	0.02	0.02	0.02
I0.5-FA30-5	0.05	0.04	0.04	0.05	0.04	0.04	0.04	0.03	0.03	0.03	0.03	0.03	0.03	0.03	0.03	0.03	0.03	0.03	0.03	0.03	0.03	0.03	0.03	0.02
I0.5-FA50-3	0.01	0.01	0.01	0.01	0.01	0.01	0.02	0.02	0.02	0.01	0.01	0.02	0.27	0.34	0.34	0.34	1.14	1.30	1.19	0.98	0.86	0.78	0.72	0.73
I0.5-FA50-5	0.01	0.01	0.01	0.01	0.02	0.01	0.01	0.01	0.01	0.02	0.01	0.01	0.03	0.02	0.01	0.01	0.53	0.39	0.56	0.54	0.74	0.51	0.50	0.41
I0.6-OPC-3	0.03	0.03	0.03	0.03	0.03	0.03	0.03	0.02	0.02	0.02	0.02	0.02	0.02	0.02	0.02	0.02	0.02	0.02	0.02	0.02	0.02	0.02	0.02	0.01
I0.6-OPC-5	0.03	0.11	0.03	0.03	0.04	0.02	0.02	0.02	0.02	0.02	0.01	0.01	0.01	0.01	0.02	0.01	0.01	0.00	0.01	0.01	0.00	0.00	0.00	0.00
I0.6-FA20-3	0.04	0.07	0.03	0.04	0.04	0.04	0.04	0.02	0.01	0.02	0.01	0.01	0.01	0.01	0.01	0.01	0.01	0.00	0.01	0.01	0.01	0.01	0.01	0.01
I0.6-FA20-5	0.01	0.01	0.01	-0.03	0.01	0.00	0.00	0.00	0.00	0.00	0.01	0.05	0.06	0.06	0.06	0.06	0.03	0.04	0.02	0.02	0.03	0.02	0.02	0.02
I0.6-FA30-3	0.02	0.03	0.03	0.00	0.02	0.01	0.01	0.01	0.01	0.01	0.01	0.01	0.03	0.03	0.03	0.03	0.17	0.30	0.31	0.42	0.47	0.49	0.46	0.43
I0.6-FA30-5	0.09	0.00	-0.03	0.00	-0.01	0.00	0.00	0.00	0.00	0.00	0.00	0.00	0.00	0.00	0.00	0.00	0.00	0.00	0.00	0.00	0.00	0.00	0.00	0.06
I0.6-FA50-3	0.03	-0.10	-0.15	0.24	0.11	0.24	0.29	0.33	0.44	0.45	0.60	0.70	0.85	0.68	0.68	1.06	1.06	1.10	1.10	1.22	1.36	1.37	1.22	1.15
I0.6-FA50-5	0.01	0.02	0.02	0.05	0.02	0.04	0.04	0.03	0.03	0.02	0.07	0.26	0.38	0.30	0.30	0.86	0.86	0.97	0.97	1.06	1.19	1.19	1.09	1.11

Table C.3 Average corrosion current density values of fly-ash concrete exposed to NaCl solution

uA/cm^2	25	26	27	28	30	32	34	36	38	40	42	44	46	48	50	52	54	56	58	60	62	64	66	68
I0.4-OPC-3	0.06	0.06	0.01	0.04	0.04	0.03	0.03	0.03	0.01	0.03	0.01	0.04	0.06	0.03	0.01	0.05	0.06	0.07	0.03	0.07	0.04	0.45	0.55	0.56
I0.4-OPC-5	0.02	0.03	0.02	0.01	0.01	0.01	0.01	0.00	0.03	0.05	0.06	0.03	0.05	0.02	0.07	0.08	0.03	0.02	0.05	0.06	0.09	0.02	0.09	0.24
I0.4-FA20-3	0.03	0.03	0.02	0.01	0.00	0.00	0.00	0.00	0.03	0.35	0.34	0.56	0.43	0.76	0.24	0.33	0.54	0.34	0.53	0.55	0.54	0.65	0.34	0.22
I0.4-FA20-5	0.02	0.02	0.02	0.01	0.01	0.01	0.01	0.01	0.03	0.02	0.04	0.06	0.04	0.07	0.45	0.55	0.50	0.54	0.56	0.34	0.67	0.55	0.54	0.35
I0.4-FA30-3	0.02	0.03	0.32	0.31	0.21	0.61	0.67	0.57	0.45	0.55	0.34	0.64	0.67	0.65	0.78	0.34	0.33	0.32	0.23	0.21	0.14	0.23	0.21	0.45
I0.4-FA30-5	0.50	0.51	0.46	0.37	0.78	0.69	0.72	0.65	0.74	0.75	0.45	0.34	0.43	0.23	0.33	0.34	0.64	0.33	0.42	0.53	0.64	0.34	0.44	0.43
I0.4-FA50-3	0.49	0.49	0.34	0.32	0.26	0.23	0.21	0.38	0.32	0.45	0.34	0.55	0.53	0.43	0.43	0.55	0.23	0.45	0.43	0.23	0.22	0.54	0.22	0.11
I0.4-FA50-5	0.11	0.08	0.03	0.10	0.55	0.65	0.55	0.50	0.34	0.45	0.53	0.33	0.43	0.32	0.54	0.34	0.55	0.65	0.29	0.39	0.32	0.22	0.11	0.22
I0.5-OPC-3	0.02	0.03	0.03	0.02	0.01	0.04	0.01	0.01	0.04	0.05	0.00	0.00	0.03	0.56	0.45	0.55	0.50	0.54	0.56	0.34	0.67	0.55	0.54	0.35
I0.5-OPC-5	0.01	0.02	0.01	0.01	0.01	0.01	0.01	0.01	0.00	0.00	0.00	0.02	0.02	0.00	0.00	0.00	0.09	0.66	0.45	0.43	0.55	0.78	0.23	0.45
I0.5-FA20-3	0.02	0.02	0.03	0.05	1.77	1.94	1.95	1.97	0.45	0.35	0.55	0.78	1.00	0.98	0.34	0.22	0.23	0.89	0.45	0.55	0.60	0.45	0.55	0.27
I0.5-FA20-5	0.80	0.97	1.30	1.05	1.75	1.74	1.29	1.08	0.45	0.56	0.66	0.87	0.89	0.78	0.89	0.96	0.66	0.75	0.89	0.94	0.57	0.77	0.78	0.34
I0.5-FA30-3	0.02	0.02	0.02	0.02	0.13	0.10	0.00	0.16	0.57	0.67	0.55	0.65	0.67	0.45	0.67	0.87	0.24	0.13	0.04	0.45	0.67	0.45	0.89	0.45
I0.5-FA30-5	0.02	0.02	0.02	0.02	0.05	0.03	0.02	0.04	0.06	0.56	0.45	0.64	0.78	0.68	0.45	0.53	0.45	0.43	0.78	0.76	0.56	0.67	0.54	0.34
I0.5-FA50-3	0.73	0.69	0.62	0.54	0.47	0.41	0.30	0.32	0.23	0.43	0.34	0.23	0.56	0.68	0.89	0.67	0.56	0.34	0.56	0.78	0.34	0.23	0.43	0.44
I0.5-FA50-5	0.35	0.55	0.48	0.22	0.58	0.66	0.68	0.50	0.50	0.45	0.54	0.50	0.53	0.53	0.34	0.53	0.57	0.67	0.65	0.45	0.76	0.54	0.65	0.67
I0.6-OPC-3	0.01	0.02	0.01	0.01	0.01	0.01	0.01	0.01	0.00	0.00	0.00	0.56	0.97	1.20	1.40	0.89	0.56	0.99	1.45	1.22	1.33	1.56	0.87	0.56
I0.6-OPC-5	0.00	0.00	0.00	0.00	0.00	0.00	0.00	0.00	0.04	0.05	0.06	0.05	0.05	0.06	0.06	0.07	0.04	0.05	0.03	0.05	0.08	0.78	0.77	0.65
I0.6-FA20-3	0.02	0.01	0.02	0.02	0.07	0.08	0.08	0.08	0.98	0.99	0.89	0.78	0.99	0.89	0.78	0.87	0.99	1.50	0.34	0.35	0.34	0.44	0.43	0.60
I0.6-FA20-5	0.01	0.01	0.01	0.00	0.01	0.01	0.00	0.00	0.00	0.00	0.00	0.00	0.00	0.56	0.56	0.54	0.56	0.67	0.44	0.45	0.67	0.32	0.12	0.11
I0.6-FA30-3	0.44	0.46	0.44	0.39	0.60	0.59	0.62	0.57	0.56	0.45	0.54	0.34	0.67	0.78	0.23	0.66	0.23	0.54	0.55	0.45	0.67	0.54	0.66	0.21
I0.6-FA30-5	0.02	0.05	0.12	0.20	0.18	0.15	0.23	0.37	0.34	0.33	0.55	0.44	0.44	0.45	0.56	0.55	0.23	0.43	0.44	0.55	0.76	0.34	0.23	0.22
I0.6-FA50-3	1.18	1.16	1.17	0.91	0.81	0.65	0.54	0.37	0.33	0.43	0.33	0.67	0.54	0.55	0.45	0.64	0.65	0.45	0.23	0.66	0.55	0.56	0.57	0.54
I0.6-FA50-5	1.79	0.95	1.11	0.91	0.99	1.00	1.04	0.96	0.56	0.89	0.78	0.67	0.77	0.89	0.67	0.88	0.56	0.45	0.88	0.39	0.72	0.58	0.48	0.98

Table C.4 Average corrosion current density values of LP concrete with w/b=0.4 exposed to NaCl solution

uA/cm^2	0	2	4	6	8	10	12	14	16	18	20	22	24	26	28	30	32	34	36	38	40	42	44	46
I0.4-OPC-3	0.01	0.01	0.01	0.01	0.01	0.01	0.09	0.08	0.09	0.08	0.08	0.08	0.09	0.09	0.10	0.07	0.08	0.08	0.08	0.08	0.08	0.06	0.05	0.05
I0.4-OPC-3	0.05	0.05	0.05	0.05	0.05	0.08	0.06	0.05	0.05	0.04	0.04	0.09	0.08	0.09	0.08	0.08	0.08	0.09	0.09	0.10	0.07	0.08	0.08	0.08
I0.4-OPC-5	0.08	0.08	0.08	0.08	0.08	0.05	0.07	0.05	0.07	0.06	0.06	0.06	0.06	0.06	0.06	0.06	0.06	0.05	0.05	0.05	0.05	0.05	0.04	0.04
I0.4-OPC-5	0.01	0.01	0.01	0.01	0.01	0.02	0.02	0.02	0.02	0.02	0.01	0.03	0.02	0.03	0.02	0.02	0.02	0.03	0.01	0.02	0.03	0.02	0.02	0.03
I0.4-LP5-3	0.00	0.00	0.00	0.00	0.00	0.03	0.04	0.03	0.02	0.03	0.02	0.01	0.01	0.01	0.01	0.00	0.03	0.05	0.06	0.03	0.05	0.02	0.07	0.01
I0.4-LP5-3	0.00	0.00	0.00	0.00	0.00	0.08	0.03	0.02	0.05	0.06	0.09	0.02	0.09	0.03	0.01	0.09	0.08	0.09	0.08	0.08	0.08	0.09	0.09	0.10
I0.4-LP5-5	0.00	0.00	0.00	0.00	0.00	0.02	0.01	0.01	0.01	0.02	0.02	0.01	0.02	0.01	0.01	0.01	0.01	0.02	0.01	0.01	0.02	0.01	0.01	0.02
I0.4-LP5-5	0.00	0.00	0.00	0.00	0.00	0.02	0.01	0.01	0.01	0.01	0.01	0.01	0.02	0.02	0.01	0.02	0.01	0.01	0.02	0.03	0.03	0.02	0.01	0.01
I0.4-LP10-3	0.02	0.02	0.02	0.02	0.02	0.01	0.09	0.08	0.09	0.08	0.08	0.08	0.09	0.02	0.03	0.04	0.05	0.01	0.01	0.01	0.04	0.02	0.23	0.23
I0.4-LP10-3	0.00	0.00	0.00	0.00	0.00	0.01	0.02	0.02	0.00	0.00	0.02	0.03	0.02	0.02	0.02	0.01	0.01	0.02	0.01	0.05	0.35	0.34	0.43	0.32
I0.4-LP10-5	0.00	0.00	0.00	0.00	0.00	0.01	0.01	0.02	0.02	0.03	0.02	0.02	0.01	0.01	0.02	0.03	0.05	0.05	0.05	0.05	0.05	0.05	0.05	0.03
I0.4-LP10-5	0.00	0.00	0.00	0.00	0.00	0.02	0.00	0.02	0.03	0.02	0.00	0.00	0.00	0.20	0.00	0.02	0.01	0.03	0.08	0.05	0.04	0.05	0.02	0.04
I0.4-LP15-3	0.00	0.00	0.00	0.00	0.00	0.01	0.01	0.01	0.01	0.02	0.01	0.01	0.01	0.01	0.02	0.01	0.01	0.03	0.02	0.01	0.01	0.23	0.34	0.35
I0.4-LP15-3	0.00	0.00	0.00	0.00	0.00	0.03	0.03	0.03	0.03	0.03	0.04	0.05	0.04	0.04	0.04	0.03	0.02	0.04	0.04	0.02	0.04	0.04	0.02	0.03
I0.4-LP15-5	0.00	0.00	0.00	0.00	0.00	0.03	0.03	0.03	0.03	0.01	0.09	0.08	0.09	0.08	0.08	0.08	0.09	0.09	0.10	0.07	0.08	0.08	0.08	0.08
I0.4-LP15-5	0.00	0.00	0.00	0.00	0.00	0.00	0.00	0.00	0.00	0.02	0.02	0.02	0.02	0.01	0.01	0.01	0.01	0.02	0.02	0.02	0.03	0.04	0.03	0.02
I0.4-L10F20-3	0.00	0.00	0.00	0.00	0.00	0.00	0.00	0.00	0.00	0.00	0.00	0.00	0.00	0.00	0.00	0.03	0.02	0.02	0.02	0.02	0.01	0.01	0.01	0.01
I0.4-L10F20-3	0.00	0.00	0.00	0.00	0.00	0.03	0.04	0.08	0.08	0.08	0.08	0.05	0.07	0.05	0.07	0.03	0.02	0.02	0.02	0.02	0.01	0.03	0.02	0.02
I0.4-L10F20-5	0.00	0.00	0.00	0.00	0.00	0.03	0.03	0.04	0.03	0.02	0.00	0.00	0.00	0.00	0.04	0.02	0.20	0.03	0.02	0.02	0.04	0.04	0.04	0.04
I0.4-L10F20-5	0.00	0.00	0.00	0.00	0.00	0.02	0.00	0.00	0.00	0.00	0.00	0.00	0.00	0.03	0.03	0.03	0.03	0.02	0.02	0.03	0.03	0.02	0.03	0.03

Table C.4 Average corrosion current density values of LP concrete with w/b=0.4 exposed to NaCl solution

uA/cm^2	48	50	52	54	56	58	60	62	64	66	68	70	72	74	76	78	80	82	84	86	88	90	92
I0.4-OPC-3	0.04	0.04	0.01	0.01	0.01	0.02	0.01	0.01	0.02	0.01	0.01	0.23	0.64	0.23	0.12	0.59	0.03	0.21	0.55	0.01	0.45	0.89	0.66
I0.4-OPC-3	0.08	0.03	0.09	0.08	0.09	0.08	0.08	0.08	0.09	0.09	0.10	0.35	0.67	0.60	0.80	1.20	1.50	1.90	2.30	2.80	2.40	2.60	2.10
I0.4-OPC-5	0.04	0.04	0.00	0.00	0.00	0.00	0.00	0.03	0.04	0.03	0.02	0.03	0.02	0.03	0.05	0.01	0.01	0.00	0.23	0.32	0.12	0.35	0.68
I0.4-OPC-5	0.02	0.01	0.02	0.02	0.01	0.01	0.01	0.01	0.02	0.02	0.02	0.03	0.00	0.00	0.00	0.03	0.02	0.00	0.02	0.16	0.65	0.35	0.45
I0.4-LP5-3	0.02	0.02	0.02	0.06	0.45	0.65	0.54	0.52	0.42	0.36	0.25	0.57	0.28	0.69	0.85	0.41	1.59	2.68	3.56	0.89	0.85	0.55	3.85
I0.4-LP5-3	0.07	0.08	0.03	0.09	0.05	0.02	0.35	0.25	0.13	0.89	0.63	0.56	2.36	1.59	0.99	1.25	2.58	4.56	0.99	0.88	1.58	1.58	1.69
I0.4-LP5-5	0.02	0.01	0.00	0.00	0.00	0.00	0.00	0.05	0.06	0.33	0.56	0.26	0.66	2.36	3.25	1.36	0.55	0.69	0.98	1.25	0.36	0.55	0.55
I0.4-LP5-5	0.02	0.01	0.00	0.00	0.06	0.05	0.04	0.00	0.15	0.36	0.26	0.59	2.44	2.31	2.99	1.56	1.40	2.50	1.40	1.60	2.70	1.20	1.20
I0.4-LP10-3	0.25	0.35	0.35	0.56	0.25	0.45	0.56	0.58	0.59	0.64	0.26	0.21	0.05	0.04	0.20	0.56	1.89	1.65	1.54	2.10	2.45	1.78	1.90
I0.4-LP10-3	0.34	0.34	0.35	0.45	0.59	0.63	0.58	0.75	0.54	0.52	0.23	0.16	0.36	1.23	2.36	2.33	2.45	1.25	2.69	2.33	1.25	0.45	0.22
I0.4-LP10-5	0.02	0.03	0.00	0.00	0.00	0.05	0.26	0.96	2.30	2.90	0.89	0.42	0.56	0.66	1.25	1.85	1.96	0.99	3.22	2.12	1.22	2.58	1.99
I0.4-LP10-5	0.02	0.04	0.00	0.00	0.00	0.06	0.45	0.63	0.50	0.96	1.30	2.30	0.67	0.60	0.80	1.20	1.50	1.90	2.30	2.80	2.40	2.60	2.10
I0.4-LP15-3	0.23	0.67	2.60	3.30	2.50	1.60	2.30	2.50	2.30	2.60	2.50	3.20	2.33	1.26	2.56	2.66	2.85	2.66	3.45	1.25	1.23	1.22	0.99
I0.4-LP15-3	0.01	0.02	0.00	0.00	0.01	0.00	0.00	0.33	1.20	2.20	1.30	3.60	3.33	1.26	2.56	3.33	2.00	1.25	2.63	1.25	1.44	1.55	1.36
I0.4-LP15-5	0.04	0.03	0.00	0.00	0.38	0.60	0.90	1.30	2.20	2.10	2.20	3.50	2.33	1.26	1.55	2.66	2.66	2.45	2.89	2.69	3.59	2.85	3.99
I0.4-LP15-5	0.02	0.02	0.00	0.00	0.33	1.20	1.30	2.20	2.80	3.20	2.20	2.50	2.44	2.31	2.99	1.56	1.40	2.50	1.40	1.60	2.70	1.20	1.20
I0.4-L10F20-3	0.02	0.02	0.00	0.00	0.00	0.02	0.56	0.90	1.20	0.60	0.50	0.90	0.05	0.04	0.20	0.56	1.89	1.65	1.54	2.10	2.45	1.78	1.90
I0.4-L10F20-3	0.03	0.03	0.00	0.32	0.60	0.50	0.40	0.60	0.50	0.30	2.60	3.60	2.33	0.99	2.56	2.45	3.33	2.48	2.96	2.56	2.55	1.36	1.99
I0.4-L10F20-5	0.05	0.03	0.00	0.00	0.00	0.00	0.00	0.08	0.06	0.02	0.01	0.02	0.00	0.00	0.00	0.01	0.36	0.25	0.33	0.55	2.63	3.66	1.26
I0.4-L10F20-5	0.02	0.01	0.00	0.02	0.05	0.06	0.02	0.00	0.00	0.00	0.08	0.04	0.00	0.00	0.06	0.00	0.99	2.36	1.56	2.33	2.55	3.89	1.25

Table C.5 Average corrosion current density values of LP concrete with w/b=0.5 exposed to NaCl solution

uA/cm^2	0	2	4	6	8	10	12	14	16	18	20	22	24	26	28	30	32	34	36	38	40	42	44	46
I0.5-OPC-3	0.00	0.00	0.00	0.00	0.00	0.00	0.00	0.00	0.00	0.00	0.00	0.00	0.02	0.02	0.03	0.04	0.04	0.02	0.01	0.01	0.30	0.02	0.02	0.03
I0.5-OPC-3	0.05	0.05	0.05	0.05	0.05	0.01	0.09	0.08	0.09	0.08	0.08	0.08	0.09	0.01	0.01	0.03	0.04	0.04	0.04	0.04	0.04	0.04	0.04	0.03
I0.5-OPC-5	0.00	0.00	0.00	0.00	0.00	0.00	0.00	0.00	0.00	0.00	0.00	0.00	0.02	0.02	0.02	0.02	0.02	0.03	0.03	0.00	0.02	0.02	0.02	0.03
I0.5-OPC-5	0.01	0.01	0.01	0.01	0.01	0.01	0.01	0.01	0.01	0.02	0.01	0.01	0.01	0.01	0.02	0.01	0.01	0.03	0.02	0.01	0.01	0.03	0.04	0.03
I0.5-LP5-3	0.02	0.02	0.02	0.02	0.02	0.02	0.02	0.02	0.02	0.02	0.03	0.03	0.03	0.03	0.01	0.02	0.02	0.02	0.04	0.04	0.04	0.03	0.02	0.34
I0.5-LP5-3	0.00	0.00	0.00	0.00	0.00	0.03	0.02	0.02	0.03	0.03	0.08	0.08	0.08	0.08	0.05	0.07	0.05	0.07	0.02	0.03	0.03	0.02	0.23	0.34
I0.5-LP5-5	0.00	0.00	0.00	0.00	0.00	0.02	0.02	0.02	0.00	0.02	0.02	0.02	0.03	0.04	0.05	0.05	0.05	0.05	0.05	0.00	0.00	0.00	0.00	0.00
I0.5-LP5-5	0.02	0.02	0.02	0.02	0.02	0.02	0.02	0.04	0.04	0.03	0.02	0.02	0.02	0.00	0.00	0.00	0.00	0.00	0.02	0.02	0.02	0.02	0.03	0.04
I0.5-LP10-3	0.00	0.00	0.00	0.00	0.00	0.03	0.03	0.03	0.03	0.02	0.03	0.03	0.05	0.03	0.02	0.00	0.00	0.03	0.03	0.35	0.43	0.55	0.55	0.55
I0.5-LP10-3	0.00	0.00	0.00	0.00	0.00	0.03	0.04	0.04	0.04	0.04	0.04	0.04	0.04	0.05	0.00	0.03	0.03	0.23	0.35	0.56	0.57	0.89	0.03	0.03
I0.5-LP10-5	0.00	0.00	0.00	0.00	0.00	0.01	0.09	0.08	0.09	0.08	0.08	0.08	0.09	0.02	0.02	0.02	0.02	0.00	0.00	0.00	0.00	0.00	0.00	0.00
I0.5-LP10-5	0.00	0.00	0.00	0.00	0.00	0.00	0.00	0.00	0.00	0.00	0.00	0.00	0.02	0.02	0.02	0.02	0.02	0.02	0.01	0.01	0.01	0.02	0.02	0.02
I0.5-LP15-3	0.00	0.00	0.00	0.00	0.00	0.00	0.00	0.00	0.00	0.02	0.02	0.02	0.03	0.02	0.05	0.25	0.46	0.44	0.56	0.67	0.68	0.67	1.34	1.23
I0.5-LP15-3	0.00	0.00	0.00	0.00	0.00	0.00	0.00	0.00	0.00	0.03	0.03	0.03	0.03	0.04	0.03	0.03	0.03	0.35	0.45	0.49	0.78	0.66	1.34	1.55
I0.5-LP15-5	0.04	0.04	0.04	0.04	0.04	0.02	0.02	0.08	0.08	0.08	0.08	0.05	0.07	0.05	0.07	0.02	0.02	0.02	0.02	0.04	0.04	0.04	0.00	0.44
I0.5-LP15-5	0.00	0.00	0.00	0.00	0.00	0.02	0.02	0.02	0.00	0.02	0.02	0.02	0.03	0.04	0.05	0.05	0.05	0.05	0.05	0.03	0.03	0.03	0.04	0.06
I0.5-L10F20-3	0.00	0.00	0.00	0.00	0.00	0.02	0.02	0.04	0.04	0.03	0.02	0.02	0.02	0.00	0.00	0.00	0.00	0.00	0.02	0.05	0.05	0.44	0.56	0.66
I0.5-L10F20-3	0.00	0.00	0.00	0.00	0.00	0.03	0.03	0.03	0.03	0.02	0.03	0.03	0.05	0.03	0.02	0.00	0.00	0.03	0.03	0.04	0.04	0.04	0.34	0.30
I0.5-L10F20-5	0.00	0.00	0.00	0.00	0.00	0.01	0.09	0.08	0.09	0.08	0.08	0.08	0.09	0.00	0.00	0.00	0.02	0.02	0.04	0.00	0.00	0.00	0.03	0.02
I0.5-L10F20-5	0.03	0.03	0.03	0.03	0.03	0.02	0.02	0.02	0.00	0.02	0.02	0.02	0.03	0.00	0.00	0.00	0.03	0.03	0.03	0.00	0.00	0.00	0.02	0.02

Table C.5 Average corrosion current density values of LP concrete with w/b=0.5 exposed to NaCl solution

uA/cm^2	48	50	52	54	56	58	60	62	64	66	68	70	72	74	76	78	80	82	84	86	88	90	92
I0.5-OPC-3	0.04	0.04	0.00	0.00	0.02	0.02	0.01	0.22	0.30	0.50	1.50	0.60	0.63	1.26	1.85	1.96	1.56	2.96	3.66	0.99	2.56	2.85	3.46
I0.5-OPC-3	0.03	0.04	0.06	0.02	0.00	0.00	0.00	0.00	0.05	0.04	0.33	2.30	1.36	2.36	2.56	2.63	1.23	0.69	0.99	2.36	3.89	3.58	2.66
I0.5-OPC-5	0.01	0.02	0.00	0.00	0.00	0.00	0.02	0.05	0.05	0.03	0.01	0.05	0.00	0.00	0.99	2.36	2.35	3.26	1.26	3.96	2.58	2.45	2.76
I0.5-OPC-5	0.03	0.03	0.00	0.00	0.00	0.00	0.00	0.02	0.03	0.04	0.05	0.12	0.36	3.26	2.33	1.26	3.45	2.56	3.56	1.85	3.69	2.11	0.99
I0.5-LP5-3	0.34	0.45	0.60	0.60	1.50	2.60	1.50	2.60	2.80	2.40	1.20	1.10	0.05	0.04	0.20	0.56	1.89	1.65	1.54	2.10	2.45	1.78	1.90
I0.5-LP5-3	0.46	0.56	0.65	0.23	0.02	0.12	0.56	0.90	1.90	1.60	3.20	3.20	0.36	1.23	2.36	2.33	2.45	1.25	2.69	2.33	1.25	0.45	0.22
I0.5-LP5-5	0.00	0.00	0.00	0.02	0.03	0.11	0.90	0.98	1.30	1.50	2.20	1.20	0.56	0.66	1.25	1.85	1.96	0.99	3.22	2.12	1.22	2.58	1.99
I0.5-LP5-5	0.03	0.08	0.02	0.02	0.01	0.19	0.30	0.10	0.90	1.50	1.40	2.60	0.67	0.60	0.80	1.20	1.50	1.90	2.30	2.80	2.40	2.60	2.10
I0.5-LP10-3	0.57	0.67	0.60	1.20	1.30	1.20	2.20	1.30	2.20	2.20	2.50	1.90	0.99	0.99	2.36	2.56	0.99	1.26	2.96	2.56	2.89	2.65	2.78
I0.5-LP10-3	0.02	0.01	1.60	1.50	1.80	2.60	2.90	2.20	2.20	2.10	1.90	1.80	2.44	2.31	2.99	1.56	1.40	2.50	1.40	1.60	2.70	1.20	1.20
I0.5-LP10-5	0.00	0.00	0.68	1.20	0.90	0.99	1.50	1.60	2.50	1.50	1.90	2.80	2.33	2.65	3.26	2.89	1.65	2.89	2.96	2.36	1.25	2.35	2.45
I0.5-LP10-5	0.01	0.01	0.00	0.33	1.20	1.60	1.90	2.40	1.90	1.80	2.60	2.80	2.33	1.26	2.56	2.66	2.85	2.66	3.45	1.25	1.23	1.22	0.99
I0.5-LP15-3	1.33	1.45	2.20	2.30	2.60	1.50	1.80	2.70	3.20	1.20	2.20	0.50	0.36	0.22	0.63	3.25	2.45	2.98	2.85	2.55	2.68	2.75	2.65
I0.5-LP15-3	1.67	1.99	2.60	2.60	2.80	1.30	0.90	1.50	1.80	2.70	2.90	3.10	0.67	0.60	0.80	1.20	1.50	1.90	2.30	2.80	2.40	2.60	2.10
I0.5-LP15-5	0.55	0.67	0.60	0.80	1.20	1.50	1.90	2.30	2.80	2.40	2.60	2.10	2.33	1.26	2.56	2.66	2.85	2.66	3.45	1.25	1.23	1.22	0.99
I0.5-LP15-5	0.24	0.35	0.35	0.22	0.11	0.75	0.89	1.50	1.60	2.50	2.80	2.40	0.36	2.36	2.56	1.36	2.89	3.58	1.26	2.36	2.45	2.59	3.25
I0.5-L10F20-3	0.75	0.33	0.38	0.89	1.60	2.10	1.60	1.80	1.20	1.70	2.20	2.90	0.67	0.60	0.80	1.20	1.50	1.90	2.30	2.80	2.40	2.60	2.10
I0.5-L10F20-3	0.56	0.55	0.15	0.35	0.77	1.50	1.60	1.80	2.30	2.40	1.50	1.70	2.36	2.35	2.12	1.25	1.36	3.25	2.36	2.25	3.25	2.36	2.85
I0.5-L10F20-5	0.02	0.33	0.22	0.15	0.65	0.48	1.56	1.85	2.13	0.78	0.65	1.56	2.36	2.36	2.36	2.25	2.36	3.24	1.25	1.95	3.59	2.86	2.45
I0.5-L10F20-5	0.04	0.29	3.30	0.60	1.25	2.30	1.65	1.45	2.63	2.58	2.68	2.45	0.36	1.25	1.63	0.36	2.59	2.78	1.36	2.78	2.36	2.55	3.55

Table C.6 Average corrosion current density values of LP concrete with w/b=0.6 exposued to NaCl solution

uA/cm^2	0	2	4	6	8	10	12	14	16	18	20	22	24	26	28	30	32	34	36	38	40	42	44	46
I0.6-OPC-3	0.02	0.02	0.02	0.02	0.02	0.02	0.02	0.04	0.04	0.03	0.02	0.02	0.02	0.00	0.00	0.00	0.00	0.00	0.02	0.00	0.00	0.00	0.03	0.03
I0.6-OPC-3	0.00	0.00	0.00	0.00	0.00	0.03	0.03	0.03	0.03	0.02	0.03	0.03	0.05	0.03	0.02	0.00	0.00	0.03	0.03	0.00	0.00	0.00	0.03	0.03
I0.6-OPC-5	0.00	0.00	0.00	0.00	0.00	0.00	0.00	0.00	0.00	0.00	0.02	0.02	0.02	0.00	0.02	0.02	0.02	0.03	0.04	0.05	0.05	0.05	0.04	0.05
I0.6-OPC-5	0.00	0.00	0.00	0.00	0.00	0.01	0.01	0.01	0.01	0.02	0.01	0.01	0.01	0.01	0.02	0.01	0.01	0.03	0.02	0.01	0.01	0.03	0.03	0.03
I0.6-LP5-3	0.00	0.00	0.00	0.00	0.00	0.00	0.00	0.00	0.02	0.02	0.04	0.05	0.04	0.36	0.47	0.88	1.67	1.48	1.74	2.44	2.48	0.67	0.05	0.85
I0.6-LP5-3	0.00	0.00	0.00	0.00	0.00	0.00	0.00	0.00	0.03	0.03	0.03	0.00	0.26	0.46	0.99	1.57	1.94	2.35	2.33	0.44	0.45	0.03	0.20	0.02
I0.6-LP5-5	0.00	0.00	0.00	0.00	0.00	0.03	0.03	0.03	0.02	0.02	0.02	0.00	0.02	0.02	0.04	0.04	0.03	0.03	0.03	0.39	0.34	0.45	0.76	0.89
I0.6-LP5-5	0.00	0.00	0.00	0.00	0.00	0.01	0.09	0.08	0.09	0.08	0.08	0.08	0.09	0.02	0.03	0.03	0.04	0.04	0.04	0.04	0.19	0.44	0.93	1.93
I0.6-LP10-3	0.00	0.00	0.00	0.00	0.00	0.04	0.04	0.24	0.84	1.57	2.55	2.39	0.66	0.95	1.44	1.56	1.77	2.34	2.30	0.34	0.33	0.02	0.03	0.04
I0.6-LP10-3	0.00	0.00	0.00	0.00	0.02	0.02	0.04	0.04	0.03	0.33	1.24	1.88	2.33	2.04	2.56	2.45	2.34	0.35	0.44	0.45	0.56	0.34	0.56	0.79
I0.6-LP10-5	0.00	0.00	0.00	0.00	0.03	0.03	0.03	0.03	0.02	0.28	0.33	0.46	0.46	0.55	0.54	0.55	0.77	0.95	1.56	1.67	1.02	1.56	1.34	0.99
I0.6-LP10-5	0.00	0.00	0.00	0.00	0.03	0.04	0.04	0.04	0.04	0.36	0.33	0.56	0.74	0.89	1.45	1.67	1.56	2.57	2.05	1.56	1.45	0.99	1.23	1.05
I0.6-LP15-3	0.00	0.00	0.00	0.00	0.01	0.09	0.08	0.09	0.08	0.27	0.33	0.54	0.32	0.54	0.43	0.67	1.56	1.44	2.45	2.75	2.45	2.34	0.35	0.44
I0.6-LP15-3	0.00	0.00	0.00	0.00	0.00	0.00	0.00	0.00	0.00	0.04	0.27	0.34	0.44	0.42	0.05	0.95	1.45	1.33	1.85	1.58	2.54	2.94	2.03	1.45
I0.6-LP15-5	0.00	0.00	0.00	0.00	0.00	0.00	0.00	0.00	0.02	0.00	0.00	0.00	0.00	0.03	0.31	0.45	0.55	0.23	0.99	1.34	1.54	1.33	1.94	2.50
I0.6-LP15-5	0.00	0.00	0.00	0.03	0.03	0.03	0.02	0.02	0.02	0.00	0.02	0.02	0.04	0.32	0.45	0.67	1.23	1.74	1.45	2.34	2.64	0.22	0.30	3.33
I0.6-L10F20-3	0.00	0.00	0.00	0.00	0.00	0.02	0.02	0.02	0.02	0.02	0.04	0.34	0.47	0.57	0.77	1.24	1.67	2.32	1.98	1.93	2.55	2.45	2.44	2.33
I0.6-L10F20-3	0.00	0.00	0.00	0.00	0.00	0.00	0.00	0.00	0.03	0.03	0.03	0.04	0.47	0.99	0.45	0.34	0.22	0.93	1.25	1.89	2.45	2.33	1.09	1.43
I0.6-L10F20-5	0.00	0.00	0.00	0.00	0.00	0.01	0.01	0.01	0.01	0.02	0.01	0.01	0.01	0.01	0.02	0.45	0.57	0.57	0.89	1.22	1.34	2.99	1.83	1.97
I0.6-L10F20-5	0.00	0.00	0.00	0.00	0.00	0.08	0.08	0.08	0.08	0.05	0.07	0.05	0.07	0.03	0.03	0.32	0.33	0.47	0.99	0.45	1.46	1.89	1.78	2.40

Table C.6 Average corrosion current density values of LP concrete with w/b=0.6 exposed to NaCl solution

uA/cm^2	48	50	52	54	56	58	60	62	64	66	68	70	72	74	76	78	80	82	84	86	88	90	92
I0.6-OPC-3	0.03	0.04	0.00	0.35	0.90	1.20	2.10	1.60	2.80	2.70	2.45	1.26	2.36	2.56	3.45	2.69	3.48	2.69	2.55	2.33	1.23	0.96	0.32
I0.6-OPC-3	0.02	0.33	0.56	1.00	0.02	0.02	1.59	1.86	2.60	2.45	2.85	2.75	0.36	2.36	3.45	2.96	3.56	1.58	1.44	1.22	1.36	3.26	2.25
I0.6-OPC-5	0.05	0.05	0.00	0.00	0.00	0.02	0.01	0.33	0.90	2.50	2.80	1.80	2.44	2.31	2.99	1.56	1.40	2.50	1.40	1.60	2.70	1.20	1.20
I0.6-OPC-5	0.03	0.03	0.00	0.00	0.00	0.00	0.02	0.01	0.05	0.32	0.60	0.98	1.23	2.36	2.33	1.26	1.59	1.85	1.36	2.56	3.33	2.56	1.26
I0.6-LP5-3	0.69	2.56	1.78	2.69	2.48	1.23	1.59	1.48	1.53	1.69	1.28	1.75	0.67	0.60	0.80	1.20	1.50	1.90	2.30	2.80	2.40	2.60	2.10
I0.6-LP5-3	0.02	0.02	0.30	2.00	0.22	0.48	1.56	1.85	1.75	0.90	1.65	2.00	3.26	2.36	2.33	3.15	2.15	0.36	0.66	2.36	3.36	2.22	1.36
I0.6-LP5-5	1.04	1.05	1.56	2.00	2.30	1.20	1.80	0.90	1.75	1.68	1.95	1.56	3.66	2.65	1.09	0.99	3.26	2.59	3.55	2.66	2.45	2.55	2.85
I0.6-LP5-5	2.44	2.31	2.99	1.56	1.40	2.50	1.40	1.60	2.70	1.20	1.20	0.90	2.44	2.31	2.99	1.56	1.40	2.50	1.40	1.60	2.70	1.20	1.20
I0.6-LP10-3	0.05	0.04	0.20	0.56	1.89	1.65	1.54	2.10	2.45	1.78	1.90	1.80	2.33	1.25	0.99	1.56	2.63	2.58	3.54	3.58	2.45	2.85	3.69
I0.6-LP10-3	1.45	1.23	2.30	2.60	2.50	1.45	1.85	1.66	2.20	1.20	1.45	1.75	2.44	2.31	2.99	1.56	1.40	2.50	1.40	1.60	2.70	1.20	1.20
I0.6-LP10-5	0.33	0.45	0.32	0.25	1.85	1.89	1.85	1.45	2.31	2.15	1.78	0.02	0.90	3.26	2.59	3.45	2.66	2.66	3.45	3.89	2.55	1.33	0.99
I0.6-LP10-5	1.04	1.04	1.25	0.33	2.50	2.45	1.26	1.25	2.05	3.24	1.25	0.90	2.44	2.31	2.99	1.56	1.40	2.50	1.40	1.60	2.70	1.20	1.20
I0.6-LP15-3	0.56	0.34	0.36	2.10	1.20	1.56	1.85	2.60	2.45	2.22	1.05	0.95	2.36	1.36	2.59	3.56	2.58	2.66	3.25	2.45	2.66	3.22	3.12
I0.6-LP15-3	1.22	0.32	0.35	0.23	0.10	1.20	1.36	1.59	1.56	1.85	2.45	0.96	0.67	0.60	0.80	1.20	1.50	1.90	2.30	2.80	2.40	2.60	2.10
I0.6-LP15-5	2.31	0.53	0.65	1.26	1.35	2.56	2.89	2.22	2.45	2.22	3.12	0.25	0.36	3.25	2.33	2.25	2.15	3.69	2.59	3.66	3.84	2.58	3.99
I0.6-LP15-5	3.20	2.10	2.20	2.02	1.03	2.56	0.09	0.96	2.15	1.26	2.54	1.25	1.26	3.26	2.58	2.46	3.75	2.96	3.56	3.26	1.36	2.54	2.55
I0.6-L10F20-3	2.03	1.83	2.20	2.20	2.20	2.32	2.12	1.65	1.54	1.68	1.36	1.25	2.33	2.63	3.56	2.34	3.85	2.99	3.56	2.58	3.26	3.55	2.22
I0.6-L10F20-3	1.24	1.45	1.36	2.35	2.22	1.25	1.45	0.90	0.96	1.25	1.25	1.45	2.44	2.31	2.99	1.56	1.40	2.50	1.40	1.60	2.70	1.20	1.20
I0.6-L10F20-5	0.90	0.90	0.02	0.65	1.25	1.30	2.65	1.96	1.25	2.44	2.48	2.55	0.67	0.60	0.80	1.20	1.50	1.90	2.30	2.80	2.40	2.60	2.10
I0.6-L10F20-5	2.64	1.97	2.33	2.45	2.85	2.66	0.90	0.65	2.20	1.25	2.85	1.99	2.33	1.26	2.56	2.66	2.85	2.66	3.45	1.25	1.23	1.22	0.99